Accessory Kinesin-2 Motors in Cerebellar Development

by

Bridget Waas

A dissertation submitted in partial fulfillment
of the requirements for the degree of
Doctor of Philosophy
(Cell and Developmental Biology)
in the University of Michigan
2023

Doctoral Committee:

Professor Kristen Verhey, Chair
Associate Professor Benjamin Allen
Professor Ryoma Ohi
Professor Jason Spence
Associate Professor Sunny Wong

Bridget Waas

bwaas@umich.edu

ORCID iD: 0000-0003-1581-5985

Acknowledgements

Firstly, I'd like to thank my mentor, Ben Allen. Thank you for pushing me and my science over the years. I can't count the number of times I walked into your office, convinced I was full of it, but I always walked out of your office feeling confident about my project. Thank you for your support, even when that meant leaving the lab for three months to go to Genentech. You are incredible mentor, and I feel privileged to be a part of the Allen lab.

Thank you to my thesis committee members (Kristen Verhey, Sunny Wong, Jason Spence, and Puck Ohi) for the helpful and insightful comments over the years. Many of the experiments and analysis in this thesis stemmed from our discussions. Kristen - thank you for being a great thesis committee head and a role model.

I would like to acknowledge and thank all those who contributed to the work in this thesis, either intellectually or experimentally. Thank you to the entire Allen lab! Brandon Carpenter, for leaving me with one tough but fascinating thesis project. Olivia Merchant for not only her beautiful illustrations but teaching me how to be a mentor. Nicole Franks for your insightful comments, help in collecting data while I was 9 months pregnant and for making sure the Allen lab doesn't burn down. From lab meetings to late nights to journal clubs, all past and present members have positively shaped my graduate school career. A special thank you to Justine, Martha, and Mike for showing me the ropes and being positive role models. Anna – I wouldn't have wanted anyone else to go through all the highs and lows of graduate school with. Thanks to Tyler, Hannah and Haeyoung for being great lab mates and making long days in lab fly by.

Thank you to the collaborating CDB labs for sharing resources and protocols to our hallway conversations – in particular the Spence, Giger and Verhey labs. Thank you to the CDB admin staff for their help over the years.

Thank you to all the teachers and professors that have shaped my scientific career prior to graduate school. My favorite science teacher, Mrs. Rausch; my undergraduate mentor, Robert Belton, and my Perrigo fellowship mentor, Ivan Maillard.

I'd like to thank parents - my mom for being my #1 cheerleader in whatever I do, and my dad, for answering my endless questions for the past 28 years. Especially when I call late at night while standing in the cold room to ask whether I need to double the amps for transferring twice as many western blots. You don't know what western blots are, but you saved my experiment (Figure 2.8C).

Last and most importantly, thank you to my little family. My husband Ryan for your endless support and love. From applying to graduate schools to defending my thesis, I couldn't have done it without you. My two dogs, Max and Sofie, for their never-ending entertaining antics and for taking me on walks. Thank you to my sweet daughter Sadie, for keeping me company these late nights writing my thesis.

Table of Contents

List of Tables

List of Figures

Abstract

Since its initial discovery in Drosophila nearly forty years ago, the Hedgehog (HH) signaling pathway has been demonstrated to directs certain aspects of development and maintenance of nearly every organ system across invertebrate, vertebrate, and mammalian animal models. In summary, HH ligands binds to the receptor Patched1 (PTCH1) to relieve the inhibition on Smoothened (SMO), promoting activation of HH target genes through the family of GLI transcription factors. The cerebellum relies on proper HH signaling to control the size and complexity of the tissue. One of the HH ligands, Sonic Hedgehog (SHH) promotes proliferation of cerebellar granule neural progenitors (CGNPs), which gives rise to cerebellar granule neurons (CGNs), the most abundant cell type in the central nervous system.

A key organelle that regulates HH signaling is the primary cilium, a microtubule-based projection from the cell membrane that serves as signaling centers for multiple pathways, including the HH pathway. Several HH pathway components localize to the primary cilia, and cilia are required for proper GLI processing. Kinesin-2 motor proteins are responsible for anterograde transport of cargo through primary cilia. There are three motor complexes in the kinesin-2 family: heterodimeric motor KIF3A/KIF3B, homodimeric KIF17, and heterodimeric KIF3A/KIF3C. In mice, KIF3A/KIF3B is required for ciliogenesis and therefore proper HH signaling. *Kif3a* deletion results in an inability to respond to SHH ligand, leading to a reduction in cerebellar granule neural progenitors (CGNP) proliferation. KIF17 and KIF3C do not have clear roles in mammalian embryogenesis or ciliogenesis, so these motors are known as accessory kinesin-2 motors. Furthermore, the role(s) of accessory kinesin-2 motors in HH signaling transduction or cerebellar

development are unknown. The goal of this dissertation is to investigate the contribution of accessory kinesin-2 motors in HH-dependent cerebellar development.

In chapter 2, I investigate the role of homodimeric KIF17 in cerebellar development. *Kif17* expression was detected in SHH-producing Purkinje cells and HH-responsive CGNPs. Deletion of *Kif17* in Purkinje cells phenocopies germline *Kif17* deletion – reduced EGL thickness due to decreased CGNP proliferation and reduced HH target gene expression. Reduced levels of SHH protein are observed within Purkinje cells in *Kif17*$^{-/-}$ cerebella, demonstrating KIF17 is required in Purkinje cells to promote CGNP proliferation. These data suggest reduced SHH protein levels in *Kif17*$^{-/-}$ cerebella results in reduced HH signaling levels and decreased CGNP proliferation, resulting in cerebellar hypoplasia. On the contrary, CGNP-specific *Kif17* deletion increased HH target gene expression and EGL thickness due to increased CGNP proliferation. Levels of GLI3 repressor are significantly reduced with *Kif17* deletion, suggesting KIF17 additionally restricts CGNP proliferation in a cell autonomous fashion. This work identifies dual and opposing roles for KIF17 in HH-dependent cerebellar development– first, as a positive regulator of HH signaling through regulation of SHH protein levels within Purkinje cells, and second, as a negative regulator of HH signaling through regulation of GLI transcription factors in CGNPs.

In chapter 3, I explored the contribution of KIF3C to the postnatal cerebellum. Differing from *Kif17*, *Kif3c* expression was detected ubiquitously in the cerebellum. Germline *Kif3c* mutants displayed cerebellar hypoplasia, albeit less severe than *Kif17* deletion animals. Notably, even with reduced CGNP proliferation, HH signaling remains intact in *Kif3c*$^{-/-}$ cerebella. In addition to decreased expression of Notch target, *Hes1*, we observed abnormal patterning of Bergmann glia in *Kif3c* mutants. Collectively, these data demonstrate KIF3C's requirement in the cerebellum and suggest a novel role in regulating Notch signaling during development. Collectively, this

dissertation demonstrates essential roles for both KIF17 and KIF3C in cerebellar development. First, I identified dual and opposing roles for KIF17 in HH signaling at the level of SHH ligand and GLI processing, and second, I explored a role for KIF3C in Bergmann glia patterning.

Chapter 1 Introduction

1.1 Abstract

The cerebellum is part of the central nervous system, classically known for its roles in coordination and movement. Recent work has uncovered an important role for the cerebellum in higher level processes such as cognitive function, including attention, language, and regulating the fear response. Dysfunction in development or homeostasis can result in diseases such as cerebellar hypoplasia, medulloblastoma, and cerebellar ataxia. Elucidating the molecular mechanisms of proper cerebellar development is vital for developing treatments for developmental cerebellar defects and adult cerebellar diseases in the future. A better understanding of normal developmental processes can be applied to investigating when these processes go awry. One signaling pathway demonstrated to be essential in cerebellar development and disease is the Hedgehog (HH) signaling pathway. In this chapter, I will review the known molecular mechanisms of HH signaling, with an emphasis on cerebellar development, including 1) an overview of HH signal transduction, 2) the mechanisms regulating HH ligand production, processing and release, 3) transcriptional control of HH pathway activity through the regulation of GLI processing and function, 4) primary cilia and kinesin-2 motors as regulators of HH pathway activity, and 5) the role of HH signaling specifically in cerebellar development. This introduction will also provide the rationale for my doctoral work investigating accessory kinesin-2 motor functions in HH-dependent cerebellar development.

1.2 HH Pathway Overview

Hedgehog (HH) signaling was initially discovered through *Drosophila* genetic screens over forty years ago (Nusslein-Volhard and Wieschaus, 1980). This screen identified the *hedgehog* (*hh*) gene, which was subsequently demonstrated to encode for a secreted ligand in the pathway (Lee et al., 1992); *hh* mutations result in segmental patterning defects in *Drosophila* larvae (Nusslein-Volhard and Wieschaus, 1980). Molecular characterization discovered that Hh provides patterning cues to neighboring cells in *Drosophila* larvae (Lee *et al.*, 1992; Mohler and Vani, 1992; Tabata et al., 1992; Taylor et al., 1993). Hedgehog ligands are evolutionarily conserved and provide segmental and body plan identity for organisms ranging from invertebrates to vertebrates [reviewed in (Ingham et al., 2011)]. Importantly, Sonic Hedgehog (SHH) has been demonstrated to be a key mitogen in the developing cerebellum (Dahmane and Ruiz i Altaba, 1999; Lewis et al., 2004; Wallace, 1999; Wechsler-Reya and Scott, 1999).

The main receptor for HH ligands is Patched (PTC) in *Drosophila*, Patched1 (PTCH1) in mammals, a twelve-pass transmembrane protein (Hooper and Scott, 1989; Marigo et al., 1996; Nakano et al., 1989). In the absence of Hh/HH ligand (Figure 1.1, left), PTC/PTCH1 inhibits a G protein-coupled like receptor Smoothened [SMO, (Chen and Struhl, 1996; Marigo and Tabin, 1996; Stone et al., 1996)]. Additionally, proper cell surface regulation of HH pathway activity is dependent on three co-receptors – GAS1, CDON and BOC (Allen et al., 2011; Allen et al., 2007; Cobourne et al., 2004; Lee et al., 2001a; Lum et al., 2003; Martinelli and Fan, 2007; Tenzen et al., 2006; Yao et al., 2006). Two of the HH co-receptors, BOC and GAS1, have been demonstrated to be essential for proper HH signal transduction in the developing cerebellum (Izzi et al., 2011). When HH ligand is present (Figure 1.1, right), it binds to PTC/PTCH1, relieving the inhibition on SMO, resulting in a signal transduction cascade that leads to modulation of the HH transcriptional

effectors, Cubitus interruptus (CI, *Drosophila*) and glioma-associated oncogene (GLI, mammals) zinc finger transcription factors (Alexandre et al., 1996; Taipale et al., 2002). In the absence of ligand, Ci/GLI transcription factors are cleaved to form a transcriptional repressor, inhibiting HH target gene expression. In the presence of HH ligand, CI/GLIs are post-translationally modified to form transcriptional activators, inducing HH target gene expression [(Alexandre *et al.*, 1996; Chen and Struhl, 1996; Taipale *et al.*, 2002); reviewed in (Aberger and Ruiz i Altaba, 2014; Falkenstein and Vokes, 2014; Huangfu and Anderson, 2006; Hui and Angers, 2011)]. Notably, *Gli2* and *Gli3* are required for proper cerebellar development (Blaess et al., 2006; Blaess et al., 2008; Corrales et al., 2006; Corrales et al., 2004).

One aspect of vertebrate HH signaling that distinguishes it from flies is the requirement for the primary cilium, a microtubule-based projection from the cell surface. Once thought to be a vestigial organelle, the primary cilium has been demonstrated to be necessary for proper HH signal transduction [(Huangfu et al., 2003); reviewed in (Bangs and Anderson, 2017; Goetz and Anderson, 2010)]. Several pathway components localize to the primary cilium, and the absence of primary cilia leads to dysregulated HH signaling across several developing tissues and organs (Corbit et al., 2005; Haycraft et al., 2005; Liu et al., 2005; Rohatgi et al., 2007). Importantly, loss of primary cilia during cerebellar development results in an inability to respond to SHH ligand, leading to a reduction in cerebellar granule neural progenitors (CGNP) proliferation (Spassky et al., 2008). Ciliogenesis and ciliary trafficking is dependent on the kinesin-2 family of motors (Figure 1.2A-B), specifically the heterodimeric motor complex KIF3A/KIF3B. Loss of either one of these subunits in mice results in defective ciliogenesis (Nonaka et al., 1998; Takeda et al., 1999). In addition to KIF3A/KIF3B motor complex, there are two accessory kinesin-2 motors, heterodimeric KIF3A/KIF3C and homodimeric KIF17 [reviewed in (Hirokawa et al., 2009)]. Loss

of either accessory motor in mice does not result in embryonic lethality or any gross defects in ciliogenesis (Yang et al., 2001; Yin et al., 2011). For my dissertation, I will focus on the accessory kinesin-2 motors and investigate the potential contributions of these motors to HH signal transduction within postnatal cerebellar development.

1.3 HH Ligands

1.3.1 Translation and Intracellular Processing

In mammals, there are three different HH ligands, Sonic Hedgehog (*Shh*), Indian Hedgehog (*Ihh*) and Desert Hedgehog (*Dhh*) (Echelard et al., 1993; Krauss et al., 1993; Riddle et al., 1993). Expression analyses revealed some overlapping areas of expression of these ligands as well as unique areas of expression, suggesting some non-redundant functions of the three ligands (Bitgood and McMahon, 1995). The most studied HH ligand is *Shh*, which has well-described roles in neural tube specification and digit specification (Echelard *et al.*, 1993; Riddle *et al.*, 1993; Roelink et al., 1994; Roelink et al., 1995). The cerebellum also requires *Shh* for proper levels of HH signaling to drive postnatal expansion of CGNPs (Lewis *et al.*, 2004), as SHH promotes proliferation of CGNPs (Dahmane and Ruiz i Altaba, 1999; Wechsler-Reya and Scott, 1999). During ossification, *Ihh* functions in chondrogenesis and osteogenesis (Chung et al., 2001; Vortkamp et al., 1996), while *Dhh* is vital for spermatogenesis (Bitgood et al., 1996; Clark et al., 2000) and peripheral nerve ensheathment (Parmantier et al., 1999). Importantly, *Shh* is the only ligand expressed in the cerebellum; *Ihh* and *Dhh* are not expressed in the cerebellum (Traiffort et al., 1998).

All Hedgehog ligands are initially translated as a 45 kDa precursor including an N-terminal signal sequence, N-terminal signaling molecule and C-terminal domain (Figure 1.3). The polypeptide undergoes autocatalytic cleavage to generate an N-terminal 19 kDa active signaling component and a C-terminal 25 kDa fragment (Lee et al., 1994; Porter et al., 1995). The

autocleavage process results in cholesterol modification to the C-terminus of the active N-terminal fragment due to the cholesterol transferase activity of the 25 kDa C-terminal fragment (Porter et al., 1996a; Porter et al., 1996b). Full length HH retains a significant level of activity (Tokhunts et al., 2010), while the C-terminal fragment is not sufficient to drive a HH gain-of-function phenotype (Porter *et al.*, 1995). In the absence of the C-terminal domain, the N-terminal signaling fragment was able to travel further extracellularly in the imaginal discs of *Drosophila* (Porter *et al.*, 1996a), suggesting the C-terminus and cholesterol modification are required for proper localization of the N-terminal fragment. Furthermore, within the developing *Drosophila* retina, the C-terminal domain has been shown to drive localization of the N-terminal ligand to the axons and growth cones of neurons (Chu et al., 2006). Cleaved N-HH is retained in the retina, while the full length HH was transported down axons (Daniele et al., 2017). In mice, the cholesterol modification is required for the proper range of SHH (Feng et al., 2004; Lewis et al., 2001; Li et al., 2006). In NIH/3T3 and 293T cells, the C-terminal fragment is degraded within the ER (Chen et al., 2011). It remains to be investigated if the C-terminal domain is degraded in the ER or required for trafficking or localization of the ligand in cells that endogenously produce HH ligands in mice.

Another post-translation modification of HH ligands is palmitoylation (Pepinsky et al., 1998). Identified in *Drosophila*, Skinny Hedgehog (Ski), a transmembrane acyltransferase, is responsible for palmitoylating the N-terminus of the active signaling fragment (Amanai and Jiang, 2001; Chamoun et al., 2001; Micchelli et al., 2002). Loss of the palmitoylate, either through mutating the palmitoylate site or through loss of *ski*, results in a reduction of activity in HH ligand. However, this was not due to a change in HH abundance, localization, or cholesterol modification (Chamoun *et al.*, 2001; Micchelli *et al.*, 2002; Pepinsky *et al.*, 1998). In *Drosophila*, expression of HH lacking palmitoylate acts as a dominant negative over the endogenous HH ligand (Lee et

al., 2001b). In mammals, mutation of the palmitoylation site resulted in a less active SHH ligand in ventralizing the embryonic mouse forebrain but could induce a polydactyl phenotype in the developing limb (Kohtz et al., 2001; Lee *et al.*, 2001b). Deletion of mouse homologue acetyltransferase *Hhat* revealed loss of palmitoylate affects the multimeric complex of SHH, therefore affecting long-range HH signaling (Chen et al., 2004). Importantly, full length SHH can be palmitoylated, suggesting autocleavage and cholesterol modification is not required for palmitoylation (Chen *et al.*, 2004). Collectively, these data propose a model where sorting of SHH is dependent on whether SHH remains full length or processed (Figure 1.3).

1.3.2 Extracellular Processing

DISP, initially identified through a *Drosophila* genetic screen, is a twelve-pass transmembrane protein from the resistance-nodulation division (RND) transporter family. DISP mediates the release of dually lipidated HH ligand from HH-producing cells (Burke et al., 1999; Caspary et al., 2002; Kawakami et al., 2002; Ma et al., 2002; Tian et al., 2005a). Loss of *disp* in *Drosophila* results in segment polarity phenotypes consistent with a HH loss-of-function phenotype; specifically, *disp* mutation results in an accumulation of HH ligand within HH-producing cells (Burke *et al.*, 1999). Importantly, this effect was not observed in HH protein lacking the cholesterol modification (Burke *et al.*, 1999; Tian *et al.*, 2005a). In zebrafish, loss of *disp1* disrupts HH signaling through its essential role in secretion of lipid-modified HH ligand (Nakano et al., 2004). In mice, there are two DISP homologues, DISP1 and DISP2 (Caspary *et al.*, 2002; Kawakami *et al.*, 2002; Ma *et al.*, 2002). In mice, loss of *Disp1* loss results in embryonic lethality with left-right asymmetry and defects the face, forebrain, and neural tube, phenocopying *Smo* mutants (Caspary *et al.*, 2002; Kawakami *et al.*, 2002; Ma *et al.*, 2002). Importantly,

conditional deletion of *Disp1* in *Shh*-expressing cells results in midline and neural tube patterning defects, confirming DISP1 is required in HH-producing cells (Tian *et al.*, 2005a). Unlike *Disp1*, *Disp2* is not expressed embryonically, and overexpression of DISP2 does not increase SHH export (Ma *et al.*, 2002). With its sterol sensing domain, DISP1 is structurally similar to PTCH1, the HH ligand receptor (Burke *et al.*, 1999; Caspary *et al.*, 2002). The sterol sensing domain is important for DISP1 activity on HH ligand in a cholesterol-dependent manner (Creanga et al., 2012; Ma *et al.*, 2002; Tukachinsky et al., 2012). Another important domain for DISP1 function is its Furin cleavage site, which has been demonstrated to be essential for proper SHH release (Stewart et al., 2018). While further studies are required to elucidate the exact molecular mechanism of DISP, another pathway component has been demonstrated to be required for proper HH ligand activity – SCUBE2 [signal peptide, CUB domain, EGF (epidermal growth factor)-like protein 2] (Creanga *et al.*, 2012; Hollway et al., 2006; Kawakami et al., 2005; Tukachinsky *et al.*, 2012; Woods and Talbot, 2005).

SCUBE2 was initially identified in mutagenic screen in zebrafish (van Eeden et al., 1996). *Scube2/you*^{ty97} mutants displayed classic HH defects, such as myotome and neural tube defects (Hollway *et al.*, 2006; Kawakami *et al.*, 2005; van Eeden *et al.*, 1996; Woods and Talbot, 2005). SCUBE2 is conserved from zebrafish to mice and humans but interestingly not in *Drosophila* (Grimmond et al., 2000; Grimmond et al., 2001; Hollway *et al.*, 2006; Kawakami *et al.*, 2005; Woods and Talbot, 2005). Loss of *Scube2* in mice causes a defect in endochondral bone formation, a phenotype associated with HH loss-of-function (Lin et al., 2015), but surprisingly no other HH phenotypes have been reported despite its wide expression during embryogenesis (Grimmond *et al.*, 2001; Kawakami *et al.*, 2005; Woods and Talbot, 2005). Notably, *Scube2* deletion in the cerebellum has not been examined. SCUBE2 belongs to a family of proteins which also contains

SCUBE1 and SCUBE3. In zebrafish, loss of all SCUBE family members results in a total lack of HH activity (Johnson et al., 2012), while compound mutants of *Scube* in mice have not been published. However, recent work demonstrate mice with *Scube3* deletion are viable, but they display impaired endochondral bone formation and chondrogenesis, similar to *Scube2*$^{-/-}$ mice (Lin et al., 2021; Lin *et al.*, 2015). Mutations in *SCUBE3* in humans results in reduced growth, skeletal features, distinctive craniofacial appearance, and dental anomalies through modulating BMP signaling (Lin *et al.*, 2021). In addition, human SCUBE1 has been demonstrated to promote BMP signaling *in vitro* (Liao et al., 2016).

It is thought that SCUBE2 is responsible for long-range HH signaling through its interaction with cholesterol modified HH ligands and increasing its solubility in the extracellular environment (Creanga *et al.*, 2012; Hollway *et al.*, 2006; Kawakami *et al.*, 2005; Tukachinsky *et al.*, 2012; Woods and Talbot, 2005). SCUBE2 has been demonstrated to interact with SHH and PTCH1 within lipid rafts (Tsai et al., 2009), but there is conflicting evidence whether palmityl moiety on HH ligands is required for SCUBE2-mediated release (Creanga *et al.*, 2012; Tukachinsky *et al.*, 2012). SCUBE proteins contain nine EGF repeats, followed by a spacer region then three cysteine-rich motifs and a CUB domain at the C-terminus (Hollway *et al.*, 2006; Kawakami *et al.*, 2005; Tsai *et al.*, 2009). Both spacer regions and the cysteine-rich motifs are required for proper localization in SCUBE2 and SCUBE1 (Liao *et al.*, 2016; Tsai *et al.*, 2009). Deletion of the cysteine-rich motifs and CUB domain (*Scube2*$^{\Delta CUB}$) impairs its ability to secrete HH ligand (Tukachinsky *et al.*, 2012). Altogether, it is believed SHH secretion is accomplished through the sterol sensing domain of DISP1 and transfers it to SCUBE2 in a cholesterol-dependent manner (Creanga *et al.*, 2012; Tukachinsky *et al.*, 2012).

1.4 GLI Transcription Factors

1.4.1 Overlapping and distinct functions of GLI proteins

Initially, *Drosophila* Ci was demonstrated as both a transcriptional repressor and activator (Dominguez et al., 1996). In mice, activator and repressor functions are split between three proteins – GLI1, GLI2 and GLI3 (Figure 1.4). Initial observations describe while GLI1 only contained an activator domain, GLI3 contained both activator and repressor domains (Dai et al., 1999). GLI3 activity is dependent on SHH ligand; in the absence of SHH, GLI3 is processed as a repressor. In the presence of SHH ligand, GLI3 can bind to *Gli1* locus, suggesting it was also a target of the pathway (Dai *et al.*, 1999). Follow up examination revealed activator and repressor domains were present in GLI2 as well, and deletion of the repressor domains increased in activator function (Sasaki et al., 1999). GLI2 is most often described as an activator, while GLI3 is primarily a transcriptional repressor (Ding et al., 1998; Sasaki et al., 1997; Sasaki *et al.*, 1999). In *Gli2*$^{-/-}$*;Gli3*$^{-/-}$ compound mutants, *Gli1* expression is not detected, suggesting GLI1 acts as a positive feedback loop to propagate HH signal transduction (Bai et al., 2004). The loss of *Gli2* or *Gli3* result in embryonic lethality, while *Gli1* deletion does not result in embryonic defects unless there is a concurrent reduction in *Gli2* (Bai et al., 2002; Park et al., 2000).

GLI1 and GLI2 have overlapping and distinct roles for GLI activator function. In the neural tube, *Gli1* mutants do not display patterning defects, while *Gli1*$^{-/-}$*;Gli2*$^{+/-}$ compound mutants have a slight defect in floor plate and V3 interneuron progenitor cells that require the highest level of HH signaling (Bai *et al.*, 2002; Bai *et al.*, 2004). This suggests GLI2 can compensate for GLI1 to attain ventral cell types in the neural tube. In further support of this notion, replacing the endogenous *Gli2* allele with *Gli1* can rescue *Gli2* mutants in the developing neural tube (Bai and Joyner, 2001). In the cerebellum, *Gli1* deletion does not impact cerebellar development, while loss

of *Gli2* results in HH loss-of-function phenotype (Corrales *et al.*, 2006). However, similar to the neural tube, loss of *Gli1* in *Gli2* conditional deletion animals worsens the cerebellar phenotype, suggesting GLI1 can partially compensate for GLI2 in this tissue (Corrales *et al.*, 2006).

GLI3 is most often classified as a repressor, but there are contexts where GLI3 activator is observed. In dorsal neural tube, *Gli3* deletion results in HH gain-of-function phenotype, but in the ventral neural tube, *Gli3* mutants have reduced *Gli1* expression, demonstrating both GLI3 activator and repressor are required for proper neural tube specification (Bai *et al.*, 2004). In the developing jaw, GLI3 has been described to cooperate with HAND2 to activate mandibular prominence target genes (Elliott et al., 2020). Examination of *Gli2/Gli3* compound mutants reveal GLI2 and GLI3 have overlapping and distinct roles as activators (Mo et al., 1997). *Gli2* mutant mice display a narrow oesophagus and trachea and lung hypoplasia, and further loss of one allele of *Gli3* (*Gli2*$^{-/-}$*;Gli3*$^{+/-}$) significantly worsens the phenotype, while *Gli2*$^{-/-}$*;Gli3*$^{-/-}$ mice lack lungs, oesophagus (Motoyama et al., 1998). This dosage-dependent phenotype suggests there are partially redundant roles for GLI2 and GLI3 (Motoyama *et al.*, 1998). Replacing the *Gli2* endogenous allele with *Gli3* can partially rescue neural tube patterning (Bai *et al.*, 2004), providing additional support that GLI2 and GLI3 have overlapping roles. It is unknown whether GLI3 can act as a transcriptional activator in the developing cerebellum, but *Gli3* deletion results in a defect in embryonic cerebellar patterning through increased FGF8, a HH gain-of-function phenotype (Blaess *et al.*, 2008).

While GLI2 is typically described as an activator, there are instances where GLI2 repressor has been described. The abundance of GLI2 repressor increases when *Shh* is deleted (Pan et al., 2006). In the sclerotome, GLI2 has been observed to repress expression of HH target gene, *Pax1* (Buttitta et al., 2003). GLI2 represses hypaxial genes in the absence of *Gli3* in the developing skeletal muscle (McDermott et al., 2005). It is unknown whether GLI2 can act as a transcriptional

repressor in the cerebellum, but conditional deletion of *Gli2* in the cerebellum results in reduced CGNP proliferation and cerebellar hypoplasia, a HH loss-of-function phenotype. Altogether, these data highlight the importance of GLI transcription factors and their cell-specific roles in modulating the HH response.

1.4.2 GLI processing

GLI transcriptional activity is dependent on its post-translational modifications (Figure 1.4). Initially described in Drosophila, Ci is proteolytically cleaved to form a transcriptional repressor in the absence of ligand (Aza-Blanc et al., 1997). Extensive work described Ci phosphorylation by protein kinase A (PKA), glycogen synthase kinase 3 (GSK3), and casein kinase I (CKI) were required for proteolytical cleavage by $SCF^{Slimb/\beta\text{-}TRCP}$ ubiquitin ligase (Chen et al., 1999; Jia et al., 2002; Jia et al., 2005; Jiang and Struhl, 1998; Price and Kalderon, 2002; Smelkinson and Kalderon, 2006; Wang et al., 1999). Degradation of Ci can be prevented through mutation of the protein degradation domain (Methot and Basler, 1999; Tian et al., 2005b). Vertebrate HH signaling is also dependent on PKA phosphorylation (Epstein et al., 1996; Hammerschmidt et al., 1996). GLI3 has been demonstrated to be phosphorylated by PKA and processed into a repressor by $SCF^{\beta TrCP}$ ubiquitin E3 ligase [Figure 1.4; black asterisks, P1-P6 (Tempe et al., 2006; Wang et al., 2000; Wang and Li, 2006). While GLI2 can also be phosphorylated by PKA, only a small fraction is processed into a repressor and the rest is degraded (Pan *et al.*, 2006; Pan et al., 2009). GLI1 does not contain the entire PKA phosphorylation cluster and cannot be processed into a repressor (Pan and Wang, 2007; Price and Kalderon, 2002). However, PKA does have a negative impact on GLI1 transcriptional activity (Kaesler et al., 2000). PKA can also regulate GLI activator function as well (Niewiadomski et al., 2013). A differential

set of phosphorylation clusters are required for full activator function of GLI2 and GLI3 (Niewiadomski et al., 2014). Phosphomimetic mutations of Pc-g clusters resulted in increased activity of GLI2 and GLI3 [Figure 1.4; blue asterisks, Pc-g (Niewiadomski *et al.*, 2014)].

Another important component of regulating GLI processing is Suppressor of Fused (SUFU). Initial identification of SUFU was in flies, where *sufu* deletion suppresses phenotypes in *fu* mutants, a kinase downstream of SMO (Preat, 1992; Preat et al., 1993; Therond et al., 1993). In mice, *Sufu* deletion results in mid-gestation lethality with HH gain-of-function phenotypes, resembling *Ptch1* mutants (Svard et al., 2006). Importantly, SUFU has been demonstrated to restrict CGNP proliferation through promoting GLI3 repressor formation and repressing GLI2 activator (Jiwani et al., 2020). Similar to *Gli3* deletion, *Sufu* deletion results in increased FGF8 in the cerebellum (Jiwani *et al.*, 2020).

SUFU interacts with GLI2 and GLI3 and promotes repressor formation, and activation of HH signaling induces GLI proteins to dissociate from SUFU (Humke et al., 2010). Deletion of *Sufu* leads to unstable full length GLIs, while SUFU overexpression stabilizes full length GLIs (Wang et al., 2010). Cerebellar conditional deletion of *Sufu* results in reduced GLI1 and GLI3 but increased GLI2 (Jiwani *et al.*, 2020). Further, PKA activation promotes SUFU-GLI interaction, inhibiting GLI activator function (Humke *et al.*, 2010). SUFU interacts with GLIs through a SYGH motif [Figure 1.4; orange box (Dunaeva et al., 2003)]. Mutation of this site in GLI1 results in constitute nuclear localization (Dunaeva *et al.*, 2003; Svard *et al.*, 2006).

Initially identified in the mouse brain, RAB23 is another negative regulator of HH signaling (Eggenschwiler et al., 2006; Eggenschwiler et al., 2001; Guo et al., 2006). *Rab23* deletion in mice results in mid-gestation lethality and phenocopies *Sufu* mutants (Eggenschwiler *et al.*, 2006; Eggenschwiler *et al.*, 2001). RAB23 suppresses HH signaling through repression of

GLI activator; *Rab23* deletion results in an increase of full length GLI proteins (Eggenschwiler *et al.*, 2006). Conditional deletion of *Rab23* in the developing cerebellum results in increased CGNP proliferation and mis-patterning of the cerebellum (Hor et al., 2021). Importantly, RAB23 localizes to cilia and regulates ciliary localization of overexpressed KIF17 in NIH/3T3 cells (Lim and Tang, 2015).

1.4.3 Primary cilia and GLI proteins

Primary cilia are microtubule-based projections from the cell surface that was originally believed to be a vestigial organelle. The observation that HH signaling is disrupted in primary cilia mutants significantly altered the field of HH signaling (Huangfu *et al.*, 2003). In addition to HH signaling, the primary cilia regulates several essential developmental processes [reviewed in (Goetz and Anderson, 2010)]. Intraflagellar transport is accomplished with IFT A and IFT B particles, which are trafficked with kinesin-2 motors (anterograde) and dynein (retrograde). Mutations in IFT particles have been associated with dysregulation of HH signaling (Gorivodsky et al., 2009; Haycraft *et al.*, 2005; Huangfu and Anderson, 2005; Huangfu *et al.*, 2003; Keady et al., 2012; Liu *et al.*, 2005; Ocbina et al., 2011; Qin et al., 2011; Yang et al., 2015). Intriguingly, most ciliary mutants display HH loss-of-function phenotypes in the neural tube (Huangfu and Anderson, 2005; Huangfu *et al.*, 2003), some ciliary mutants display polydactyl, a HH gain-of-function phenotype (Haycraft *et al.*, 2005; Liu *et al.*, 2005). These contradictory results are likely due to the net reduction of GLI activator and repressor in these tissues, as proper GLI processing is dependent on intact primary cilia.

Full length GLI1, GLI2 and GLI3 localize to the tips of primary cilia even in the absence of HH stimulation, while processed repressors do not (Chen et al., 2009; Kim et al., 2009; Wen et

al., 2010). Notably, the presence of primary cilia can restrict the activity of constitutively active GLI2 (Engelke et al., 2019; Wong et al., 2009). PKA localizes to the base of the primary cilia, and the HH gain-of-function phenotype with PKA loss is dependent on cilia (Tuson et al., 2011). Deletion of PKA phosphorylation sites in GLI2 negatively affect activator function and ciliary localization (Liu et al., 2015a), while point mutations in PKA phosphorylation sites enhances activator function and does not impact ciliary localization (Niewiadomski *et al.*, 2014; Zeng et al., 2010). Mutations of other sites in GLI2 have also reduced ciliary localization; however, GLI2 constructs also lacking those resides still localize to primary cilia (Han et al., 2017; Santos and Reiter, 2014). These conflicting data demonstrate GLI ciliary localization is a complex process that requires further study.

Importantly, SUFU and GLI co-localize at the tips of cilia (Haycraft *et al.*, 2005). GLI dissociation from SUFU is cilia-dependent, and SUFU ciliary localization is dependent on GLI2 and GLI3 (Humke *et al.*, 2010; Tukachinsky et al., 2010). Collectively, these data suggest a model where in the absence of HH stimulation, GLI is bound to SUFU at the tips of primary cilia and is processed into repressors through PKA phosphorylation of P1-P6 sites; in the presence of ligand, GLI dissociates from SUFU and PKA phosphorylates Pc-G clusters for transcriptional activation.

1.5 Accessory Kinesin-2 Motors

1.5.1 Kinesin-2 Overview

Intracellular transport through kinesin motors is required for essential cellular functions. Passive transport of small molecules is accomplished by diffusion, but movement of large cargo (organelles, vesicles etc.) must be actively transported. Cellular trafficking along microtubules is accomplished through kinesin and dynein motors. First identified in the giant axon of the squid

(Allen et al., 1982; Brady et al., 1982; Vale et al., 1985), kinesin proteins contain a motor domain, which uses ATP hydrolysis to carry cargo anterograde – from the minus ends of microtubules to the plus ends at the periphery of the cell or the tip of primary cilium. In addition to the motor domain, kinesins typically contain a coiled-coiled region to dimerize and a tail domain for cargo binding. In mammals, there are over forty different kinesin proteins highlighting the importance of specialized transport within the cell [reviewed in (Hirokawa *et al*., 2009)]. One family of motors is kinesin-2, initially identified from sea urchin eggs (Cole et al., 1993). The kinesin-2 family contains heterodimeric KIF3A/KIF3B, homodimeric KIF17 and heterodimeric KIF3A/KIF3C [reviewed in (Hirokawa *et al*., 2009)], Figure 1.2A-B). The latter two motors are known as accessory motors, as they do not have clear roles within mammalian ciliogenesis or embryonic development (Yang *et al*., 2001; Yin *et al*., 2011).

1.5.2 Heterodimeric KIF3A/KIF3B

KIF3A was the first kinesin-2 motor to be cloned from mouse brain cDNA libraries (Aizawa et al., 1992) and observed as an anterograde axonal motor in the brain (Kondo et al., 1994). KIF3B was subsequently identified from mouse brain cDNA libraries and demonstrated to form a heterodimeric motor with KIF3A to transport vesicles in axons (Yamazaki et al., 1995). While axonal (Aizawa *et al*., 1992; Kondo *et al*., 1994; Takeda et al., 2000) and cytoplasmic (Brown et al., 2005; Stauber et al., 2006; Yamazaki *et al*., 1995) trafficking roles have been established, KIF3A/KIF3B is well-known for its role in primary cilia [reviewed in (Scholey, 2013)]. Anterograde transport within the primary cilia is accomplished by one main motor in mice – heterodimeric kinesin-2 motor KIF3A/KIF3B. Loss of either one of these subunits in mice, *Kif3a* or *Kif3b*, lead to defective ciliogenesis, embryonic lethality and dysregulation of HH

signaling (Huangfu *et al*., 2003; Nonaka *et al*., 1998; Takeda *et al*., 1999). In addition to its role in ciliogenesis, inhibition of KIF3A/KIF3B resulted in primary ciliary deconstruction in a matter of hours, suggesting there is an additional requirement for this motor in cilia maintenance (Engelke *et al*., 2019). Furthermore, previous work in our laboratory has found that KIF3A and its adaptor protein, KAP3, directly binds and regulates GLI transcription factors (Carpenter et al., 2015). Importantly, loss of *Kif3a* within the HH-responsive cells in the developing cerebellum leads to cerebellar hypoplasia due to reduced CGNP proliferation and loss of mitogenic response to SHH ligand (Spassky *et al*., 2008). Recent work has implicated KIF3B in contributing to the SHH gradient in the developing limb (Wang et al., 2022), but it remains to be explored whether KIF3A/KIF3B functions within the SHH-producing Purkinje cells in the cerebellum.

1.5.3 Homodimeric KIF17

KIF17 is a homodimeric kinesin motor, initially identified and mapped using cDNA libraries from 4 week old kidney from mice (Nakagawa et al., 1997). KIF17 has orthologues ranging from Tetrahymena (Awan et al., 2004) and sea urchin (Morris et al., 2006) to humans (Nagase et al., 2000). Loss of *Kif17* is well-tolerated in across several model organisms, though KIF17 does have defined roles within neuronal tissues. Within *C. elegans*, loss of KIF17 homologue, OSM-3, leads to a disrupted distal primary cilia compartment within neurons (Evans et al., 2006; Signor et al., 1999; Snow et al., 2004). In *Danio rerio*, loss of KIF17 led to disrupted photoreceptor outer segment development (Insinna et al., 2008; Lewis et al., 2018; Lewis et al., 2017), as well as morphological changes to olfactory cilia (Zhao et al., 2012). Loss of KIF17 in mice leads to short term memory issues, learning disabilities and a disruption of NR2B trafficking in the hippocampus (Yin et al., 2012; Yin *et al*., 2011). Knock-down of *Kif17* in mice spinal cord

led to reduced pain perception (Liu et al., 2015b; Liu et al., 2014). Observational studies in humans revealed mutations in *KIF17* were associated with schizophrenia (Tarabeux et al., 2010), dementia with Lewy bodies (Goldstein et al., 2021), microphthalmia, coloboma (Riva et al., 2021), and male infertility (Markantoni et al., 2021). Overexpression of KIF17 in mice resulted in improved memory (Wong et al., 2002) but also increased the severity of epileptic activity (Liu et al., 2022).

Whether KIF17 can compensate for the loss of other kinesin-2 motors varies significantly across different organisms. In *C. elegans* amphid-channel sensory cilia, KIF17/OSM-3 can compensate for the loss of KIF3A/KIF3B homologue, KLP20/KLP11 (Evans *et al*., 2006; Snow *et al*., 2004). In the developing zebrafish, injection of *Kif17* RNA was able to partially rescue the loss of *Kif3b* (Zhao *et al.*, 2012). However, KIF17 cannot rescue ciliogenesis in *Kif3a*$^{-/-}$*;Kif3b*$^{-/-}$ NIH/3T3 mouse fibroblasts (Engelke *et al.*, 2019).

In the mouse, KIF17 has been demonstrated to traffic NR2B, a sub-unit of the NMDA receptor in the dendrites of hippocampal neurons and regulating synaptic plasticity and memory (Guillaud et al., 2003; Guillaud et al., 2008; Yin *et al*., 2012; Yin *et al*., 2011). Outside of the central nervous system, another tissue where *Kif17* has notable expression is the testis (Macho et al., 2002). Overexpression studies examining KIF17 function revealed co-localization with the transcription factor Activator of CREM in Testis (ACT) in specific stages of spermatogenesis, and *in vitro* analyses revealed KIF17 shuttled ACT between the cytoplasm and nucleus (Macho *et al*., 2002), as well as the mRNAs dependent on CREM binding (Chennathukuzhi et al., 2003). KIF17 has also been noted to localize to chromatoid bodies and could interact with Piwi-like protein 1, MIWI (Kotaja et al., 2006). Additionally, KIF17 co-localizes with Spatial during spermatid differentiation (Saade et al., 2007) and neuron differentiation (Irla et al., 2007). While human male infertility has been linked to *KIF17* (Markantoni *et al*., 2021), mice lacking *Kif17* are viable and

fertile (Lewis *et al*., 2017; Yin *et al*., 2011), suggesting redundancy in KIF17 function in the mouse testis.

KIF17/OSM-3 is a fast, processive motor (Guillaud *et al*., 2003; Hammond et al., 2010; Setou et al., 2000). When not bound to cargo, inhibition of kinesin motors is essential to avoid unnecessary ATP hydrolysis and congestion on microtubule tracks (Blasius et al., 2007; Verhey and Hammond, 2009). Previous work revealed two mechanisms of autoinhibition for KIF17 (Hammond *et al*., 2010). A region of the tail domain binds to the motor domain to prevent microtubule binding, while another region in the coiled-coiled 2 domain also binds to the motor to prevent processive movement [Figure 1.2C, (Hammond *et al*., 2010)]. KIF17 activity can be further modulated through phosphorylation by Calcium/calmodulin-dependent protein kinase II (CaMKII) on the tail domain (Guillaud *et al*., 2008; Lewis *et al*., 2018). Phospho-mimetic mutations in the tail domain of KIF17 increased ciliary localization across multiple cell lines and the distal outer segment of zebrafish larvae (Lewis *et al*., 2018). Another important region of KIF17 is the ciliary localization signal (CLS) in the tail domain, which was found to be necessary and sufficient for ciliary localization (Dishinger et al., 2010). Surprisingly, removal of the motor domain does not affect ciliary localization of KIF17, suggesting KIF17 can act as cargo for KIF3A/KIF3B (Jiang et al., 2015; Williams et al., 2014). While there has been work demonstrating KIF17's function across several cell types, a role for KIF17 in HH signaling has not been investigated.

1.5.4 Heterodimeric KIF3A/KIF3C

The remaining kinesin-2 motor, *Kif3c*, was first identified from cDNA libraries isolated from mouse brain, spinal cord and retina (Yang et al., 1997). Similar to *Kif17*, loss of *Kif3c* does

not perturb embryonic development in several model organisms. Morpholinos for *kif3c* and *kif3c-like* do not result in ciliary phenotypes or embryonic development defects in *Danio rerio* (Zhao *et al.*, 2012). In mice, *Kif3c* mutants are viable, fertile and display grossly normal development (Jimeno et al., 2006; Yang *et al.*, 2001); but *Kif3c*$^{-/-}$ neurons display defects in axon growth in neuron regeneration (Gumy et al., 2013). In both the zebrafish retina and mouse dorsal root ganglia neurons, *Kif3c* expression restricted to the adult tissue (Gumy *et al.*, 2013; Zhao *et al.*, 2012). In humans, mutations in *KIF3C* have been associated with sporadic infantile spasm syndrome (Dimassi et al., 2016), and expression of *KIF3C* has been observed in several human cancer cell lines (Gao et al., 2020; Liu et al., 2021; Ma et al., 2021; Wang et al., 2015; Yao et al., 2021).

Unlike the other kinesin-2 motors, KIF3C has not been observed in cilia, and *Kif3c* loss does not result in ciliary phenotypes (Jimeno *et al.*, 2006; Yang *et al.*, 2001; Zhao *et al.*, 2012). Injection of *Kif3c* RNA was able to partially rescue the loss of *Kif3b* in the developing zebrafish (Zhao *et al.*, 2012). However, KIF3C overexpression cannot rescue ciliogenesis in *Kif3a*$^{-/-}$*;Kif3b*$^{-/-}$ NIH/3T3 mouse fibroblasts (Engelke *et al.*, 2019).

KIF3C forms a motor complex with KIF3A, but not KIF3B, for anterograde axonal transport of vesicles [Figure 1.2A, B, D, (Muresan et al., 1998; Yang and Goldstein, 1998)]. In contrast to KIF3B, a significant subset of KIF3C is not bound to KIF3A, raising the possibilities KIF3C interacts with another motor or has an independent function (Muresan *et al.*, 1998). KIF3C preferentially binds to tyrosinated (unstable) microtubules, and treatment with Taxol, a microtubule stabilizer, resulted in KIF3C release from microtubules (Gumy *et al.*, 2013). Additionally, forced homodimeric motor KIF3C/KIF3C has been observed to increase the catastrophe frequency of microtubules without altering the rate of microtubule growth (Guzik-Lendrum et al., 2017). Through its tail domain, KIF3C can interact with end-binding protein 3

(EB3), which is necessary for localization at growing ends of microtubules within the growth cones of regenerating dorsal root ganglion cells (Gumy *et al.*, 2013). In adult regenerating dorsal root ganglion axons, KIF3C loss led to stable, overgrown, and looped microtubules at the growth cones. Overexpression of *Kif3c* in embryonic dorsal root ganglion cells (which do not express *Kif3c*) is detrimental to axon growth (Gumy *et al.*, 2013). While embryonic *Kif3c* expression has not been detected, it remains to be investigated whether loss of KIF3C results in any defects in tissues that develop postnatally, such as the cerebellum.

1.6 Cerebellar Morphogenesis

1.6.1 Specification of cerebellar cell types

The developing cerebellum contains four cell layers (Figure 1.5). Positioned most externally are the CGNPs, which reside next to the basement membrane. The next layer is the molecular layer, consisting of Purkinje cells and Bergmann glia. CGNs are subsequently positioned, while the white matter lays most internally. Initially, all cerebellar neurons are specified alar plate of r1, which give rise to the rhombic lip and ventricular zone [reviewed in (Butts et al., 2014; Leto et al., 2016)]. Purkinje cells precursors (PCPs) arise from the ventricular zone between E10-E13 and give rise to a transient structure called the Purkinje cell plate, which will transform into the molecular monolayer in the later cerebellum (Goffinet, 1983; Yuasa et al., 1991). Bergmann glia are derived from the ventricular zone around E14.0 and initially migrate to the precursor white matter (Anthony and Heintz, 2008; Mori et al., 2006; Yuasa, 1996) before they settle adjacent to Purkinje cells in the molecular layer. One subset of Bergmann glia is differentiated early in development, while another subset undergoes a proliferative wave up to postnatal day 7 (P7; reviewed in (Leto *et al.*, 2016)]. Cerebellar granule neural progenitors

(CGNPs) are derived from the rhombic lip and express *Atoh1* (Alder et al., 1999; Machold and Fishell, 2005; Wang et al., 2005). During E12.0 to E16.5, CGNPs will migrate to the dorsal surface of cerebellar anlagen and form the external granule layer [EGL, (Miale and Sidman, 1961)]. Several mitogenic pathways promote expansion of the EGL, starting with a thin layer of cells to a cell layer consisting of six to eight cells deep. SHH is the main driver behind CGNP expansion (Corrales *et al.*, 2006; Dahmane and Ruiz i Altaba, 1999; Lewis *et al.*, 2004; Wallace, 1999; Wechsler-Reya and Scott, 1999); Notch signaling participates in driving proliferation and antagonizing BMP signaling (Solecki et al., 2001; Zhao et al., 2008). As development progresses, CGNPs will exit the cell cycle aided by BMP and WNT3 signaling (Anne et al., 2013). Semaphorin 6A and Plexin A2 provide the molecular cue for post-mitotic CGNPs to migrate using the radial fibers from the Bergmann glia into the inner granule layer (IGL), where they differentiate and become mature CGNs [summarized in Figure 1.5, (Kerjan et al., 2005; Renaud et al., 2008)].

1.6.2 HH-dependent cerebellar development

Hedgehog signaling was first implicated in cerebellar development when human medulloblastomas were noted to have mutations in *PTCH1* (Raffel et al., 1997). It was then observed *Ptch1*$^{+/-}$ mice also had increased incidence of medulloblastoma, and *Ptch1* is expressed in the cerebellum (Goodrich et al., 1997). It was then noted Hedgehog pathway components were expressed during cerebellar development – *Shh* within Purkinje cells, *Ptch1* in Bergmann glia, cerebellar granule neurons (CGNs) and cerebellar granule neural progenitors (CGNPs) and *Smo* within CGNPs (Figure 1.5) (Traiffort *et al.*, 1998). Further examination revealed *Ptch2*, *Gli1*, *Gli2,* and *Gli3* were also expressed in CGNPs, Bergmann glia and CGNs [summarized in Figure 1.(Corrales *et al.*, 2004; Dahmane and Ruiz i Altaba, 1999; Wallace, 1999; Wechsler-Reya and

Scott, 1999). SHH ligand induced CGNP proliferation and inhibited differentiation (Dahmane and Ruiz i Altaba, 1999; Wechsler-Reya and Scott, 1999). Further, injection of hybridoma cells secreting SHH blocking antibody (5E1) led to thinning of the external granule layer (EGL), where CGNPs reside (Dahmane and Ruiz i Altaba, 1999; Wallace, 1999; Wechsler-Reya and Scott, 1999).

Starting at E16.5 and continuing through adulthood, *Shh* is expressed in Purkinje cells starting at E16.5 and continuing through adulthood (42, 283). SHH is the only HH ligand in the cerebellum; *Ihh* and *Dhh* expression are not detected in this tissue (Traiffort *et al.*, 1998). Cerebellar size and foliation are influenced by the levels of ligand – deletion of *Shh* results in cerebellar hypoplasia and reduced number of lobes, while an additional allele of *Shh* increases cerebellar size and the number of lobes (Corrales *et al.*, 2006; Lewis *et al.*, 2004). It is unknown how SHH is processed, trafficked, or released from Purkinje cells.

SHH ligand drives CGNP proliferation and activates HH signaling in the surrounding Bergmann glia and CGNs. SHH binds to PTCH1, relieving the inhibition of SMO; deletion of *Smo* in the cerebellum results in reduced expression of HH target genes and lack of foliation in the tissue (Corrales *et al.*, 2006). CGNP specific deletion of *Smo* similarly resulted in cerebellar hypoplasia and reduced CGNP proliferation, and conditional deletion of *Smo* in Bergmann glia results in a mild patterning defect in the molecular layer and reduced proliferation of CGNPs (Cheng et al., 2018). Two of the HH co-receptors, BOC and GAS1 have been demonstrated to be essential for proper HH signal transduction in the developing cerebellum; loss of either of these co-receptors results in reduced CGNP proliferation in a cell-autonomous manner (Izzi *et al.*, 2011). *Boc* is ubiquitously expressed in the cerebellum, while *Gas1* is restricted to CGNPs (Izzi *et al.*,

2011). Notably, *Cdon* expression is not detected, and its deletion did not impact embryonic cerebellar development (Izzi *et al.*, 2011).

Gli1, *Gli2* and *Gli3* are expressed in all three HH-responsive cells [Figure 1.5, (Corrales *et al.*, 2004)]. *Gli1* deletion does not impact cerebellar size unless there is additional deletion of an allele of *Gli2* (Corrales *et al.*, 2006). Examination of $Gli2^{-/-}$ mouse embryos at embryonic day 18.5 (E18.5) revealed decrease of EGL thickness, while $Gli3^{-/-}$ embryos displayed a thicker EGL (Corrales *et al.*, 2004). GLI2 activator function is required for the postnatal expansion of the cerebellum, as *Gli2* conditional deletion reduced cerebellar size and number of lobes (Corrales *et al.*, 2006). Additionally, GLI3 repressor plays an important role in setting up the embryonic primordium in maintaining *Fgf8* expression from E9.5-E12.5, as well as defining the cerebellar foliation pattern (Blaess *et al.*, 2006; Blaess *et al.*, 2008). GLI3 function in the postnatal cerebellum has not been investigated.

Loss of other repressive components of HH signaling result in increased CGNP proliferation and patterning defects. *Sufu* deletion results in increased FGF8 in the cerebellum, phenocopying *Gli3* mutants (Jiwani *et al.*, 2020). SUFU promotes GLI3 repressor formation and represses GLI2 activator to restrict CGNP proliferation (Jiwani *et al.*, 2020). Conditional deletion of *Rab23* in the developing cerebellum results in increased CGNP proliferation and mis-patterning of the cerebellum (Hor *et al.*, 2021). Collectively, these data establish the importance of HH signaling in cerebellar development.

1.7 Conclusion

The postnatal expansion of the cerebellum is dependent on proper levels of HH signaling; deletion of HH pathway components significantly impact cerebellar size and foliation. Loss-of-

function mutations result in reduced CGNP proliferation and cerebellar hypoplasia, while gain-of-function mutations lead to increased CGNP proliferation, disrupted cell layers, and medulloblastoma. The primary cilium is required for proper HH signaling and processing of the transcriptional effectors, GLI proteins. Loss of the primary cilia lead to lack of both repressor and activator forms of GLI. Heterodimeric kinesin-2 motor, KIF3A/KIF3B, is responsible for anterograde transport in primary cilia in mice. Deletion of either *Kif3a* or *Kif3b* result in defective ciliogenesis, abnormal GLI processing, and cerebellar hypoplasia. Deletion of accessory kinesin-2 motors, homodimeric KIF17 and heterodimeric KIF3A/KIF3C do not result in obvious ciliary phenotypes in mice. For my thesis, I investigate what, if any, roles do accessory kinesin-2 motors play in HH-dependent cerebellar development?

Chapter 2 focuses on homodimeric KIF17 and its conflicting roles in HH signaling within the developing cerebellum. The first role for KIF17 is as a positive regulator SHH ligand, where *Kif17* deletion in SHH-producing Purkinje cells causes a loss-of-function phenotype. The second opposing role described for KIF17 is as a positive regulator of GLI3 repressor in HH-responsive CGNPs, where *Kif17* specific deletion results in a HH gain-of-function phenotype. Chapter 3 focuses on KIF3C's contribution to cerebellar development. Similar to *Kif17*, *Kif3c* deletion results in reduced cerebellar size. However, *Kif3c* deletion does not impact HH signaling but Notch signaling instead. Collectively, the data presented in this thesis demonstrate while loss of accessory kinesin-2 motors does not impact embryogenesis or ciliogenesis in mice, KIF17 and KIF3C have unique and non-redundant roles in postnatal cerebellar development.

1.8 Figures

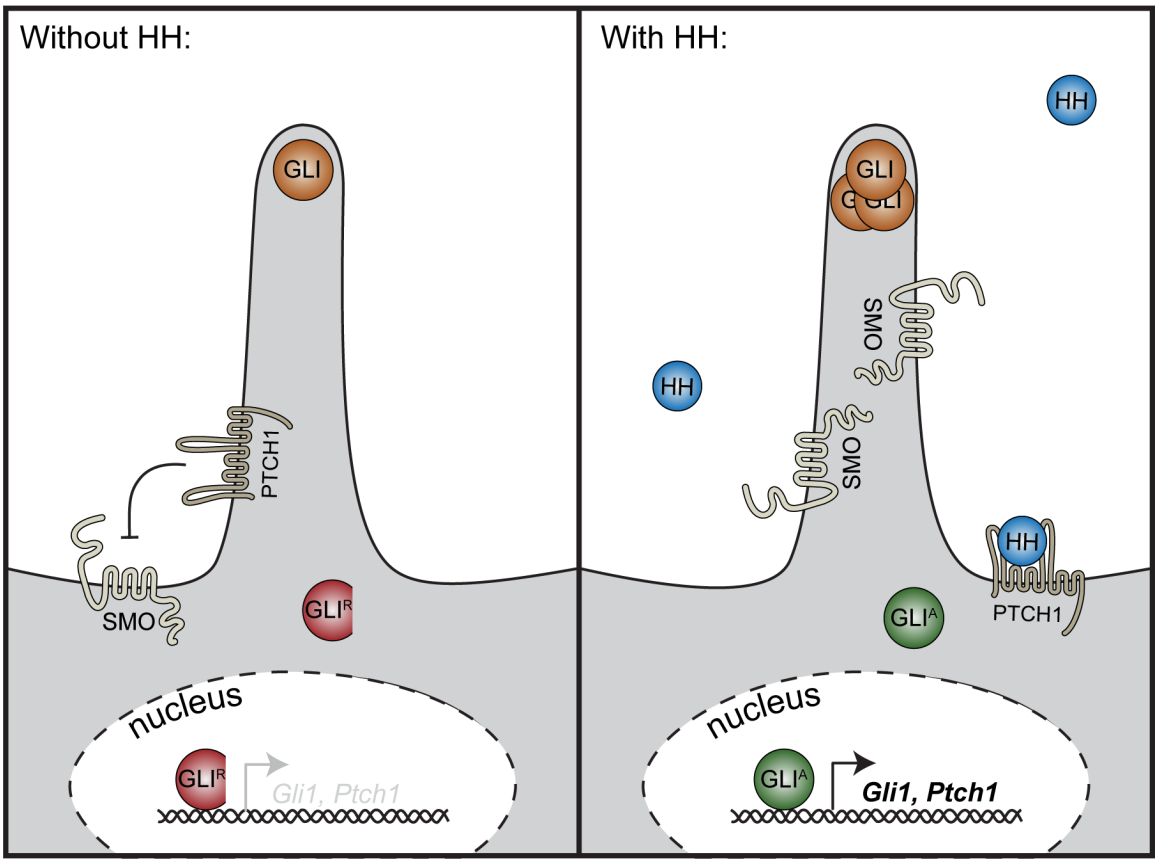

Figure 1.1 Schematic of Hedgehog signaling in primary cilia.

In the absence of HH ligand (blue), PTCH1 lays at the base of cilia, repressing SMO. Full length GLIs (orange) are processed into repressors (red) to inhibit HH target genes. In the presence of HH ligand, HH binds to PTCH1, relieving inhibition on SMO. This results in full length GLIs processed into activators which turn on expression of HH target genes, like *Gli1* and *Ptch1*.

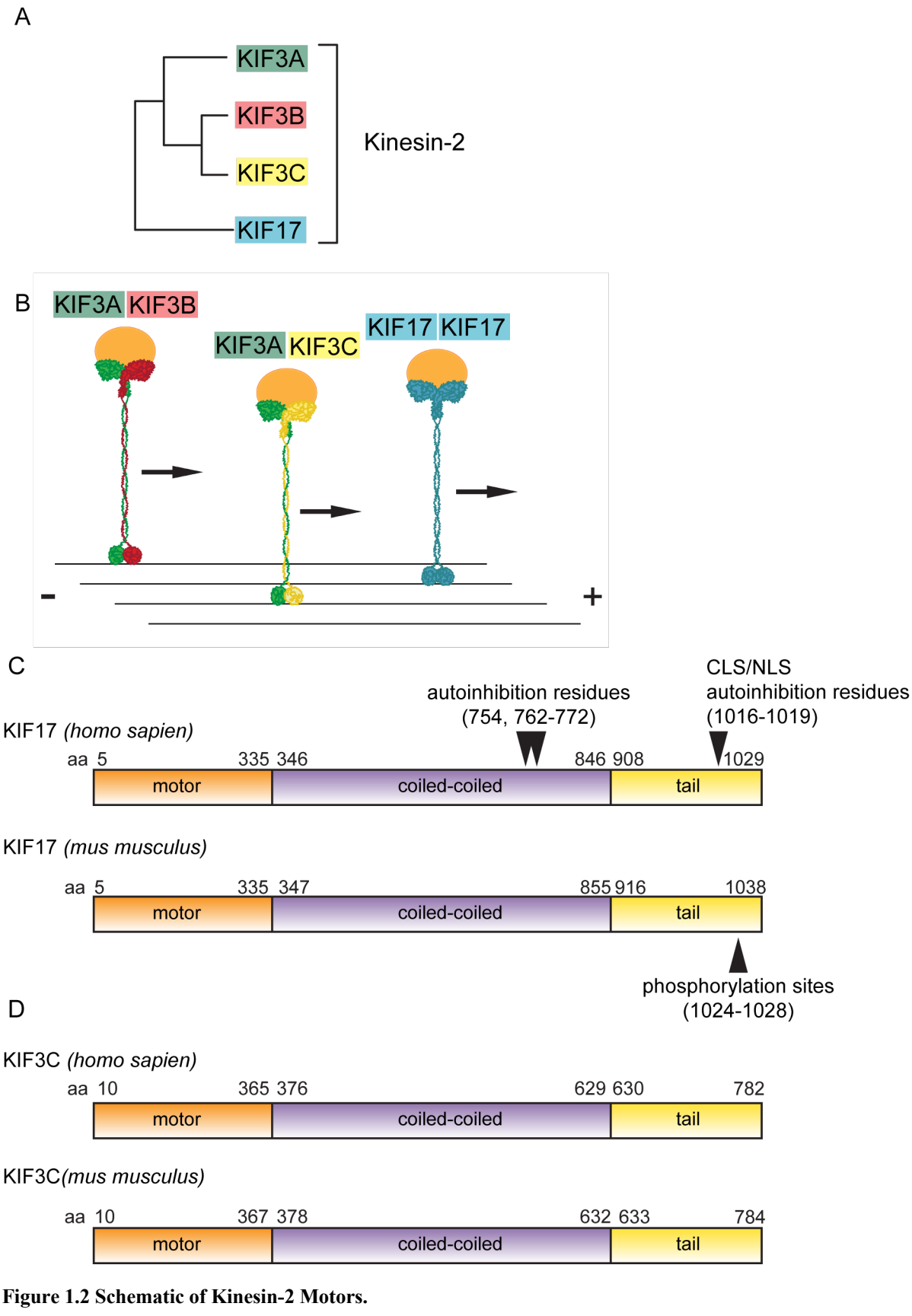

Figure 1.2 Schematic of Kinesin-2 Motors.

(A) Phylogeny tree of mouse kinesin-2 motors. (B) Schematic of three kinesin-2 motor complexes carrying cargo (orange oval) to the plus ends of microtubules. (C) Polypeptide schematic of human and mouse KIF17. (D) Polypeptide schematic of human and mouse KIF3C.

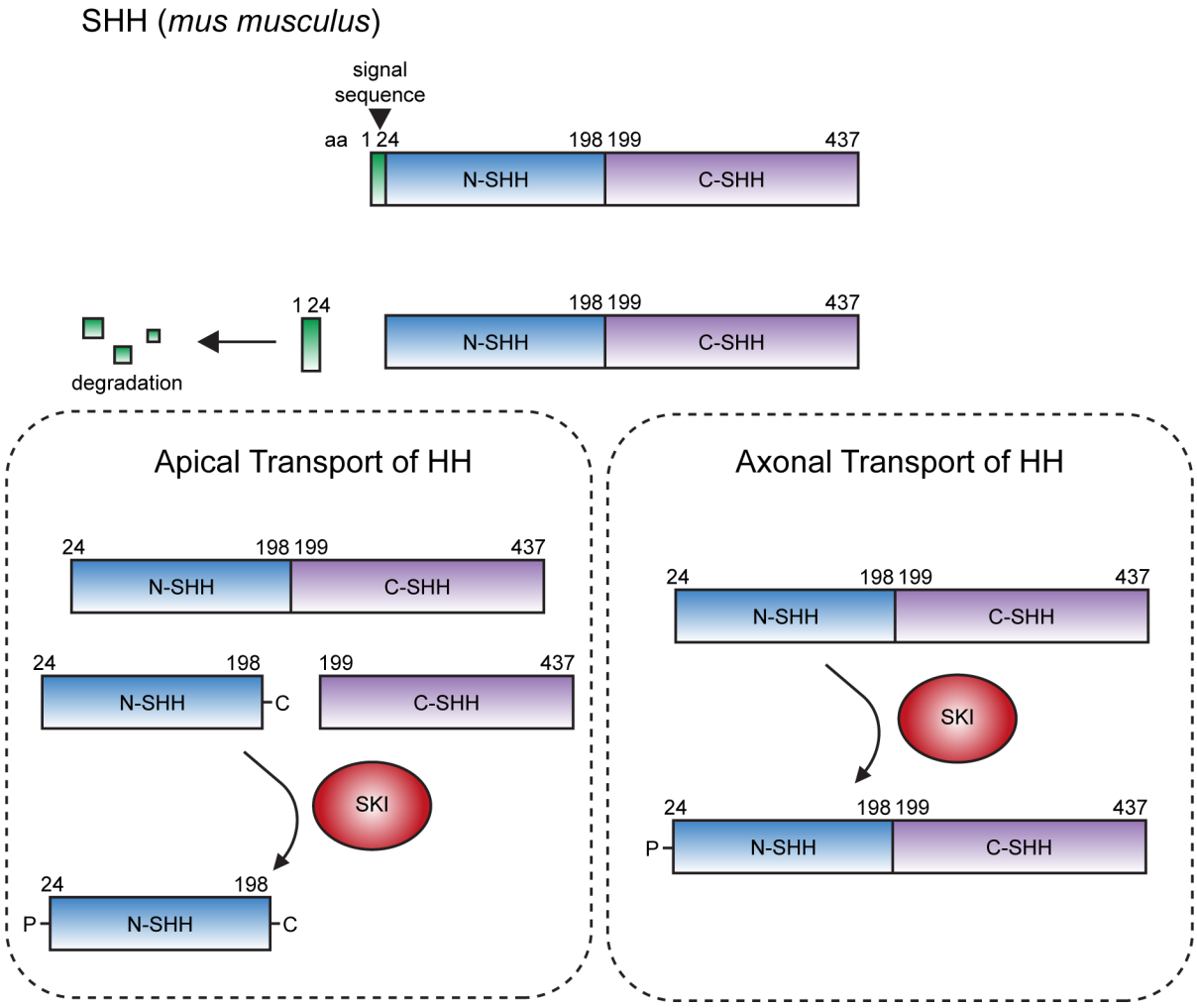

Figure 1.3 SHH processing schematic.

Schematic displaying SHH ligand polypeptide with a signal sequence (green), N-terminal signaling domain (N-SHH) and C-terminal fragment (C-SHH). Autocleavage between N-SHH and C-SHH results in the addition of cholesterol at the C terminus of N-SHH (labeled as C). Skinny Hedgehog (SKI, red) transfers the palmitoylate to the N-terminus of N-SHH.

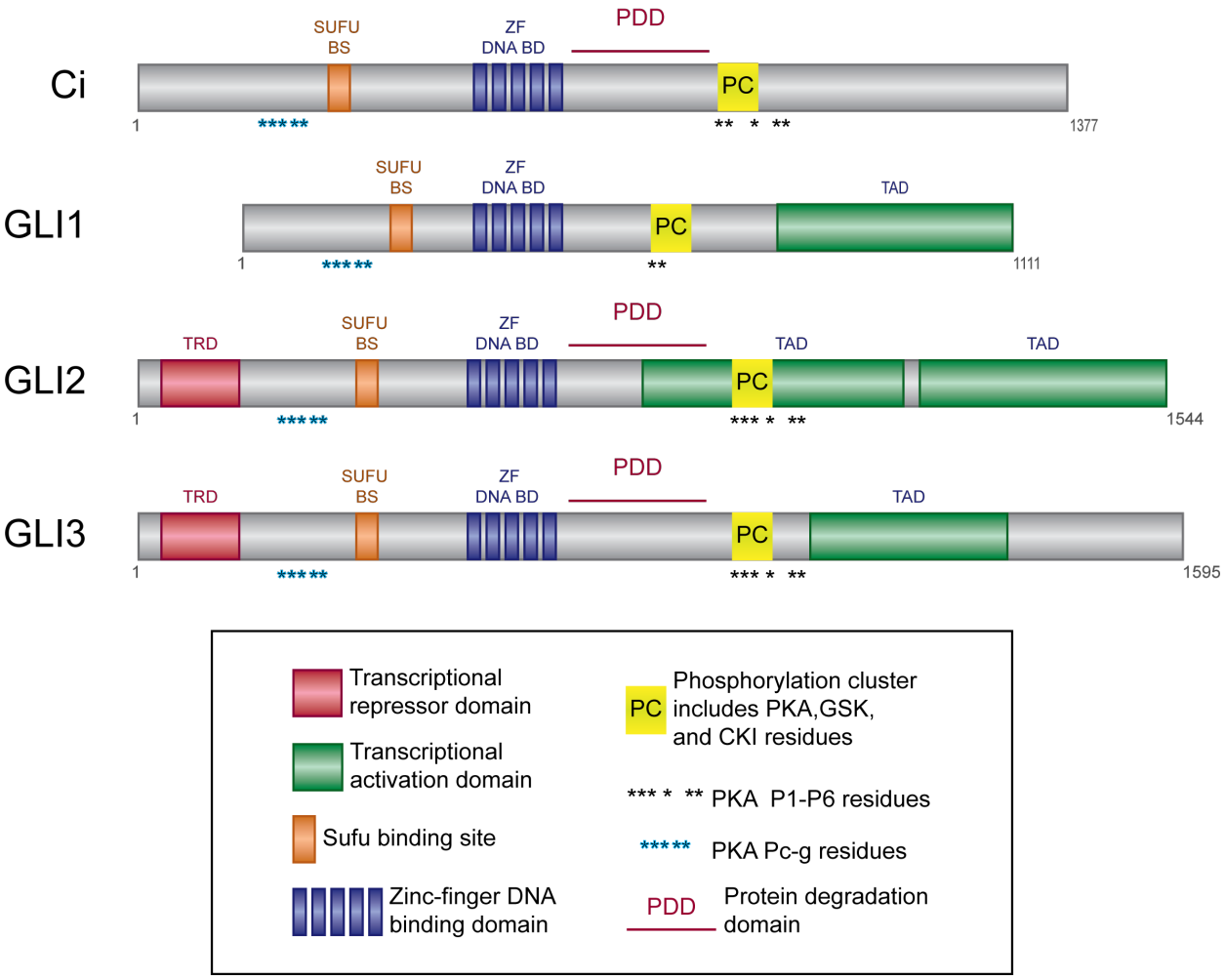

Figure 1.4 GLI/Ci Processing Schematic.

Schematic displaying *Drosophila* Ci and mammalian GLIs with their domains, binding sites and phosphorylation sites labeled. Figure adapted from Brandon Carpenter's thesis.

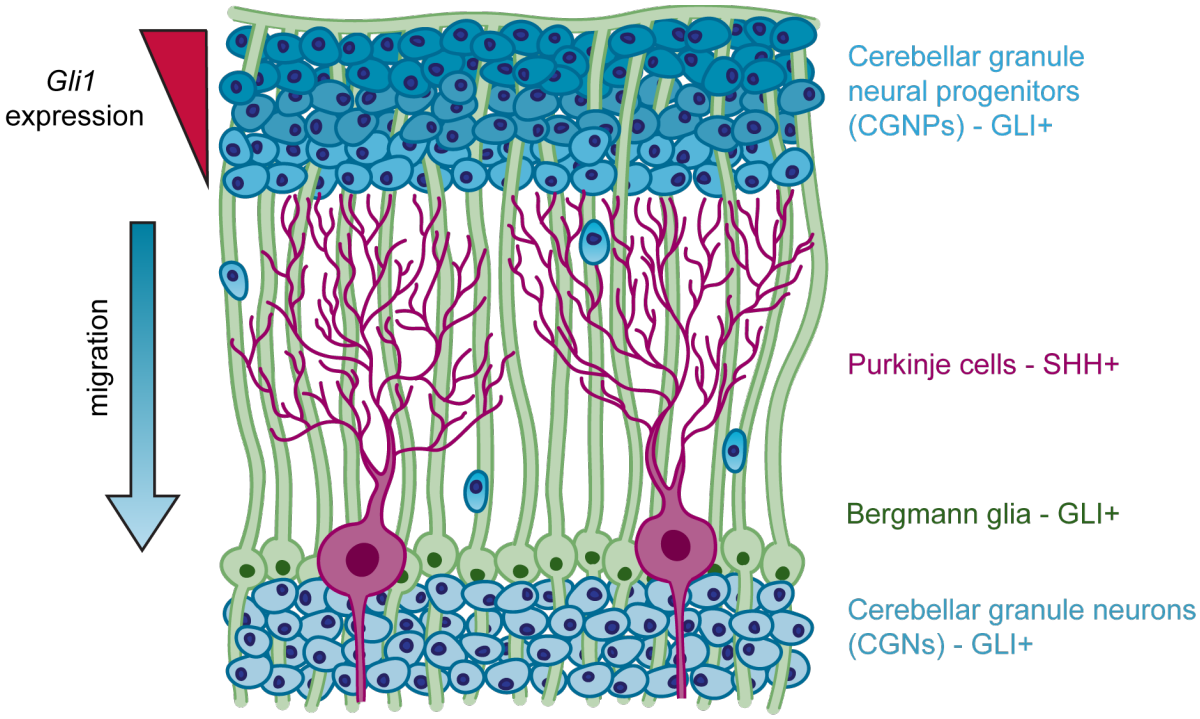

Figure 1.5 Schematic demonstrating postnatal cerebellar development.

Purkinje cells (magenta) express Shh, which drives HH target genes like *Gli1* and proliferation of CGNPs (dark blue). As development progresses, CGNPs exit the cell cycle and use the fibers of the Bergmann glia (green) to migrate to the inner granule layer where they differentiate and become mature neurons (light blue).

1.9 References

Aberger, F., and Ruiz i Altaba, A. (2014). Context-dependent signal integration by the GLI code: the oncogenic load, pathways, modifiers and implications for cancer therapy. Semin Cell Dev Biol *33*, 93-104. 10.1016/j.semcdb.2014.05.003.

Aizawa, H., Sekine, Y., Takemura, R., Zhang, Z., Nangaku, M., and Hirokawa, N. (1992). Kinesin family in murine central nervous system. J Cell Biol *119*, 1287-1296. 10.1083/jcb.119.5.1287.

Alder, J., Lee, K.J., Jessell, T.M., and Hatten, M.E. (1999). Generation of cerebellar granule neurons in vivo by transplantation of BMP-treated neural progenitor cells. Nat Neurosci *2*, 535-540. 10.1038/9189.

Alexandre, C., Jacinto, A., and Ingham, P.W. (1996). Transcriptional activation of hedgehog target genes in Drosophila is mediated directly by the cubitus interruptus protein, a member of the GLI family of zinc finger DNA-binding proteins. Genes Dev *10*, 2003-2013. 10.1101/gad.10.16.2003.

Allen, B.L., Song, J.Y., Izzi, L., Althaus, I.W., Kang, J.S., Charron, F., Krauss, R.S., and McMahon, A.P. (2011). Overlapping roles and collective requirement for the coreceptors GAS1, CDO, and BOC in SHH pathway function. Dev Cell *20*, 775-787. 10.1016/j.devcel.2011.04.018.

Allen, B.L., Tenzen, T., and McMahon, A.P. (2007). The Hedgehog-binding proteins Gas1 and Cdo cooperate to positively regulate Shh signaling during mouse development. Genes Dev *21*, 1244-1257. 10.1101/gad.1543607.

Allen, R.D., Metuzals, J., Tasaki, I., Brady, S.T., and Gilbert, S.P. (1982). Fast axonal transport in squid giant axon. Science *218*, 1127-1129. 10.1126/science.6183744.

Amanai, K., and Jiang, J. (2001). Distinct roles of Central missing and Dispatched in sending the Hedgehog signal. Development *128*, 5119-5127. 10.1242/dev.128.24.5119.

Anne, S.L., Govek, E.E., Ayrault, O., Kim, J.H., Zhu, X., Murphy, D.A., Van Aelst, L., Roussel, M.F., and Hatten, M.E. (2013). WNT3 inhibits cerebellar granule neuron progenitor proliferation and medulloblastoma formation via MAPK activation. PLoS One *8*, e81769. 10.1371/journal.pone.0081769.

Anthony, T.E., and Heintz, N. (2008). Genetic lineage tracing defines distinct neurogenic and gliogenic stages of ventral telencephalic radial glial development. Neural Dev *3*, 30. 10.1186/1749-8104-3-30.

Awan, A., Bernstein, M., Hamasaki, T., and Satir, P. (2004). Cloning and characterization of Kin5, a novel Tetrahymena ciliary kinesin II. Cell Motil Cytoskeleton *58*, 1-9. 10.1002/cm.10170.

Aza-Blanc, P., Ramirez-Weber, F.A., Laget, M.P., Schwartz, C., and Kornberg, T.B. (1997). Proteolysis that is inhibited by hedgehog targets Cubitus interruptus protein to the nucleus and converts it to a repressor. Cell *89*, 1043-1053. 10.1016/s0092-8674(00)80292-5.

Bai, C.B., Auerbach, W., Lee, J.S., Stephen, D., and Joyner, A.L. (2002). Gli2, but not Gli1, is required for initial Shh signaling and ectopic activation of the Shh pathway. Development *129*, 4753-4761. 10.1242/dev.129.20.4753.

Bai, C.B., and Joyner, A.L. (2001). Gli1 can rescue the in vivo function of Gli2. Development *128*, 5161-5172. 10.1242/dev.128.24.5161.

Bai, C.B., Stephen, D., and Joyner, A.L. (2004). All mouse ventral spinal cord patterning by hedgehog is Gli dependent and involves an activator function of Gli3. Dev Cell *6*, 103-115. 10.1016/s1534-5807(03)00394-0.

Bangs, F., and Anderson, K.V. (2017). Primary Cilia and Mammalian Hedgehog Signaling. Cold Spring Harb Perspect Biol *9*. 10.1101/cshperspect.a028175.

Bitgood, M.J., and McMahon, A.P. (1995). Hedgehog and Bmp genes are coexpressed at many diverse sites of cell-cell interaction in the mouse embryo. Dev Biol *172*, 126-138. 10.1006/dbio.1995.0010.

Bitgood, M.J., Shen, L., and McMahon, A.P. (1996). Sertoli cell signaling by Desert hedgehog regulates the male germline. Curr Biol *6*, 298-304. 10.1016/s0960-9822(02)00480-3.

Blaess, S., Corrales, J.D., and Joyner, A.L. (2006). Sonic hedgehog regulates Gli activator and repressor functions with spatial and temporal precision in the mid/hindbrain region. Development *133*, 1799-1809. 10.1242/dev.02339.

Blaess, S., Stephen, D., and Joyner, A.L. (2008). Gli3 coordinates three-dimensional patterning and growth of the tectum and cerebellum by integrating Shh and Fgf8 signaling. Development *135*, 2093-2103. 10.1242/dev.015990.

Blasius, T.L., Cai, D., Jih, G.T., Toret, C.P., and Verhey, K.J. (2007). Two binding partners cooperate to activate the molecular motor Kinesin-1. J Cell Biol *176*, 11-17. 10.1083/jcb.200605099.

Brady, S.T., Lasek, R.J., and Allen, R.D. (1982). Fast axonal transport in extruded axoplasm from squid giant axon. Science *218*, 1129-1131. 10.1126/science.6183745.

Brown, C.L., Maier, K.C., Stauber, T., Ginkel, L.M., Wordeman, L., Vernos, I., and Schroer, T.A. (2005). Kinesin-2 is a motor for late endosomes and lysosomes. Traffic *6*, 1114-1124. 10.1111/j.1600-0854.2005.00347.x.

Burke, R., Nellen, D., Bellotto, M., Hafen, E., Senti, K.A., Dickson, B.J., and Basler, K. (1999). Dispatched, a novel sterol-sensing domain protein dedicated to the release of cholesterol-modified hedgehog from signaling cells. Cell *99*, 803-815. 10.1016/s0092-8674(00)81677-3.

Buttitta, L., Mo, R., Hui, C.C., and Fan, C.M. (2003). Interplays of Gli2 and Gli3 and their requirement in mediating Shh-dependent sclerotome induction. Development *130*, 6233-6243. 10.1242/dev.00851.

Butts, T., Green, M.J., and Wingate, R.J. (2014). Development of the cerebellum: simple steps to make a 'little brain'. Development *141*, 4031-4041. 10.1242/dev.106559.

Carpenter, B.S., Barry, R.L., Verhey, K.J., and Allen, B.L. (2015). The heterotrimeric kinesin-2 complex interacts with and regulates GLI protein function. J Cell Sci *128*, 1034-1050. 10.1242/jcs.162552.

Caspary, T., Garcia-Garcia, M.J., Huangfu, D., Eggenschwiler, J.T., Wyler, M.R., Rakeman, A.S., Alcorn, H.L., and Anderson, K.V. (2002). Mouse Dispatched homolog1 is required for long-range, but not juxtacrine, Hh signaling. Curr Biol *12*, 1628-1632. 10.1016/s0960-9822(02)01147-8.

Chamoun, Z., Mann, R.K., Nellen, D., von Kessler, D.P., Bellotto, M., Beachy, P.A., and Basler, K. (2001). Skinny hedgehog, an acyltransferase required for palmitoylation and activity of the hedgehog signal. Science *293*, 2080-2084. 10.1126/science.1064437.

Chen, M.H., Li, Y.J., Kawakami, T., Xu, S.M., and Chuang, P.T. (2004). Palmitoylation is required for the production of a soluble multimeric Hedgehog protein complex and long-range signaling in vertebrates. Genes Dev *18*, 641-659. 10.1101/gad.1185804.

Chen, M.H., Wilson, C.W., Li, Y.J., Law, K.K., Lu, C.S., Gacayan, R., Zhang, X., Hui, C.C., and Chuang, P.T. (2009). Cilium-independent regulation of Gli protein function by Sufu in Hedgehog signaling is evolutionarily conserved. Genes Dev *23*, 1910-1928. 10.1101/gad.1794109.

Chen, X., Tukachinsky, H., Huang, C.H., Jao, C., Chu, Y.R., Tang, H.Y., Mueller, B., Schulman, S., Rapoport, T.A., and Salic, A. (2011). Processing and turnover of the Hedgehog protein in the endoplasmic reticulum. J Cell Biol *192*, 825-838. 10.1083/jcb.201008090.

Chen, Y., Cardinaux, J.R., Goodman, R.H., and Smolik, S.M. (1999). Mutants of cubitus interruptus that are independent of PKA regulation are independent of hedgehog signaling. Development *126*, 3607-3616. 10.1242/dev.126.16.3607.

Chen, Y., and Struhl, G. (1996). Dual roles for patched in sequestering and transducing Hedgehog. Cell *87*, 553-563. 10.1016/s0092-8674(00)81374-4.

Cheng, F.Y., Fleming, J.T., and Chiang, C. (2018). Bergmann glial Sonic hedgehog signaling activity is required for proper cerebellar cortical expansion and architecture. Dev Biol *440*, 152-166. 10.1016/j.ydbio.2018.05.015.

Chennathukuzhi, V., Morales, C.R., El-Alfy, M., and Hecht, N.B. (2003). The kinesin KIF17b and RNA-binding protein TB-RBP transport specific cAMP-responsive element modulator-regulated mRNAs in male germ cells. Proc Natl Acad Sci U S A *100*, 15566-15571. 10.1073/pnas.2536695100.

Chu, T., Chiu, M., Zhang, E., and Kunes, S. (2006). A C-terminal motif targets Hedgehog to axons, coordinating assembly of the Drosophila eye and brain. Dev Cell *10*, 635-646. 10.1016/j.devcel.2006.03.003.

Chung, U.I., Schipani, E., McMahon, A.P., and Kronenberg, H.M. (2001). Indian hedgehog couples chondrogenesis to osteogenesis in endochondral bone development. J Clin Invest *107*, 295-304. 10.1172/JCI11706.

Clark, A.M., Garland, K.K., and Russell, L.D. (2000). Desert hedgehog (Dhh) gene is required in the mouse testis for formation of adult-type Leydig cells and normal development of peritubular cells and seminiferous tubules. Biol Reprod *63*, 1825-1838. 10.1095/biolreprod63.6.1825.

Cobourne, M.T., Miletich, I., and Sharpe, P.T. (2004). Restriction of sonic hedgehog signalling during early tooth development. Development *131*, 2875-2885. 10.1242/dev.01163.

Cole, D.G., Chinn, S.W., Wedaman, K.P., Hall, K., Vuong, T., and Scholey, J.M. (1993). Novel heterotrimeric kinesin-related protein purified from sea urchin eggs. Nature *366*, 268-270. 10.1038/366268a0.

Corbit, K.C., Aanstad, P., Singla, V., Norman, A.R., Stainier, D.Y., and Reiter, J.F. (2005). Vertebrate Smoothened functions at the primary cilium. Nature *437*, 1018-1021. 10.1038/nature04117.

Corrales, J.D., Blaess, S., Mahoney, E.M., and Joyner, A.L. (2006). The level of sonic hedgehog signaling regulates the complexity of cerebellar foliation. Development *133*, 1811-1821. 10.1242/dev.02351.

Corrales, J.D., Rocco, G.L., Blaess, S., Guo, Q., and Joyner, A.L. (2004). Spatial pattern of sonic hedgehog signaling through Gli genes during cerebellum development. Development *131*, 5581-5590. 10.1242/dev.01438.

Creanga, A., Glenn, T.D., Mann, R.K., Saunders, A.M., Talbot, W.S., and Beachy, P.A. (2012). Scube/You activity mediates release of dually lipid-modified Hedgehog signal in soluble form. Genes Dev *26*, 1312-1325. 10.1101/gad.191866.112.

Dahmane, N., and Ruiz i Altaba, A. (1999). Sonic hedgehog regulates the growth and patterning of the cerebellum. Development *126*, 3089-3100. 10.1242/dev.126.14.3089.

Dai, P., Akimaru, H., Tanaka, Y., Maekawa, T., Nakafuku, M., and Ishii, S. (1999). Sonic Hedgehog-induced activation of the Gli1 promoter is mediated by GLI3. J Biol Chem *274*, 8143-8152. 10.1074/jbc.274.12.8143.

Daniele, J.R., Chu, T., and Kunes, S. (2017). A novel proteolytic event controls Hedgehog intracellular sorting and distribution to receptive fields. Biol Open *6*, 540-550. 10.1242/bio.024083.

Dimassi, S., Labalme, A., Ville, D., Calender, A., Mignot, C., Boutry-Kryza, N., de Bellescize, J., Rivier-Ringenbach, C., Bourel-Ponchel, E., Cheillan, D., et al. (2016). Whole-exome sequencing improves the diagnosis yield in sporadic infantile spasm syndrome. Clin Genet *89*, 198-204. 10.1111/cge.12636.

Ding, Q., Motoyama, J., Gasca, S., Mo, R., Sasaki, H., Rossant, J., and Hui, C.C. (1998). Diminished Sonic hedgehog signaling and lack of floor plate differentiation in Gli2 mutant mice. Development *125*, 2533-2543. 10.1242/dev.125.14.2533.

Dishinger, J.F., Kee, H.L., Jenkins, P.M., Fan, S., Hurd, T.W., Hammond, J.W., Truong, Y.N., Margolis, B., Martens, J.R., and Verhey, K.J. (2010). Ciliary entry of the kinesin-2 motor KIF17 is regulated by importin-beta2 and RanGTP. Nat Cell Biol *12*, 703-710. 10.1038/ncb2073.

Dominguez, M., Brunner, M., Hafen, E., and Basler, K. (1996). Sending and receiving the hedgehog signal: control by the Drosophila Gli protein Cubitus interruptus. Science *272*, 1621-1625. 10.1126/science.272.5268.1621.

Dunaeva, M., Michelson, P., Kogerman, P., and Toftgard, R. (2003). Characterization of the physical interaction of Gli proteins with SUFU proteins. J Biol Chem *278*, 5116-5122. 10.1074/jbc.M209492200.

Echelard, Y., Epstein, D.J., St-Jacques, B., Shen, L., Mohler, J., McMahon, J.A., and McMahon, A.P. (1993). Sonic hedgehog, a member of a family of putative signaling molecules, is implicated in the regulation of CNS polarity. Cell *75*, 1417-1430. 10.1016/0092-8674(93)90627-3.

Eggenschwiler, J.T., Bulgakov, O.V., Qin, J., Li, T., and Anderson, K.V. (2006). Mouse Rab23 regulates hedgehog signaling from smoothened to Gli proteins. Dev Biol *290*, 1-12. 10.1016/j.ydbio.2005.09.022.

Eggenschwiler, J.T., Espinoza, E., and Anderson, K.V. (2001). Rab23 is an essential negative regulator of the mouse Sonic hedgehog signalling pathway. Nature *412*, 194-198. 10.1038/35084089.

Elliott, K.H., Chen, X., Salomone, J., Chaturvedi, P., Schultz, P.A., Balchand, S.K., Servetas, J.D., Zuniga, A., Zeller, R., Gebelein, B., et al. (2020). Gli3 utilizes Hand2 to synergistically regulate tissue-specific transcriptional networks. Elife *9*. 10.7554/eLife.56450.

Engelke, M.F., Waas, B., Kearns, S.E., Suber, A., Boss, A., Allen, B.L., and Verhey, K.J. (2019). Acute Inhibition of Heterotrimeric Kinesin-2 Function Reveals Mechanisms of Intraflagellar Transport in Mammalian Cilia. Curr Biol *29*, 1137-1148 e1134. 10.1016/j.cub.2019.02.043.

Epstein, D.J., Marti, E., Scott, M.P., and McMahon, A.P. (1996). Antagonizing cAMP-dependent protein kinase A in the dorsal CNS activates a conserved Sonic hedgehog signaling pathway. Development *122*, 2885-2894. 10.1242/dev.122.9.2885.

Evans, J.E., Snow, J.J., Gunnarson, A.L., Ou, G., Stahlberg, H., McDonald, K.L., and Scholey, J.M. (2006). Functional modulation of IFT kinesins extends the sensory repertoire of ciliated neurons in Caenorhabditis elegans. J Cell Biol *172*, 663-669. 10.1083/jcb.200509115.

Falkenstein, K.N., and Vokes, S.A. (2014). Transcriptional regulation of graded Hedgehog signaling. Semin Cell Dev Biol *33*, 73-80. 10.1016/j.semcdb.2014.05.010.

Feng, J., White, B., Tyurina, O.V., Guner, B., Larson, T., Lee, H.Y., Karlstrom, R.O., and Kohtz, J.D. (2004). Synergistic and antagonistic roles of the Sonic hedgehog N- and C-terminal lipids. Development *131*, 4357-4370. 10.1242/dev.01301.

Gao, Y., Zheng, H., Li, L., Zhou, C., Chen, X., Zhou, X., and Cao, Y. (2020). KIF3C Promotes Proliferation, Migration, and Invasion of Glioma Cells by Activating the PI3K/AKT Pathway and Inducing EMT. Biomed Res Int *2020*, 6349312. 10.1155/2020/6349312.

Goetz, S.C., and Anderson, K.V. (2010). The primary cilium: a signalling centre during vertebrate development. Nat Rev Genet *11*, 331-344. 10.1038/nrg2774.

Goffinet, A.M. (1983). The embryonic development of the cerebellum in normal and reeler mutant mice. Anat Embryol (Berl) *168*, 73-86. 10.1007/BF00305400.

Goldstein, O., Gana-Weisz, M., Shiner, T., Attar, R., Mordechai, Y., Waldman, Y.Y., Bar-Shira, A., Thaler, A., Gurevich, T., Mirelman, A., et al. (2021). R869C mutation in molecular motor KIF17 gene is involved in dementia with Lewy bodies. Alzheimers Dement (Amst) *13*, e12143. 10.1002/dad2.12143.

Goodrich, L.V., Milenkovic, L., Higgins, K.M., and Scott, M.P. (1997). Altered neural cell fates and medulloblastoma in mouse patched mutants. Science *277*, 1109-1113. 10.1126/science.277.5329.1109.

Gorivodsky, M., Mukhopadhyay, M., Wilsch-Braeuninger, M., Phillips, M., Teufel, A., Kim, C., Malik, N., Huttner, W., and Westphal, H. (2009). Intraflagellar transport protein 172 is essential for primary cilia formation and plays a vital role in patterning the mammalian brain. Dev Biol *325*, 24-32. 10.1016/j.ydbio.2008.09.019.

Grimmond, S., Larder, R., Van Hateren, N., Siggers, P., Hulsebos, T.J., Arkell, R., and Greenfield, A. (2000). Cloning, mapping, and expression analysis of a gene encoding a novel mammalian EGF-related protein (SCUBE1). Genomics *70*, 74-81. 10.1006/geno.2000.6370.

Grimmond, S., Larder, R., Van Hateren, N., Siggers, P., Morse, S., Hacker, T., Arkell, R., and Greenfield, A. (2001). Expression of a novel mammalian epidermal growth factor-related gene during mouse neural development. Mech Dev *102*, 209-211. 10.1016/s0925-4773(00)00586-4.

Guillaud, L., Setou, M., and Hirokawa, N. (2003). KIF17 dynamics and regulation of NR2B trafficking in hippocampal neurons. J Neurosci *23*, 131-140. 10.1523/JNEUROSCI.23-01-00131.2003.

Guillaud, L., Wong, R., and Hirokawa, N. (2008). Disruption of KIF17-Mint1 interaction by CaMKII-dependent phosphorylation: a molecular model of kinesin-cargo release. Nat Cell Biol *10*, 19-29. 10.1038/ncb1665.

Gumy, L.F., Chew, D.J., Tortosa, E., Katrukha, E.A., Kapitein, L.C., Tolkovsky, A.M., Hoogenraad, C.C., and Fawcett, J.W. (2013). The kinesin-2 family member KIF3C regulates microtubule dynamics and is required for axon growth and regeneration. J Neurosci *33*, 11329-11345. 10.1523/JNEUROSCI.5221-12.2013.

Guo, A., Wang, T., Ng, E.L., Aulia, S., Chong, K.H., Teng, F.Y., Wang, Y., and Tang, B.L. (2006). Open brain gene product Rab23: expression pattern in the adult mouse brain and functional characterization. J Neurosci Res *83*, 1118-1127. 10.1002/jnr.20788.

Guzik-Lendrum, S., Rayment, I., and Gilbert, S.P. (2017). Homodimeric Kinesin-2 KIF3CC Promotes Microtubule Dynamics. Biophys J *113*, 1845-1857. 10.1016/j.bpj.2017.09.015.

Hammerschmidt, M., Bitgood, M.J., and McMahon, A.P. (1996). Protein kinase A is a common negative regulator of Hedgehog signaling in the vertebrate embryo. Genes Dev *10*, 647-658. 10.1101/gad.10.6.647.

Hammond, J.W., Blasius, T.L., Soppina, V., Cai, D., and Verhey, K.J. (2010). Autoinhibition of the kinesin-2 motor KIF17 via dual intramolecular mechanisms. J Cell Biol *189*, 1013-1025. 10.1083/jcb.201001057.

Han, Y., Xiong, Y., Shi, X., Wu, J., Zhao, Y., and Jiang, J. (2017). Regulation of Gli ciliary localization and Hedgehog signaling by the PY-NLS/karyopherin-beta2 nuclear import system. PLoS Biol *15*, e2002063. 10.1371/journal.pbio.2002063.

Haycraft, C.J., Banizs, B., Aydin-Son, Y., Zhang, Q., Michaud, E.J., and Yoder, B.K. (2005). Gli2 and Gli3 localize to cilia and require the intraflagellar transport protein polaris for processing and function. PLoS Genet *1*, e53. 10.1371/journal.pgen.0010053.

Hirokawa, N., Noda, Y., Tanaka, Y., and Niwa, S. (2009). Kinesin superfamily motor proteins and intracellular transport. Nat Rev Mol Cell Biol *10*, 682-696. 10.1038/nrm2774.

Hollway, G.E., Maule, J., Gautier, P., Evans, T.M., Keenan, D.G., Lohs, C., Fischer, D., Wicking, C., and Currie, P.D. (2006). Scube2 mediates Hedgehog signalling in the zebrafish embryo. Dev Biol *294*, 104-118. 10.1016/j.ydbio.2006.02.032.

Hooper, J.E., and Scott, M.P. (1989). The Drosophila patched gene encodes a putative membrane protein required for segmental patterning. Cell *59*, 751-765. 10.1016/0092-8674(89)90021-4.

Hor, C.H.H., Lo, J.C.W., Cham, A.L.S., Leong, W.Y., and Goh, E.L.K. (2021). Multifaceted Functions of Rab23 on Primary Cilium-Mediated and Hedgehog Signaling-Mediated Cerebellar Granule Cell Proliferation. J Neurosci *41*, 6850-6863. 10.1523/JNEUROSCI.3005-20.2021.

Huangfu, D., and Anderson, K.V. (2005). Cilia and Hedgehog responsiveness in the mouse. Proc Natl Acad Sci U S A *102*, 11325-11330. 10.1073/pnas.0505328102.

Huangfu, D., and Anderson, K.V. (2006). Signaling from Smo to Ci/Gli: conservation and divergence of Hedgehog pathways from Drosophila to vertebrates. Development *133*, 3-14. 10.1242/dev.02169.

Huangfu, D., Liu, A., Rakeman, A.S., Murcia, N.S., Niswander, L., and Anderson, K.V. (2003). Hedgehog signalling in the mouse requires intraflagellar transport proteins. Nature *426*, 83-87. 10.1038/nature02061.

Hui, C.C., and Angers, S. (2011). Gli proteins in development and disease. Annu Rev Cell Dev Biol *27*, 513-537. 10.1146/annurev-cellbio-092910-154048.

Humke, E.W., Dorn, K.V., Milenkovic, L., Scott, M.P., and Rohatgi, R. (2010). The output of Hedgehog signaling is controlled by the dynamic association between Suppressor of Fused and the Gli proteins. Genes Dev *24*, 670-682. 10.1101/gad.1902910.

Ingham, P.W., Nakano, Y., and Seger, C. (2011). Mechanisms and functions of Hedgehog signalling across the metazoa. Nat Rev Genet *12*, 393-406. 10.1038/nrg2984.

Insinna, C., Pathak, N., Perkins, B., Drummond, I., and Besharse, J.C. (2008). The homodimeric kinesin, Kif17, is essential for vertebrate photoreceptor sensory outer segment development. Dev Biol *316*, 160-170. 10.1016/j.ydbio.2008.01.025.

Irla, M., Saade, M., Fernandez, C., Chasson, L., Victorero, G., Dahmane, N., Chazal, G., and Nguyen, C. (2007). Neuronal distribution of spatial in the developing cerebellum and hippocampus and its somatodendritic association with the kinesin motor KIF17. Exp Cell Res *313*, 4107-4119. 10.1016/j.yexcr.2007.09.006.

Izzi, L., Levesque, M., Morin, S., Laniel, D., Wilkes, B.C., Mille, F., Krauss, R.S., McMahon, A.P., Allen, B.L., and Charron, F. (2011). Boc and Gas1 each form distinct Shh receptor complexes with Ptch1 and are required for Shh-mediated cell proliferation. Dev Cell *20*, 788-801. 10.1016/j.devcel.2011.04.017.

Jia, J., Amanai, K., Wang, G., Tang, J., Wang, B., and Jiang, J. (2002). Shaggy/GSK3 antagonizes Hedgehog signalling by regulating Cubitus interruptus. Nature *416*, 548-552. 10.1038/nature733.

Jia, J., Zhang, L., Zhang, Q., Tong, C., Wang, B., Hou, F., Amanai, K., and Jiang, J. (2005). Phosphorylation by double-time/CKIepsilon and CKIalpha targets cubitus interruptus for Slimb/beta-TRCP-mediated proteolytic processing. Dev Cell *9*, 819-830. 10.1016/j.devcel.2005.10.006.

Jiang, J., and Struhl, G. (1998). Regulation of the Hedgehog and Wingless signalling pathways by the F-box/WD40-repeat protein Slimb. Nature *391*, 493-496. 10.1038/35154.

Jiang, L., Tam, B.M., Ying, G., Wu, S., Hauswirth, W.W., Frederick, J.M., Moritz, O.L., and Baehr, W. (2015). Kinesin family 17 (osmotic avoidance abnormal-3) is dispensable for photoreceptor morphology and function. FASEB J *29*, 4866-4880. 10.1096/fj.15-275677.

Jimeno, D., Lillo, C., Roberts, E.A., Goldstein, L.S., and Williams, D.S. (2006). Kinesin-2 and photoreceptor cell death: requirement of motor subunits. Exp Eye Res *82*, 351-353. 10.1016/j.exer.2005.10.026.

Jiwani, T., Kim, J.J., and Rosenblum, N.D. (2020). Suppressor of fused controls cerebellum granule cell proliferation by suppressing Fgf8 and spatially regulating Gli proteins. Development *147*. 10.1242/dev.170274.

Johnson, J.L., Hall, T.E., Dyson, J.M., Sonntag, C., Ayers, K., Berger, S., Gautier, P., Mitchell, C., Hollway, G.E., and Currie, P.D. (2012). Scube activity is necessary for Hedgehog signal transduction in vivo. Dev Biol *368*, 193-202. 10.1016/j.ydbio.2012.05.007.

Kaesler, S., Luscher, B., and Ruther, U. (2000). Transcriptional activity of GLI1 is negatively regulated by protein kinase A. Biol Chem *381*, 545-551. 10.1515/BC.2000.070.

Kawakami, A., Nojima, Y., Toyoda, A., Takahoko, M., Satoh, M., Tanaka, H., Wada, H., Masai, I., Terasaki, H., Sakaki, Y., et al. (2005). The zebrafish-secreted matrix protein you/scube2 is implicated in long-range regulation of hedgehog signaling. Curr Biol *15*, 480-488. 10.1016/j.cub.2005.02.018.

Kawakami, T., Kawcak, T., Li, Y.J., Zhang, W., Hu, Y., and Chuang, P.T. (2002). Mouse dispatched mutants fail to distribute hedgehog proteins and are defective in hedgehog signaling. Development *129*, 5753-5765. 10.1242/dev.00178.

Keady, B.T., Samtani, R., Tobita, K., Tsuchya, M., San Agustin, J.T., Follit, J.A., Jonassen, J.A., Subramanian, R., Lo, C.W., and Pazour, G.J. (2012). IFT25 links the signal-dependent movement of Hedgehog components to intraflagellar transport. Dev Cell *22*, 940-951. 10.1016/j.devcel.2012.04.009.

Kerjan, G., Dolan, J., Haumaitre, C., Schneider-Maunoury, S., Fujisawa, H., Mitchell, K.J., and Chedotal, A. (2005). The transmembrane semaphorin Sema6A controls cerebellar granule cell migration. Nat Neurosci *8*, 1516-1524. 10.1038/nn1555.

Kim, J., Kato, M., and Beachy, P.A. (2009). Gli2 trafficking links Hedgehog-dependent activation of Smoothened in the primary cilium to transcriptional activation in the nucleus. Proc Natl Acad Sci U S A *106*, 21666-21671. 10.1073/pnas.0912180106.

Kohtz, J.D., Lee, H.Y., Gaiano, N., Segal, J., Ng, E., Larson, T., Baker, D.P., Garber, E.A., Williams, K.P., and Fishell, G. (2001). N-terminal fatty-acylation of sonic hedgehog enhances the induction of rodent ventral forebrain neurons. Development *128*, 2351-2363. 10.1242/dev.128.12.2351.

Kondo, S., Sato-Yoshitake, R., Noda, Y., Aizawa, H., Nakata, T., Matsuura, Y., and Hirokawa, N. (1994). KIF3A is a new microtubule-based anterograde motor in the nerve axon. J Cell Biol *125*, 1095-1107. 10.1083/jcb.125.5.1095.

Kotaja, N., Lin, H., Parvinen, M., and Sassone-Corsi, P. (2006). Interplay of PIWI/Argonaute protein MIWI and kinesin KIF17b in chromatoid bodies of male germ cells. J Cell Sci *119*, 2819-2825. 10.1242/jcs.03022.

Krauss, S., Concordet, J.P., and Ingham, P.W. (1993). A functionally conserved homolog of the Drosophila segment polarity gene hh is expressed in tissues with polarizing activity in zebrafish embryos. Cell *75*, 1431-1444. 10.1016/0092-8674(93)90628-4.

Lee, C.S., Buttitta, L., and Fan, C.M. (2001a). Evidence that the WNT-inducible growth arrest-specific gene 1 encodes an antagonist of sonic hedgehog signaling in the somite. Proc Natl Acad Sci U S A *98*, 11347-11352. 10.1073/pnas.201418298.

Lee, J.D., Kraus, P., Gaiano, N., Nery, S., Kohtz, J., Fishell, G., Loomis, C.A., and Treisman, J.E. (2001b). An acylatable residue of Hedgehog is differentially required in Drosophila and mouse limb development. Dev Biol *233*, 122-136. 10.1006/dbio.2001.0218.

Lee, J.J., Ekker, S.C., von Kessler, D.P., Porter, J.A., Sun, B.I., and Beachy, P.A. (1994). Autoproteolysis in hedgehog protein biogenesis. Science *266*, 1528-1537. 10.1126/science.7985023.

Lee, J.J., von Kessler, D.P., Parks, S., and Beachy, P.A. (1992). Secretion and localized transcription suggest a role in positional signaling for products of the segmentation gene hedgehog. Cell *71*, 33-50. 10.1016/0092-8674(92)90264-d.

Leto, K., Arancillo, M., Becker, E.B., Buffo, A., Chiang, C., Ding, B., Dobyns, W.B., Dusart, I., Haldipur, P., Hatten, M.E., et al. (2016). Consensus Paper: Cerebellar Development. Cerebellum *15*, 789-828. 10.1007/s12311-015-0724-2.

Lewis, P.M., Dunn, M.P., McMahon, J.A., Logan, M., Martin, J.F., St-Jacques, B., and McMahon, A.P. (2001). Cholesterol modification of sonic hedgehog is required for long-range signaling activity and effective modulation of signaling by Ptc1. Cell *105*, 599-612. 10.1016/s0092-8674(01)00369-5.

Lewis, P.M., Gritli-Linde, A., Smeyne, R., Kottmann, A., and McMahon, A.P. (2004). Sonic hedgehog signaling is required for expansion of granule neuron precursors and patterning of the mouse cerebellum. Dev Biol *270*, 393-410. 10.1016/j.ydbio.2004.03.007.

Lewis, T.R., Kundinger, S.R., Link, B.A., Insinna, C., and Besharse, J.C. (2018). Kif17 phosphorylation regulates photoreceptor outer segment turnover. BMC Cell Biol *19*, 25. 10.1186/s12860-018-0177-9.

Lewis, T.R., Kundinger, S.R., Pavlovich, A.L., Bostrom, J.R., Link, B.A., and Besharse, J.C. (2017). Cos2/Kif7 and Osm-3/Kif17 regulate onset of outer segment development in zebrafish photoreceptors through distinct mechanisms. Dev Biol *425*, 176-190. 10.1016/j.ydbio.2017.03.019.

Li, Y., Zhang, H., Litingtung, Y., and Chiang, C. (2006). Cholesterol modification restricts the spread of Shh gradient in the limb bud. Proc Natl Acad Sci U S A *103*, 6548-6553. 10.1073/pnas.0600124103.

Liao, W.J., Tsao, K.C., and Yang, R.B. (2016). Electrostatics and N-glycan-mediated membrane tethering of SCUBE1 is critical for promoting bone morphogenetic protein signalling. Biochem J *473*, 661-672. 10.1042/BJ20151041.

Lim, Y.S., and Tang, B.L. (2015). A role for Rab23 in the trafficking of Kif17 to the primary cilium. J Cell Sci *128*, 2996-3008. 10.1242/jcs.163964.

Lin, Y.C., Niceta, M., Muto, V., Vona, B., Pagnamenta, A.T., Maroofian, R., Beetz, C., van Duyvenvoorde, H., Dentici, M.L., Lauffer, P., et al. (2021). SCUBE3 loss-of-function causes a recognizable recessive developmental disorder due to defective bone morphogenetic protein signaling. Am J Hum Genet *108*, 115-133. 10.1016/j.ajhg.2020.11.015.

Lin, Y.C., Roffler, S.R., Yan, Y.T., and Yang, R.B. (2015). Disruption of Scube2 Impairs Endochondral Bone Formation. J Bone Miner Res *30*, 1255-1267. 10.1002/jbmr.2451.

Liu, A., Wang, B., and Niswander, L.A. (2005). Mouse intraflagellar transport proteins regulate both the activator and repressor functions of Gli transcription factors. Development *132*, 3103-3111. 10.1242/dev.01894.

Liu, H., Liu, R., Hao, M., Zhao, X., and Li, C. (2021). Kinesin family member 3C (KIF3C) is a novel non-small cell lung cancer (NSCLC) oncogene whose expression is modulated by microRNA-150-5p (miR-150-5p) and microRNA-186-3p (miR-186-3p). Bioengineered *12*, 3077-3088. 10.1080/21655979.2021.1942768.

Liu, J., Zeng, H., and Liu, A. (2015a). The loss of Hh responsiveness by a non-ciliary Gli2 variant. Development *142*, 1651-1660. 10.1242/dev.119669.

Liu, M., Liu, Y., Hou, B., Bu, D., Shi, L., Gu, X., and Ma, Z. (2015b). Kinesin superfamily protein 17 contributes to the development of bone cancer pain by participating in NR2B transport in the spinal cord of mice. Oncol Rep *33*, 1365-1371. 10.3892/or.2015.3706.

Liu, Y., Liang, Y., Hou, B., Liu, M., Yang, X., Liu, C., Zhang, J., Zhang, W., Ma, Z., and Gu, X. (2014). The inhibitor of calcium/calmodulin-dependent protein kinase II KN93 attenuates bone cancer pain via inhibition of KIF17/NR2B trafficking in mice. Pharmacol Biochem Behav *124*, 19-26. 10.1016/j.pbb.2014.05.003.

Liu, Y., Tian, X., Ke, P., Gu, J., Ma, Y., Guo, Y., Xu, X., Chen, Y., Yang, M., Wang, X., and Xiao, F. (2022). KIF17 Modulates Epileptic Seizures and Membrane Expression of the NMDA Receptor Subunit NR2B. Neurosci Bull *38*, 841-856. 10.1007/s12264-022-00888-9.

Lum, L., Yao, S., Mozer, B., Rovescalli, A., Von Kessler, D., Nirenberg, M., and Beachy, P.A. (2003). Identification of Hedgehog pathway components by RNAi in Drosophila cultured cells. Science *299*, 2039-2045. 10.1126/science.1081403.

Ma, H., Zhang, F., Zhong, Q., and Hou, J. (2021). METTL3-mediated m6A modification of KIF3C-mRNA promotes prostate cancer progression and is negatively regulated by miR-320d. Aging (Albany NY) *13*, 22332-22344. 10.18632/aging.203541.

Ma, Y., Erkner, A., Gong, R., Yao, S., Taipale, J., Basler, K., and Beachy, P.A. (2002). Hedgehog-mediated patterning of the mammalian embryo requires transporter-like function of dispatched. Cell *111*, 63-75. 10.1016/s0092-8674(02)00977-7.

Macho, B., Brancorsini, S., Fimia, G.M., Setou, M., Hirokawa, N., and Sassone-Corsi, P. (2002). CREM-dependent transcription in male germ cells controlled by a kinesin. Science *298*, 2388-2390. 10.1126/science.1077265.

Machold, R., and Fishell, G. (2005). Math1 is expressed in temporally discrete pools of cerebellar rhombic-lip neural progenitors. Neuron *48*, 17-24. 10.1016/j.neuron.2005.08.028.

Marigo, V., Davey, R.A., Zuo, Y., Cunningham, J.M., and Tabin, C.J. (1996). Biochemical evidence that patched is the Hedgehog receptor. Nature *384*, 176-179. 10.1038/384176a0.

Marigo, V., and Tabin, C.J. (1996). Regulation of patched by sonic hedgehog in the developing neural tube. Proc Natl Acad Sci U S A *93*, 9346-9351. 10.1073/pnas.93.18.9346.

Markantoni, M., Sarafidou, T., Kyrgiafini, M.A., Chatziparasidou, A., Christoforidis, N., Dafopoulos, K., and Mamuris, Z. (2021). Replicating a GWAS: two novel candidate markers for oligospermia in Greek population. Mol Biol Rep *48*, 4967-4972. 10.1007/s11033-021-06470-2.

Martinelli, D.C., and Fan, C.M. (2007). Gas1 extends the range of Hedgehog action by facilitating its signaling. Genes Dev *21*, 1231-1243. 10.1101/gad.1546307.

McDermott, A., Gustafsson, M., Elsam, T., Hui, C.C., Emerson, C.P., Jr., and Borycki, A.G. (2005). Gli2 and Gli3 have redundant and context-dependent function in skeletal muscle formation. Development *132*, 345-357. 10.1242/dev.01537.

Methot, N., and Basler, K. (1999). Hedgehog controls limb development by regulating the activities of distinct transcriptional activator and repressor forms of Cubitus interruptus. Cell *96*, 819-831. 10.1016/s0092-8674(00)80592-9.

Miale, I.L., and Sidman, R.L. (1961). An autoradiographic analysis of histogenesis in the mouse cerebellum. Exp Neurol *4*, 277-296. 10.1016/0014-4886(61)90055-3.

Micchelli, C.A., The, I., Selva, E., Mogila, V., and Perrimon, N. (2002). Rasp, a putative transmembrane acyltransferase, is required for Hedgehog signaling. Development *129*, 843-851. 10.1242/dev.129.4.843.

Mo, R., Freer, A.M., Zinyk, D.L., Crackower, M.A., Michaud, J., Heng, H.H., Chik, K.W., Shi, X.M., Tsui, L.C., Cheng, S.H., et al. (1997). Specific and redundant functions of Gli2 and Gli3 zinc finger genes in skeletal patterning and development. Development *124*, 113-123. 10.1242/dev.124.1.113.

Mohler, J., and Vani, K. (1992). Molecular organization and embryonic expression of the hedgehog gene involved in cell-cell communication in segmental patterning of Drosophila. Development *115*, 957-971. 10.1242/dev.115.4.957.

Mori, T., Tanaka, K., Buffo, A., Wurst, W., Kuhn, R., and Gotz, M. (2006). Inducible gene deletion in astroglia and radial glia--a valuable tool for functional and lineage analysis. Glia *54*, 21-34. 10.1002/glia.20350.

Morris, R.L., Hoffman, M.P., Obar, R.A., McCafferty, S.S., Gibbons, I.R., Leone, A.D., Cool, J., Allgood, E.L., Musante, A.M., Judkins, K.M., et al. (2006). Analysis of cytoskeletal and motility proteins in the sea urchin genome assembly. Dev Biol *300*, 219-237. 10.1016/j.ydbio.2006.08.052.

Motoyama, J., Liu, J., Mo, R., Ding, Q., Post, M., and Hui, C.C. (1998). Essential function of Gli2 and Gli3 in the formation of lung, trachea and oesophagus. Nat Genet *20*, 54-57. 10.1038/1711.

Muresan, V., Abramson, T., Lyass, A., Winter, D., Porro, E., Hong, F., Chamberlin, N.L., and Schnapp, B.J. (1998). KIF3C and KIF3A form a novel neuronal heteromeric kinesin that associates with membrane vesicles. Mol Biol Cell *9*, 637-652. 10.1091/mbc.9.3.637.

Nagase, T., Kikuno, R., Ishikawa, K.I., Hirosawa, M., and Ohara, O. (2000). Prediction of the coding sequences of unidentified human genes. XVI. The complete sequences of 150 new cDNA clones from brain which code for large proteins in vitro. DNA Res *7*, 65-73. 10.1093/dnares/7.1.65.

Nakagawa, T., Tanaka, Y., Matsuoka, E., Kondo, S., Okada, Y., Noda, Y., Kanai, Y., and Hirokawa, N. (1997). Identification and classification of 16 new kinesin superfamily (KIF) proteins in mouse genome. Proc Natl Acad Sci U S A *94*, 9654-9659. 10.1073/pnas.94.18.9654.

Nakano, Y., Guerrero, I., Hidalgo, A., Taylor, A., Whittle, J.R., and Ingham, P.W. (1989). A protein with several possible membrane-spanning domains encoded by the Drosophila segment polarity gene patched. Nature *341*, 508-513. 10.1038/341508a0.

Nakano, Y., Kim, H.R., Kawakami, A., Roy, S., Schier, A.F., and Ingham, P.W. (2004). Inactivation of dispatched 1 by the chameleon mutation disrupts Hedgehog signalling in the zebrafish embryo. Dev Biol *269*, 381-392. 10.1016/j.ydbio.2004.01.022.

Niewiadomski, P., Kong, J.H., Ahrends, R., Ma, Y., Humke, E.W., Khan, S., Teruel, M.N., Novitch, B.G., and Rohatgi, R. (2014). Gli protein activity is controlled by multisite phosphorylation in vertebrate Hedgehog signaling. Cell Rep *6*, 168-181. 10.1016/j.celrep.2013.12.003.

Niewiadomski, P., Zhujiang, A., Youssef, M., and Waschek, J.A. (2013). Interaction of PACAP with Sonic hedgehog reveals complex regulation of the hedgehog pathway by PKA. Cell Signal *25*, 2222-2230. 10.1016/j.cellsig.2013.07.012.

Nonaka, S., Tanaka, Y., Okada, Y., Takeda, S., Harada, A., Kanai, Y., Kido, M., and Hirokawa, N. (1998). Randomization of left-right asymmetry due to loss of nodal cilia generating leftward flow of extraembryonic fluid in mice lacking KIF3B motor protein. Cell *95*, 829-837. 10.1016/s0092-8674(00)81705-5.

Nusslein-Volhard, C., and Wieschaus, E. (1980). Mutations affecting segment number and polarity in Drosophila. Nature *287*, 795-801. 10.1038/287795a0.

Ocbina, P.J., Eggenschwiler, J.T., Moskowitz, I., and Anderson, K.V. (2011). Complex interactions between genes controlling trafficking in primary cilia. Nat Genet *43*, 547-553. 10.1038/ng.832.

Pan, Y., Bai, C.B., Joyner, A.L., and Wang, B. (2006). Sonic hedgehog signaling regulates Gli2 transcriptional activity by suppressing its processing and degradation. Mol Cell Biol *26*, 3365-3377. 10.1128/MCB.26.9.3365-3377.2006.

Pan, Y., and Wang, B. (2007). A novel protein-processing domain in Gli2 and Gli3 differentially blocks complete protein degradation by the proteasome. J Biol Chem *282*, 10846-10852. 10.1074/jbc.M608599200.

Pan, Y., Wang, C., and Wang, B. (2009). Phosphorylation of Gli2 by protein kinase A is required for Gli2 processing and degradation and the Sonic Hedgehog-regulated mouse development. Dev Biol *326*, 177-189. 10.1016/j.ydbio.2008.11.009.

Park, H.L., Bai, C., Platt, K.A., Matise, M.P., Beeghly, A., Hui, C.C., Nakashima, M., and Joyner, A.L. (2000). Mouse Gli1 mutants are viable but have defects in SHH signaling in combination with a Gli2 mutation. Development *127*, 1593-1605. 10.1242/dev.127.8.1593.

Parmantier, E., Lynn, B., Lawson, D., Turmaine, M., Namini, S.S., Chakrabarti, L., McMahon, A.P., Jessen, K.R., and Mirsky, R. (1999). Schwann cell-derived Desert hedgehog controls the development of peripheral nerve sheaths. Neuron *23*, 713-724. 10.1016/s0896-6273(01)80030-1.

Pepinsky, R.B., Zeng, C., Wen, D., Rayhorn, P., Baker, D.P., Williams, K.P., Bixler, S.A., Ambrose, C.M., Garber, E.A., Miatkowski, K., et al. (1998). Identification of a palmitic acid-modified form of human Sonic hedgehog. J Biol Chem *273*, 14037-14045. 10.1074/jbc.273.22.14037.

Porter, J.A., Ekker, S.C., Park, W.J., von Kessler, D.P., Young, K.E., Chen, C.H., Ma, Y., Woods, A.S., Cotter, R.J., Koonin, E.V., and Beachy, P.A. (1996a). Hedgehog patterning activity: role of a lipophilic modification mediated by the carboxy-terminal autoprocessing domain. Cell *86*, 21-34. 10.1016/s0092-8674(00)80074-4.

Porter, J.A., von Kessler, D.P., Ekker, S.C., Young, K.E., Lee, J.J., Moses, K., and Beachy, P.A. (1995). The product of hedgehog autoproteolytic cleavage active in local and long-range signalling. Nature *374*, 363-366. 10.1038/374363a0.

Porter, J.A., Young, K.E., and Beachy, P.A. (1996b). Cholesterol modification of hedgehog signaling proteins in animal development. Science *274*, 255-259. 10.1126/science.274.5285.255.

Preat, T. (1992). Characterization of Suppressor of fused, a complete suppressor of the fused segment polarity gene of Drosophila melanogaster. Genetics *132*, 725-736. 10.1093/genetics/132.3.725.

Preat, T., Therond, P., Limbourg-Bouchon, B., Pham, A., Tricoire, H., Busson, D., and Lamour-Isnard, C. (1993). Segmental polarity in Drosophila melanogaster: genetic dissection of fused in a Suppressor of fused background reveals interaction with costal-2. Genetics *135*, 1047-1062. 10.1093/genetics/135.4.1047.

Price, M.A., and Kalderon, D. (2002). Proteolysis of the Hedgehog signaling effector Cubitus interruptus requires phosphorylation by Glycogen Synthase Kinase 3 and Casein Kinase 1. Cell *108*, 823-835. 10.1016/s0092-8674(02)00664-5.

Qin, J., Lin, Y., Norman, R.X., Ko, H.W., and Eggenschwiler, J.T. (2011). Intraflagellar transport protein 122 antagonizes Sonic Hedgehog signaling and controls ciliary localization of pathway components. Proc Natl Acad Sci U S A *108*, 1456-1461. 10.1073/pnas.1011410108.

Raffel, C., Jenkins, R.B., Frederick, L., Hebrink, D., Alderete, B., Fults, D.W., and James, C.D. (1997). Sporadic medulloblastomas contain PTCH mutations. Cancer Res *57*, 842-845.

Renaud, J., Kerjan, G., Sumita, I., Zagar, Y., Georget, V., Kim, D., Fouquet, C., Suda, K., Sanbo, M., Suto, F., et al. (2008). Plexin-A2 and its ligand, Sema6A, control nucleus-centrosome coupling in migrating granule cells. Nat Neurosci *11*, 440-449. 10.1038/nn2064.

Riddle, R.D., Johnson, R.L., Laufer, E., and Tabin, C. (1993). Sonic hedgehog mediates the polarizing activity of the ZPA. Cell *75*, 1401-1416. 10.1016/0092-8674(93)90626-2.

Riva, A., Gambadauro, A., Dipasquale, V., Casto, C., Ceravolo, M.D., Accogli, A., Scala, M., Ceravolo, G., Iacomino, M., Zara, F., et al. (2021). Biallelic Variants in KIF17 Associated with Microphthalmia and Coloboma Spectrum. Int J Mol Sci *22*. 10.3390/ijms22094471.

Roelink, H., Augsburger, A., Heemskerk, J., Korzh, V., Norlin, S., Ruiz i Altaba, A., Tanabe, Y., Placzek, M., Edlund, T., Jessell, T.M., and et al. (1994). Floor plate and motor neuron induction by vhh-1, a vertebrate homolog of hedgehog expressed by the notochord. Cell *76*, 761-775. 10.1016/0092-8674(94)90514-2.

Roelink, H., Porter, J.A., Chiang, C., Tanabe, Y., Chang, D.T., Beachy, P.A., and Jessell, T.M. (1995). Floor plate and motor neuron induction by different concentrations of the amino-terminal cleavage product of sonic hedgehog autoproteolysis. Cell *81*, 445-455. 10.1016/0092-8674(95)90397-6.

Rohatgi, R., Milenkovic, L., and Scott, M.P. (2007). Patched1 regulates hedgehog signaling at the primary cilium. Science *317*, 372-376. 10.1126/science.1139740.

Saade, M., Irla, M., Govin, J., Victorero, G., Samson, M., and Nguyen, C. (2007). Dynamic distribution of Spatial during mouse spermatogenesis and its interaction with the kinesin KIF17b. Exp Cell Res *313*, 614-626. 10.1016/j.yexcr.2006.11.011.

Santos, N., and Reiter, J.F. (2014). A central region of Gli2 regulates its localization to the primary cilium and transcriptional activity. J Cell Sci *127*, 1500-1510. 10.1242/jcs.139253.

Sasaki, H., Hui, C., Nakafuku, M., and Kondoh, H. (1997). A binding site for Gli proteins is essential for HNF-3beta floor plate enhancer activity in transgenics and can respond to Shh in vitro. Development *124*, 1313-1322. 10.1242/dev.124.7.1313.

Sasaki, H., Nishizaki, Y., Hui, C., Nakafuku, M., and Kondoh, H. (1999). Regulation of Gli2 and Gli3 activities by an amino-terminal repression domain: implication of Gli2 and Gli3 as primary mediators of Shh signaling. Development *126*, 3915-3924. 10.1242/dev.126.17.3915.

Scholey, J.M. (2013). Kinesin-2: a family of heterotrimeric and homodimeric motors with diverse intracellular transport functions. Annu Rev Cell Dev Biol *29*, 443-469. 10.1146/annurev-cellbio-101512-122335.

Setou, M., Nakagawa, T., Seog, D.H., and Hirokawa, N. (2000). Kinesin superfamily motor protein KIF17 and mLin-10 in NMDA receptor-containing vesicle transport. Science *288*, 1796-1802. 10.1126/science.288.5472.1796.

Signor, D., Wedaman, K.P., Rose, L.S., and Scholey, J.M. (1999). Two heteromeric kinesin complexes in chemosensory neurons and sensory cilia of Caenorhabditis elegans. Mol Biol Cell *10*, 345-360. 10.1091/mbc.10.2.345.

Smelkinson, M.G., and Kalderon, D. (2006). Processing of the Drosophila hedgehog signaling effector Ci-155 to the repressor Ci-75 is mediated by direct binding to the SCF component Slimb. Curr Biol *16*, 110-116. 10.1016/j.cub.2005.12.012.

Snow, J.J., Ou, G., Gunnarson, A.L., Walker, M.R., Zhou, H.M., Brust-Mascher, I., and Scholey, J.M. (2004). Two anterograde intraflagellar transport motors cooperate to build sensory cilia on C. elegans neurons. Nat Cell Biol *6*, 1109-1113. 10.1038/ncb1186.

Solecki, D.J., Liu, X.L., Tomoda, T., Fang, Y., and Hatten, M.E. (2001). Activated Notch2 signaling inhibits differentiation of cerebellar granule neuron precursors by maintaining proliferation. Neuron *31*, 557-568. 10.1016/s0896-6273(01)00395-6.

Spassky, N., Han, Y.G., Aguilar, A., Strehl, L., Besse, L., Laclef, C., Ros, M.R., Garcia-Verdugo, J.M., and Alvarez-Buylla, A. (2008). Primary cilia are required for cerebellar development and Shh-dependent expansion of progenitor pool. Dev Biol *317*, 246-259. 10.1016/j.ydbio.2008.02.026.

Stauber, T., Simpson, J.C., Pepperkok, R., and Vernos, I. (2006). A role for kinesin-2 in COPI-dependent recycling between the ER and the Golgi complex. Curr Biol *16*, 2245-2251. 10.1016/j.cub.2006.09.060.

Stewart, D.P., Marada, S., Bodeen, W.J., Truong, A., Sakurada, S.M., Pandit, T., Pruett-Miller, S.M., and Ogden, S.K. (2018). Cleavage activates dispatched for Sonic Hedgehog ligand release. Elife *7*. 10.7554/eLife.31678.

Stone, D.M., Hynes, M., Armanini, M., Swanson, T.A., Gu, Q., Johnson, R.L., Scott, M.P., Pennica, D., Goddard, A., Phillips, H., et al. (1996). The tumour-suppressor gene patched encodes a candidate receptor for Sonic hedgehog. Nature *384*, 129-134. 10.1038/384129a0.

Svard, J., Heby-Henricson, K., Persson-Lek, M., Rozell, B., Lauth, M., Bergstrom, A., Ericson, J., Toftgard, R., and Teglund, S. (2006). Genetic elimination of Suppressor of fused reveals an

essential repressor function in the mammalian Hedgehog signaling pathway. Dev Cell *10*, 187-197. 10.1016/j.devcel.2005.12.013.

Tabata, T., Eaton, S., and Kornberg, T.B. (1992). The Drosophila hedgehog gene is expressed specifically in posterior compartment cells and is a target of engrailed regulation. Genes Dev *6*, 2635-2645. 10.1101/gad.6.12b.2635.

Taipale, J., Cooper, M.K., Maiti, T., and Beachy, P.A. (2002). Patched acts catalytically to suppress the activity of Smoothened. Nature *418*, 892-897. 10.1038/nature00989.

Takeda, S., Yamazaki, H., Seog, D.H., Kanai, Y., Terada, S., and Hirokawa, N. (2000). Kinesin superfamily protein 3 (KIF3) motor transports fodrin-associating vesicles important for neurite building. J Cell Biol *148*, 1255-1265. 10.1083/jcb.148.6.1255.

Takeda, S., Yonekawa, Y., Tanaka, Y., Okada, Y., Nonaka, S., and Hirokawa, N. (1999). Left-right asymmetry and kinesin superfamily protein KIF3A: new insights in determination of laterality and mesoderm induction by kif3A-/- mice analysis. J Cell Biol *145*, 825-836. 10.1083/jcb.145.4.825.

Tarabeux, J., Champagne, N., Brustein, E., Hamdan, F.F., Gauthier, J., Lapointe, M., Maios, C., Piton, A., Spiegelman, D., Henrion, E., et al. (2010). De novo truncating mutation in Kinesin 17 associated with schizophrenia. Biol Psychiatry *68*, 649-656. 10.1016/j.biopsych.2010.04.018.

Taylor, A.M., Nakano, Y., Mohler, J., and Ingham, P.W. (1993). Contrasting distributions of patched and hedgehog proteins in the Drosophila embryo. Mech Dev *42*, 89-96. 10.1016/0925-4773(93)90101-3.

Tempe, D., Casas, M., Karaz, S., Blanchet-Tournier, M.F., and Concordet, J.P. (2006). Multisite protein kinase A and glycogen synthase kinase 3beta phosphorylation leads to Gli3 ubiquitination by SCFbetaTrCP. Mol Cell Biol *26*, 4316-4326. 10.1128/MCB.02183-05.

Tenzen, T., Allen, B.L., Cole, F., Kang, J.S., Krauss, R.S., and McMahon, A.P. (2006). The cell surface membrane proteins Cdo and Boc are components and targets of the Hedgehog signaling pathway and feedback network in mice. Dev Cell *10*, 647-656. 10.1016/j.devcel.2006.04.004.

Therond, P., Busson, D., Guillemet, E., Limbourg-Bouchon, B., Preat, T., Terracol, R., Tricoire, H., and Lamour-Isnard, C. (1993). Molecular organisation and expression pattern of the segment polarity gene fused of Drosophila melanogaster. Mech Dev *44*, 65-80. 10.1016/0925-4773(93)90017-r.

Tian, H., Jeong, J., Harfe, B.D., Tabin, C.J., and McMahon, A.P. (2005a). Mouse Disp1 is required in sonic hedgehog-expressing cells for paracrine activity of the cholesterol-modified ligand. Development *132*, 133-142. 10.1242/dev.01563.

Tian, L., Holmgren, R.A., and Matouschek, A. (2005b). A conserved processing mechanism regulates the activity of transcription factors Cubitus interruptus and NF-kappaB. Nat Struct Mol Biol *12*, 1045-1053. 10.1038/nsmb1018.

Tokhunts, R., Singh, S., Chu, T., D'Angelo, G., Baubet, V., Goetz, J.A., Huang, Z., Yuan, Z., Ascano, M., Zavros, Y., et al. (2010). The full-length unprocessed hedgehog protein is an active signaling molecule. J Biol Chem *285*, 2562-2568. 10.1074/jbc.M109.078626.

Traiffort, E., Charytoniuk, D.A., Faure, H., and Ruat, M. (1998). Regional distribution of Sonic Hedgehog, patched, and smoothened mRNA in the adult rat brain. J Neurochem *70*, 1327-1330. 10.1046/j.1471-4159.1998.70031327.x.

Tsai, M.T., Cheng, C.J., Lin, Y.C., Chen, C.C., Wu, A.R., Wu, M.T., Hsu, C.C., and Yang, R.B. (2009). Isolation and characterization of a secreted, cell-surface glycoprotein SCUBE2 from humans. Biochem J *422*, 119-128. 10.1042/BJ20090341.

Tukachinsky, H., Kuzmickas, R.P., Jao, C.Y., Liu, J., and Salic, A. (2012). Dispatched and scube mediate the efficient secretion of the cholesterol-modified hedgehog ligand. Cell Rep *2*, 308-320. 10.1016/j.celrep.2012.07.010.

Tukachinsky, H., Lopez, L.V., and Salic, A. (2010). A mechanism for vertebrate Hedgehog signaling: recruitment to cilia and dissociation of SuFu-Gli protein complexes. J Cell Biol *191*, 415-428. 10.1083/jcb.201004108.

Tuson, M., He, M., and Anderson, K.V. (2011). Protein kinase A acts at the basal body of the primary cilium to prevent Gli2 activation and ventralization of the mouse neural tube. Development *138*, 4921-4930. 10.1242/dev.070805.

Vale, R.D., Reese, T.S., and Sheetz, M.P. (1985). Identification of a novel force-generating protein, kinesin, involved in microtubule-based motility. Cell *42*, 39-50. 10.1016/s0092-8674(85)80099-4.

van Eeden, F.J., Granato, M., Schach, U., Brand, M., Furutani-Seiki, M., Haffter, P., Hammerschmidt, M., Heisenberg, C.P., Jiang, Y.J., Kane, D.A., et al. (1996). Mutations affecting somite formation and patterning in the zebrafish, Danio rerio. Development *123*, 153-164. 10.1242/dev.123.1.153.

Verhey, K.J., and Hammond, J.W. (2009). Traffic control: regulation of kinesin motors. Nat Rev Mol Cell Biol *10*, 765-777. 10.1038/nrm2782.

Vortkamp, A., Lee, K., Lanske, B., Segre, G.V., Kronenberg, H.M., and Tabin, C.J. (1996). Regulation of rate of cartilage differentiation by Indian hedgehog and PTH-related protein. Science *273*, 613-622. 10.1126/science.273.5275.613.

Wallace, V.A. (1999). Purkinje-cell-derived Sonic hedgehog regulates granule neuron precursor cell proliferation in the developing mouse cerebellum. Curr Biol *9*, 445-448. 10.1016/s0960-9822(99)80195-x.

Wang, B., Fallon, J.F., and Beachy, P.A. (2000). Hedgehog-regulated processing of Gli3 produces an anterior/posterior repressor gradient in the developing vertebrate limb. Cell *100*, 423-434. 10.1016/s0092-8674(00)80678-9.

Wang, B., and Li, Y. (2006). Evidence for the direct involvement of betaTrCP in Gli3 protein processing. Proc Natl Acad Sci U S A *103*, 33-38. 10.1073/pnas.0509927103.

Wang, C., Pan, Y., and Wang, B. (2010). Suppressor of fused and Spop regulate the stability, processing and function of Gli2 and Gli3 full-length activators but not their repressors. Development *137*, 2001-2009. 10.1242/dev.052126.

Wang, C., Wang, C., Wei, Z., Li, Y., Wang, W., Li, X., Zhao, J., Zhou, X., Qu, X., and Xiang, F. (2015). Suppression of motor protein KIF3C expression inhibits tumor growth and metastasis in

breast cancer by inhibiting TGF-beta signaling. Cancer Lett *368*, 105-114. 10.1016/j.canlet.2015.07.037.

Wang, G., Wang, B., and Jiang, J. (1999). Protein kinase A antagonizes Hedgehog signaling by regulating both the activator and repressor forms of Cubitus interruptus. Genes Dev *13*, 2828-2837. 10.1101/gad.13.21.2828.

Wang, S., Tanaka, Y., Xu, Y., Takeda, S., and Hirokawa, N. (2022). KIF3B promotes a PI3K signaling gradient causing changes in a Shh protein gradient and suppressing polydactyly in mice. Dev Cell *57*, 2273-2289 e2211. 10.1016/j.devcel.2022.09.007.

Wang, V.Y., Rose, M.F., and Zoghbi, H.Y. (2005). Math1 expression redefines the rhombic lip derivatives and reveals novel lineages within the brainstem and cerebellum. Neuron *48*, 31-43. 10.1016/j.neuron.2005.08.024.

Wechsler-Reya, R.J., and Scott, M.P. (1999). Control of neuronal precursor proliferation in the cerebellum by Sonic Hedgehog. Neuron *22*, 103-114. 10.1016/s0896-6273(00)80682-0.

Wen, X., Lai, C.K., Evangelista, M., Hongo, J.A., de Sauvage, F.J., and Scales, S.J. (2010). Kinetics of hedgehog-dependent full-length Gli3 accumulation in primary cilia and subsequent degradation. Mol Cell Biol *30*, 1910-1922. 10.1128/MCB.01089-09.

Williams, C.L., McIntyre, J.C., Norris, S.R., Jenkins, P.M., Zhang, L., Pei, Q., Verhey, K., and Martens, J.R. (2014). Direct evidence for BBSome-associated intraflagellar transport reveals distinct properties of native mammalian cilia. Nat Commun *5*, 5813. 10.1038/ncomms6813.

Wong, R.W., Setou, M., Teng, J., Takei, Y., and Hirokawa, N. (2002). Overexpression of motor protein KIF17 enhances spatial and working memory in transgenic mice. Proc Natl Acad Sci U S A *99*, 14500-14505. 10.1073/pnas.222371099.

Wong, S.Y., Seol, A.D., So, P.L., Ermilov, A.N., Bichakjian, C.K., Epstein, E.H., Jr., Dlugosz, A.A., and Reiter, J.F. (2009). Primary cilia can both mediate and suppress Hedgehog pathway-dependent tumorigenesis. Nat Med *15*, 1055-1061. 10.1038/nm.2011.

Woods, I.G., and Talbot, W.S. (2005). The you gene encodes an EGF-CUB protein essential for Hedgehog signaling in zebrafish. PLoS Biol *3*, e66. 10.1371/journal.pbio.0030066.

Yamazaki, H., Nakata, T., Okada, Y., and Hirokawa, N. (1995). KIF3A/B: a heterodimeric kinesin superfamily protein that works as a microtubule plus end-directed motor for membrane organelle transport. J Cell Biol *130*, 1387-1399. 10.1083/jcb.130.6.1387.

Yang, N., Li, L., Eguether, T., Sundberg, J.P., Pazour, G.J., and Chen, J. (2015). Intraflagellar transport 27 is essential for hedgehog signaling but dispensable for ciliogenesis during hair follicle morphogenesis. Development *142*, 2860. 10.1242/dev.128751.

Yang, Z., and Goldstein, L.S. (1998). Characterization of the KIF3C neural kinesin-like motor from mouse. Mol Biol Cell *9*, 249-261. 10.1091/mbc.9.2.249.

Yang, Z., Hanlon, D.W., Marszalek, J.R., and Goldstein, L.S. (1997). Identification, partial characterization, and genetic mapping of kinesin-like protein genes in mouse. Genomics *45*, 123-131. 10.1006/geno.1997.4901.

Yang, Z., Roberts, E.A., and Goldstein, L.S. (2001). Functional analysis of mouse kinesin motor Kif3C. Mol Cell Biol *21*, 5306-5311. 10.1128/MCB.21.16.5306-5311.2001.

Yao, S., Lum, L., and Beachy, P. (2006). The ihog cell-surface proteins bind Hedgehog and mediate pathway activation. Cell *125*, 343-357. 10.1016/j.cell.2006.02.040.

Yao, W., Jia, X., Xu, L., Li, S., and Wei, L. (2021). MicroRNA-2053 involves in the progression of esophageal cancer by targeting KIF3C. Cell Cycle *20*, 1163-1172. 10.1080/15384101.2021.1929675.

Yin, X., Feng, X., Takei, Y., and Hirokawa, N. (2012). Regulation of NMDA receptor transport: a KIF17-cargo binding/releasing underlies synaptic plasticity and memory in vivo. J Neurosci *32*, 5486-5499. 10.1523/JNEUROSCI.0718-12.2012.

Yin, X., Takei, Y., Kido, M.A., and Hirokawa, N. (2011). Molecular motor KIF17 is fundamental for memory and learning via differential support of synaptic NR2A/2B levels. Neuron *70*, 310-325. 10.1016/j.neuron.2011.02.049.

Yuasa, S. (1996). Bergmann glial development in the mouse cerebellum as revealed by tenascin expression. Anat Embryol (Berl) *194*, 223-234. 10.1007/BF00187133.

Yuasa, S., Kawamura, K., Ono, K., Yamakuni, T., and Takahashi, Y. (1991). Development and migration of Purkinje cells in the mouse cerebellar primordium. Anat Embryol (Berl) *184*, 195-212. 10.1007/BF01673256.

Zeng, H., Jia, J., and Liu, A. (2010). Coordinated translocation of mammalian Gli proteins and suppressor of fused to the primary cilium. PLoS One *5*, e15900. 10.1371/journal.pone.0015900.

Zhao, C., Omori, Y., Brodowska, K., Kovach, P., and Malicki, J. (2012). Kinesin-2 family in vertebrate ciliogenesis. Proc Natl Acad Sci U S A *109*, 2388-2393. 10.1073/pnas.1116035109.

Zhao, H., Ayrault, O., Zindy, F., Kim, J.H., and Roussel, M.F. (2008). Post-transcriptional down-regulation of Atoh1/Math1 by bone morphogenic proteins suppresses medulloblastoma development. Genes Dev *22*, 722-727. 10.1101/gad.1636408.

Chapter 2 Dual and Opposing Roles for KIF17 in HH-dependent Cerebellar Development

2.1 Abstract

While the kinesin-2 motors KIF3A and KIF3B have essential roles in ciliogenesis and Hedgehog (HH) signal transduction, potential role(s) for another kinesin-2 motor, KIF17, in HH signaling have yet to be explored. Here, we investigated the contribution of KIF17 to HH-dependent cerebellar development, where *Kif17* is expressed in both HH-producing Purkinje cells and HH-responding cerebellar granule neuron progenitors (CGNPs). Germline *Kif17* deletion in mice results in cerebellar hypoplasia due to reduced CGNP proliferation, a consequence of decreased HH pathway activity mediated through decreased Sonic HH (SHH) protein. Notably, Purkinje cell-specific *Kif17* deletion phenocopies *Kif17* germline mutants. Surprisingly, CGNP-specific *Kif17* deletion results in the opposite phenotype– increased CGNP proliferation and HH target gene expression due to altered GLI transcription factor processing. Together these data identify KIF17 as a key regulator of HH-dependent cerebellar development, with dual and opposing roles in HH-producing Purkinje cells and HH-responding CGNPS.

2.2 Introduction

Hedgehog (HH) signaling is a major mitogenic stimulus for postnatal expansion of the developing cerebellum (Dahmane and Ruiz i Altaba, 1999; Wechsler-Reya and Scott, 1999). Sonic hedgehog (SHH) ligand is produced by Purkinje cells and promotes cerebellar granule neural

progenitor (CGNP) proliferation (Dahmane and Ruiz i Altaba, 1999; Lewis *et al.*, 2004; Wechsler-Reya and Scott, 1999). *Shh* deletion within Purkinje cells results in cerebellar hypoplasia and reduced CGNP proliferation (Lewis *et al.*, 2004). Conversely, increasing the dosage of *Shh* in Purkinje cells results in cerebellar hyperplasia, as well as the formation of additional cerebellar lobes (Corrales *et al.*, 2006). Genetic deletion of other HH pathway components, namely *Gli2* (a key transcriptional effector of the HH pathway), *Gas1* or *Boc* (essential HH pathway co-receptors), within CGNPs leads to cerebellar hypoplasia due to reduced CGNP proliferation (Corrales *et al.*, 2004; Izzi *et al.*, 2011).

In addition to CGNPs, mature cerebellar granule neurons (CGNs) and Bergmann glia (BG) are HH-responsive (Corrales *et al.*, 2004). Recent work demonstrated that abrogating HH signaling within BG (through conditional *Smo* deletion) results in a non-cell autonomous reduction in CGNP proliferation and mild patterning abnormalities (Cheng *et al.*, 2018). Notably, the role of HH signaling within mature CGNs remains unclear.

A key organelle that is required for proper HH signaling in mice is the primary cilium (reviewed in (Bangs and Anderson, 2017)). Primary cilia are microtubule-based organelles that project from the cell surface and act as signaling centers for the HH pathway. Anterograde transport within primary cilia is accomplished by the heterodimeric kinesin-2 motor, KIF3A/KIF3B. Loss of either subunit in mice, *Kif3a* or *Kif3b*, lead to an absence of primary cilia, dysregulation of HH signaling and embryonic lethality (Huangfu *et al.*, 2003; Nonaka *et al.*, 1998; Takeda *et al.*, 1999). Within the developing cerebellum, loss of *Kif3a* within CGNPs leads to cerebellar hypoplasia due to reduced CGNP proliferation and loss of mitogenic response to SHH ligand (Spassky *et al.*, 2008). In addition to KIF3A/KIF3B function in ciliogenesis, KIF3A and its

adaptor protein, KAP3, regulate HH signaling by binding to and regulating GLI transcription factors (Carpenter *et al.*, 2015).

The kinesin-2 motor family contains two additional motor complexes in mammals, heterodimeric KIF3A/KIF3C and homodimeric KIF17 (reviewed in (He et al., 2017; Hirokawa *et al.*, 2009)). These motors are known as accessory motors, as they do not have clear roles within mammalian ciliogenesis (Engelke *et al.*, 2019; Yang *et al.*, 2001; Yin *et al.*, 2011). Loss of *Kif17* is well-tolerated across several model organisms, though KIF17 does have defined roles within several neuronal tissues. Within *Caenorhabditis elegans*, loss of OSM-3, a KIF17 homologue, leads to disruption of the distal region of primary cilia in sensory neurons (Signor *et al.*, 1999; Snow *et al.*, 2004). In *Danio rerio*, loss of *Kif17* results in disrupted photoreceptor outer segment development (Insinna *et al.*, 2008; Lewis *et al.*, 2018; Lewis *et al.*, 2017), as well as morphological changes to olfactory cilia (Zhao *et al.*, 2012). *Kif17* deletion in mice leads to short term memory issues, learning disabilities and disruption of NR2B trafficking in the hippocampus (Yin *et al.*, 2012; Yin *et al.*, 2011). Given that KIF17 can alter primary cilia with functional consequences in multiple neuronal cell types across different species, we investigated the contribution of KIF17 to HH signaling during postnatal cerebellar development.

Here we find that *Kif17* is expressed within SHH-producing Purkinje cells and HH-responsive CGNPs. Germline *Kif17* deletion leads to cerebellar hypoplasia, reduced CGNP proliferation and decreased HH target gene expression across multiple HH-responsive cell types. Purkinje cell-specific *Kif17* deletion phenocopies the germline mutant, demonstrating a requirement for KIF17 in Purkinje cells for proper HH signaling, a finding that correlates with reduced SHH protein levels within Purkinje cells in *Kif17* mutant animals. Conversely, CGNP-specific *Kif17* deletion results in upregulation of HH target genes and increased CGNP

proliferation *in vitro* and *in vivo*, a finding that correlates with reduced GLI3 protein levels (a transcriptional repressor of HH signaling). Together these data suggest that KIF17 plays dual roles in HH-dependent cerebellar development– promoting HH signaling in Purkinje cells through the regulation of SHH ligand and restricting HH signaling in CGNPs through the regulation of GLI transcription factor processing.

2.3 Results

2.3.1 Kif17 is expressed within Purkinje cells and cerebellar granule neural progenitors and is required for normal cerebellar development.

To investigate a role for the kinesin-2 motor, KIF17, in HH signal transduction, we generated *Kif17* mutant mice on a congenic C5BL/6J background. For our analysis, we utilized $Kif17^{lacZ}$ mice (Figure 2.1A), where fourth exon is deleted and has an insertion of a *lacZ* cassette. Similar to previous work on *Kif17* (Lewis *et al.*, 2017; Yin *et al.*, 2011), but in contrast to genetic deletion of other kinesin-2 family members (Nonaka *et al.*, 1998; Takeda *et al.*, 1999), *Kif17* homozygous mutant animals are viable and fertile, with no gross morphological abnormalities. Expression analysis revealed that *Kif17* is expressed within the developing cerebellum, starting at postnatal day 4 (P4) and continuing into adulthood (Figure 2.1B-G). X-GAL staining of $Kif17^{+/+}$ and $Kif17^{lacZ/lacZ}$ pups at P10 demonstrated *Kif17* expression within the Purkinje cell layer (PCL) and to a lesser degree within the external granule layer (EGL; Figure 2.2A-B). *Kif17* is expressed in a graded fashion along the anterior-posterior axis, with the strongest signal detected within the posterior lobes (Figure 2.2A-B), similar to what has been reported for the HH pathway target *Gli1* (Corrales *et al.*, 2004). To evaluate if the loss of KIF17 impacted HH-dependent cerebellar development, we continued our analysis of $Kif17^{-/-}$ cerebella at postnatal day 10, following the

peak of HH-dependent CGNP proliferation. For our analysis, we examined mid-sagittal cerebellar sections, where lobes I-III were considered anterior, while lobes VI-VIII were considered posterior (Figure 2.1H-I).

To identify which cell(s) express *Kif17*, we performed immunofluorescence for beta-galactosidase (β-GAL) in *Kif17*$^{+/+}$ and *Kif17*$^{lacZ/lacZ}$ cerebella at P10 (Figure 2.2C-H). In posterior lobes of *Kif17*$^{lacZ/lacZ}$ cerebella, we observed punctate localization of β-GAL within the cell bodies of Purkinje cells and in a subset of dendrites (Figure 2.2G, arrowheads). Further, we observed β-GAL signal within cerebellar granule neuron progenitors (CGNPs) of the EGL (Figure 2.2G, bracket). To confirm expression within these two cell populations, we performed fluorescence *in situ* hybridization in posterior lobes (Figure 2.2I-P) and anterior lobes (Figure 2.1J-Q) of *Kif17*$^{+/+}$ and *Kif17*$^{lacZ/lacZ}$ cerebella. In both regions of *Kif17*$^{lacZ/lacZ}$ cerebella, we detected *lacZ* punctae surrounding Purkinje cell nuclei (Figure 2.2M-N, Figure 2.1N-O) and CGNP nuclei (Figure 2.2O-P, Figure 2.1P-Q), corroborating the B-GAL localization results. Notably, *Kif17* expression was not detected within Bergmann glia or mature CGNs. Additionally, *Kif17* expression persists in Purkinje cells through P21 (Figure 2.3A-D). Finally, RT-qPCR analysis confirmed *Kif17* expression in CGNPs and verified efficient *Kif17* deletion in mutant animals (Figure 2.3E-F). Together, these data indicate that *Kif17* is expressed in two cell populations in the developing cerebellum– SHH-producing Purkinje cells and SHH-responsive CGNPs.

Analysis of cortical (Figure 2.2Q) and cerebellar (Figure 2.2R) weights at P10 indicated that *Kif17* mutant cerebella are significantly smaller than *Kif17*$^{+/+}$ littermates. Notably, this difference persisted even after normalizing cerebellar weight to cortical weight (Figure 2.2S). No significant difference in cortices or cerebellar weights were detected in *Kif17*$^{+/-}$ animals (Figure 2.3G-I). Notably, cerebellar hypoplasia was still observed in *Kif17* mutant animals maintained on

a mixed C57BL/6J; 129S4/SvJaeJ background (Figure 2.3J). However, this phenotype was not observed in *Kif17* mutants maintained on a congenic 129S4/SvJaeJ background (Figure 2.3K). On a C57BL/6J background, *Kif17*$^{-/-}$ animals had non-significant reduction of cerebellar area compared to *Kif17*$^{+/-}$ animals (Figure 2.3L-N). To determine if KIF17-mediated cerebellar hypoplasia is maintained during cerebellar development, cerebellar weights were measured from postnatal day 7 to 42 (Figure 2.3O). The reduction in cerebellar weight was not observed at postnatal day 7 in *Kif17*$^{-/-}$ animals but was observed at all later time points. Together, these data suggest that KIF17 promotes cerebellar development, albeit in a genetic background-dependent fashion.

2.3.2 Kif17 germline deletion results in reduced CGNP proliferation and decreased Gli1 expression within all HH-responsive cells.

To further investigate which layers of the cerebellum are affected by KIF17 loss, we measured the length of the Purkinje cell (PC) dendrites (Figure 2.4A, Figure 2.5A). Additionally, external granule layer thickness was measured (EGL, Figure 2.4B, Figure 2.5B) where CGNPs reside. Although we did not detect significant changes in PC dendrite length, we did observe statistically significant reductions in EGL thickness within both posterior and anterior lobes of *Kif17*$^{-/-}$ cerebella (Figure 2.4B, Figure 2.5B). Since previous work demonstrated that reduced EGL thickness is associated with a reduction in CGNP proliferation (Izzi *et al.*, 2011), we next examined *in vivo* proliferation of CGNPs in *Kif17*$^{+/+}$ and *Kif17*$^{-/-}$ P10 cerebella. Within the posterior lobes, we observed a significant reduction in the percentage of Ki67^{+} cells and EdU^{+} cells out of the PAX6^{+} cells in the EGL (Figure 2.4C-J). Within the anterior lobes, we similarly observed a significant reduction in CGNP proliferation (Figure 2.5C-D), although to a lesser degree.

Intriguingly, while there is a significant reduction in the percentage of EdU^+ cells, we also observed decreased EdU fluorescence within posterior and anterior lobes of *Kif17*$^{-/-}$ cerebella (Figure 2.5E-F). Altogether, these data suggest that cerebellar hypoplasia in *Kif17*$^{-/-}$ mice is due to reduced CGNP proliferation.

To determine whether decreased CGNP proliferation was associated with alterations in the levels of HH signaling in *Kif17*$^{-/-}$ cerebella, we quantified expression of the HH target gene, *Gli1*, using RT-qPCR and found it is significantly decreased in *Kif17*$^{-/-}$ P10 cerebella (Figure 2.4K). Expression of other HH target genes, *Ptch1*, *Ptch2*, *Ccnd1*, also trend lower in *Kif17*$^{-/-}$ cerebella (Figure 2.5G-I). Since *Gli1* is expressed in several HH-responsive cells in the developing cerebellum [CGNPs, Bergmann glia and cerebellar granule neurons (CGNs)], section *in situ* hybridization for *Gli1* was performed to define which cell population(s) displayed downregulated *Gli1* expression [*Gli1* probe specificity was validated in *Gli1*$^{-/-}$ cerebella (Figure 2.5J-M)]. Surprisingly, we found that *Gli1* expression is reduced across all HH-responsive cells (Figure 2.4L-Q). Additionally, reduced *Gli1* expression persists in CGNs and Bergmann glia in P21 *Kif17*$^{-/-}$ cerebella (Figure 2.5N-Q). Reduced *Gli1* expression within CGNs could be due to a resulting defect due to *Kif17* loss in its progenitors, CGNPs. However, since we did not observe *Kif17* expression within Bergmann glia, we hypothesized that KIF17 acts in a non-cell autonomous fashion in SHH-producing Purkinje cells to regulate *Gli1* expression.

2.3.3 Purkinje cell-specific Kif17 deletion results in a non-cell autonomous HH loss-of-function phenotype.

To directly assess KIF17 function in Purkinje cells, we conditionally deleted *Kif17* within Purkinje cells using a *Shh*^{Cre} driver (Figure 2.6A). The specificity of *Shh*^{Cre} was confirmed through

breeding with *Rosa26*$^{LSL\text{-}tdT}$ reporter mice (Figure 2.7A-F). Consistent with previous reports (Harfe et al., 2004), *Shh*^{Cre} efficiently mediates recombination in Calbindin (CALB1)-positive Purkinje cells. Importantly, *Shh*^{Cre} is a loss-of-function allele; however, reducing *Shh* dosage does not alter cerebellar size in *Kif17*$^{-/-}$;*Shh*$^{+/-}$ pups compared to *Kif17*$^{-/-}$ littermates (Figure 2.7G). RT-qPCR analysis revealed significantly reduced *Kif17* expression in *Shh*^{Cre};*Kif17*$^{fl/fl}$ cerebella (Figure 2.6B), suggesting efficient deletion within Purkinje cells (note that residual *Kif17* expression is likely due to the presence of *Kif17*-expressing CGNPs). Remarkably, Purkinje cell-specific *Kif17* deletion results in cerebellar hypoplasia measured through weight (Figure 2.6C, Figure 2.7H) and cerebellar area (Figure 2.7I-K), phenocopying *Kif17* germline deletion (cf. Figure 2.2S, Figure 2.3L-N).

As with *Kif17* germline mutants, PC dendrite length is unaltered in Purkinje cell-specific *Kif17* mutant pups in either the posterior (Figure 2.6D) or anterior (Figure 2.7L) lobes. However, there is a significant reduction in EGL thickness, specifically in posterior lobes (Figure 2.6E, Figure 2.7M). Consistent with *Kif17*$^{-/-}$ mice, analysis of CGNP proliferation revealed a significant reduction in the percentage Ki67^{+} cells and EdU^{+} cells within both the posterior and anterior lobes of *Shh*$^{Cre:GFP}$;*Kif17*$^{fl/fl}$ mice compared to control littermates (Figure 2.6F-M, Figure 2.7N-O). Additionally, we observed significant reductions in the expression of multiple HH target genes, including *Gli1* and *Ptch1* (Figure 2.6N-O) as well as *Ptch2* and *Ccnd1,* as measured by RT-qPCR (Figure 2.7P-Q). Fluorescence *in situ* hybridization revealed reduced *Gli1* expression in *Shh*$^{Cre:GFP}$;*Kif17*$^{fl/fl}$ cerebella within CGNPs, BG and CGNs (Figure 2.6P-S). These data demonstrate that Purkinje cell-specific *Kif17* deletion phenocopies germline *Kif17* mutant cerebella. The HH loss-of-function phenotype could be due to reduced PC number or a change in PC morphology with *Kif17* deletion. However, we did not observe any gross differences in PC morphology or density in either *Kif17* germline deletion or PC conditional deletion cerebella

(Figure 2.7R-W). Altogether, these data establish an essential role for KIF17 within SHH-producing Purkinje cells during cerebellar development.

2.3.4 KIF17 regulates SHH protein in the developing cerebellum.

The reduction of HH target gene expression across multiple HH-responsive cells in *Kif17* mutant cerebella suggested a non-cell autonomous role for KIF17 in HH signal transduction. Given that SHH, the only HH ligand expressed in the developing cerebellum, is produced by Purkinje cells, we explored a role for KIF17 in Purkinje cell regulation of SHH localization and release. Initially, examination of *Shh* expression by RT-qPCR revealed that *Shh* transcripts are downregulated in both *Kif17*$^{-/-}$ mice (Figure 2.8A) and Purkinje cell-specific conditional *Kif17* mutants (Figure 2.8B). Next, we assessed the protein levels of SHH ligand and observed levels of N-terminal SHH are subtly but not significantly decreased in the cerebella of *Kif17* germline mutants [Figure 2.8C-D; SHH antibody specificity was validated in *Shh*$^{-/-}$ tissue (Figure 2.9A)].

We also examined levels of the HH co-receptor, BOC, which is expressed in Purkinje cells (Izzi *et al.*, 2011) and has been recently demonstrated to regulate SHH localization in cytonemes of NIH/3T3 cells (Hall et al., 2021). Notably, levels of *Boc* transcripts (Figure 2.9B-C) and BOC protein are unaltered in *Kif17* deletion cerebella (Figure 2.9D-E). However, *Scube2,* which encodes a key regulator of SHH protein release (Hollway *et al.*, 2006; Kawakami *et al.*, 2005), is significantly reduced in P10 cerebella from both *Kif17*$^{-/-}$ (Figure 2.8E) and Purkinje cell-specific *Kif17* mutant animals (Figure 2.8F). Given the reduced levels of *Scube2*, we speculated that KIF17 could impact SHH ligand release or secretion.

To assess a role for KIF17 in SHH release, we utilized a gain-of-function approach, where COS-7 cells were driven to express epitope-tagged KIF17 (KIF17:HA) and either full-length

(SHH:GFP) or N-terminal SHH (N-SHH; Figure 2.8G). While KIF17 expression does not alter the levels of secreted N-SHH (Figure 2.9F), we did observe increased levels of secreted full-length SHH (Figure 2.8H). We also observed significantly increased levels of intracellular SHH, including full length SHH:GFP, N-SHH:GFP and N-SHH when co-expressed with KIF17 (Figure 2.8I, Figure 2.9G-H).

To investigate KIF17-mediated regulation of intracellular SHH levels *in vivo*, we employed an antibody directed toward the C-terminus of SHH [SHH antibody specificity was validated in P10 cerebella of *Shh* conditional mutant animals $Shh^{CreER/lacZ}$ mice (Figure 2.9I-Q)]. Intracellular SHH is detected in the Golgi/ER (horizontal arrowheads) and within the cell bodies of Purkinje cells of $Kif17^{+/-}$ and $Kif17^{-/-}$ littermates (vertical arrowheads, Figure 2.8J-M). However, SHH levels are significantly reduced in the posterior lobes of $Kif17^{-/-}$ P10 cerebella (Figure 2.8N). Notably, SHH levels are not significantly altered in anterior lobes of $Kif17^{-/-}$ mice (Figure 2.9R). Together, these gain- and loss-of-function data suggest that KIF17 acts in Purkinje cells to stabilize intracellular SHH protein and promote SHH release. This is supported by the downregulation of HH target genes across the multiple HH-responsive cell types (CGNPs, BG and CGNs) following Purkinje cell-specific *Kif17* deletion. Reduction of SHH protein ultimately results in decreased CGNP proliferation and cerebellar hypoplasia in *Kif17* deletion mice (Figure 2.8O).

2.3.5 Kif17 deletion promotes CGNP proliferation in vitro.

To investigate a role for KIF17 in CGNPs, we isolated and cultured wildtype and $Kif17^{-/-}$ CGNPs *in vitro* isolated from mice maintained on C57BL/6J genetic background (Lee et al., 2009). HH-dependent proliferation was measured in response to treatment with either Smoothened Agonist (SAG) or N-SHH conditioned media (N-SHH CM). Surprisingly, $Kif17^{-/-}$ CGNPs display

increased baseline proliferation compared to *Kif17*$^{+/-}$ and *Kif17*$^{+/+}$ CGNPs (Figure 2.10A-F). Treatment with either SAG or N-SHH CM resulted in increased CGNP proliferation, measured by EdU/BrdU incorporation (Figure 2.10E, Figure 2.11A) or luminescence-based quantitation of ATP levels (Figure 2.10F). Additionally, we cultured CGNPs from *Kif17*$^{fl/fl}$ and *Shh*^{Cre}*;Kif17*$^{fl/fl}$ littermates and evaluated their proliferation *in vitro* (Figure 2.11B-G). We observed no significant differences of CGNP proliferation in *Kif17*$^{fl/fl}$ and *Shh*^{Cre}*;Kif17*$^{fl/fl}$ cultures, confirming increased proliferation in *Kif17*$^{-/-}$ CGNPs is a cell-autonomous phenotype. Notably, these results are distinct from those observed in CGNPs lacking *Boc*, which encodes for an essential HH co-receptor (Izzi *et al.*, 2011). Direct comparison of *Kif17*$^{-/-}$ CGNP and *Boc*$^{-/-}$ CGNP proliferation confirmed that *Kif17* deletion results in increased baseline and HH-stimulated CGNP proliferation (Figure 2.11H). These data are directly in opposition of CGNP proliferation *in vivo* (c.f. Figure 2.4C-J), suggesting KIF17 has two distinct roles in Purkinje cells and CGNPs.

Given the altered baseline CGNP proliferation, we examined the levels and processing of the HH pathway transcriptional repressor, GLI3 in *Kif17* mutant animals. Western blot analysis of GLI3 full length (GLI3^{FL}) and repressor (GLI3^{R}) in P10 cerebella revealed (Figure 5G) significant reductions in both GLI3^{FL} and GLI3^{R} in *Kif17*$^{-/-}$ cerebella (Figure 2.10H-I). Further, the ratio of GLI3^{FL} to GLI3^{R} is significantly increased in *Kif17* mutant cerebella (Figure 2.10J). These data suggest that similar to other kinesin-2 mutants (Huangfu and Anderson, 2005), KIF17 regulates GLI3 processing in CGNPs. To examine the consequences of altering *Gli3* dosage in *Kif17* mutant animals, we measured cerebellar size in P10 *Kif17*^{lacZ}*;Gli3*^{Xt} compound mutant cerebella (Figure 2.10K). Notably, loss of one *Gli3* allele causes cerebellar hyperplasia in *Kif17*$^{+/+}$ mice and rescues the cerebellar hypoplasia phenotype observed in *Kif17* mutants. Together, these data suggest that

KIF17 negatively regulates HH signaling in a cell-autonomous fashion within CGNPs, potentially through regulation of GLI3 repressor.

2.3.6 CGNP-specific Kif17 deletion results in a cell-autonomous HH gain-of-function phenotype.

To directly assess KIF17 function in CGNPs *in vivo*, we crossed *Kif17*^{flox} mice to *Atoh1Cre* animals (Figure 2.12A), which specifically drives recombination in CGNPs [(Matei et al., 2005); Figure 2.13A-F]. We used RT-qPCR to confirm efficient *Kif17* deletion in *Atoh1Cre;Kif17*$^{fl/fl}$ cerebella (Figure 2.12B, Figure 2.13G). Additionally, while *Kif17* expression is reduced in conditional deletion cerebella, we found *Kif17* expression was surprisingly increased *Atoh1Cre;Kif17*$^{+/+}$ cerebella (Figure 2.13G). Next, we assessed cerebellar size in *Atoh1Cre;Kif17*$^{fl/fl}$ animals, which is unchanged compared to control animals (Figure 2.12C, Figure 2.13H-K). These data are in striking contrast to *Kif17* germline mutants and Purkinje cell-specific *Kif17* deletion (cf. Figure 2.2S and Figure 2.6C). While length of the PC dendrites is not significantly changed in either posterior or anterior lobes of *Atoh1Cre;Kif17*$^{fl/fl}$ cerebella (Figure 2.12D, Figure 2.13L), EGL thickness is increased, specifically in posterior lobes of *Atoh1Cre;Kif17*$^{fl/fl}$ cerebella (Figure 2.12E, Figure 2.13M). Notably, increased EGL thickness appears to be due to increased CGNP proliferation (as assessed by the percentage of EdU^{+} cells out of the PAX6^{+} cells in the EGL) in both posterior (Figure 2.12M) and anterior (Figure 2.13O) lobes of *Atoh1Cre;Kif17*$^{fl/fl}$ cerebella. RT-qPCR analysis revealed increased HH target gene expression in *Atoh1Cre;Kif17*$^{fl/fl}$ cerebella compared to control littermates (Figure 2.12N-O; Figure 2.13P-R). *In situ* hybridization confirmed that the increase in HH target gene expression is restricted to CGNPs in the posterior lobe, while no changes were observed in HH-responsive Bergmann glia and CGNs (Figure 2.12P-T; Figure 2.13S). Together, these data indicate that

CGNP-specific *Kif17* deletion results in increased HH pathway activity and CGNP proliferation, leading to a thicker EGL within posterior lobes of the developing cerebellum.

2.3.7 CGNP-specific Kif17 deletion results in reduced GLI protein, increased CGNP proliferation, and elongated primary cilia in vitro.

Given that other kinesin-2 motors regulate GLI processing and trafficking, including in the cerebellum (Huangfu and Anderson, 2005; Huangfu *et al.*, 2003; Spassky *et al.*, 2008), we examined the consequences of CGNP-specific *Kif17* deletion on *Gli* expression and GLI protein levels. *Gli2* and *Gli3* expression are increased in *Atoh1Cre;Kif17*$^{fl/fl}$ cerebella (Figure 2.14A-B), similar to *Gli1*. However, western blot analysis (Figure 2.15A) revealed significantly reduced levels of GLI1 and GLI2 protein (Figure 2.15B-C). Similar to what was observed *Kif17*$^{-/-}$ cerebella (cf Figure 2.10G-J), GLI3 full length and GLI3 repressor levels are also reduced (Figure 2.15D-E); further, the ratio of full length (GLI3^{FL}) to repressor (GLI3^{R}) is increased in *Kif17* mutant CGNPs (Figure 2.15F).

We also assessed potential physical interactions between KIF17 and GLI proteins, as previously demonstrated for other Kinesin-2 motors (Carpenter *et al.*, 2015). Co-immunoprecipitation of epitope-tagged KIF17 (KIF17:HA) and GLI transcription factors (MYC:GLI1, MYC:GLI2, MYC:GLI3) suggested that KIF17 can indeed physically interact with all three GLI proteins (Figure 2.14C). Reduction of both full length and processed forms of GLI is reminiscent of SUFU loss-of-function cerebella (Jiwani *et al.*, 2020). Additionally, loss of GLI2 or GLI3 lead to loss of ciliary localization of SUFU (Tukachinsky *et al.*, 2010). We examined ciliary localization of SUFU [SUFU antibody validated in *Sufu*$^{-/-}$ MEFs (Figure 2.14D-I)] in *Kif17* conditional deletion CGNPs in response to SAG (Figure 2.14J-R). We found that SUFU was found

at the tips of cilia in both *Kif17*$^{fl/fl}$ and *Atoh1Cre;Kif17*$^{fl/fl}$ CGNPs, albeit a lower percentage of SUFU^{+} cilia were observed in *Atoh1Cre;Kif17*$^{fl/fl}$ CGNPs. Altogether these data suggest KIF17 impacts GLI stability or processing, potentially through regulating SUFU-GLI interactions.

We noted that *Atoh1* expression is increased in animals with CGNP-specific *Kif17* deletion (Figure 2.16A**)**; previous work demonstrated that ATOH1 promotes ciliogenesis and maintains CGNP responsiveness to HH (Chang et al., 2019). However, analysis of CGNP primary cilia length in *Atoh1Cre;Kif17*$^{fl/fl}$ P10 cerebella revealed no significant change *in vivo* (Figure 2.16B-C; $p = 0.4534$ for posterior lobes, $p = 0.0886$ for anterior lobes). In contrast, when we examined primary ciliary length in SAG-treated CGNPs *in vitro*, we found that CGNPs lacking *Kif17* display increased ciliary length (Figure 2.15G-L), with an average ciliary length of 1.46 μm (compared to 1.1 μm in control animals); notably, some primary cilia reached lengths of 5 μm (Figure 2.15K).

Since HH signaling also regulates cilia length (Cruz et al., 2010) and ciliogenesis (Peterson et al., 2012), we investigated whether increased ciliary length was a cause or a consequence of HH pathway activity. We antagonized HH signaling *in vitro* by adding BMP ligands, either BMP2, which has been previously shown to antagonize SHH-induced CGNP proliferation (Rios et al., 2004) or BMP10, which is significantly upregulated in *Kif17*$^{-/-}$ cerebella (Figure 2.16D). Notably, both BMP2 and BMP10 effectively attenuate HH-mediated CGNP proliferation in both *Kif17*$^{fl/fl}$ and *Atoh1Cre;Kif17*$^{fl/fl}$ cultures (Figure 2.16E-M, Figure 2.15L). However, BMP2 and BMP10 treatment reduced ciliary length specifically in *Atoh1Cre;Kif17*$^{fl/fl}$ CGNPs (Figure 2.15M-S, Figure 2.16N), resulting in average ciliary lengths of 1.18 μm (BMP2) and 1.17 μm (BMP10). Together, these data suggest that high levels of HH pathway activation in *Kif17* mutant CGNPs results in increased ciliary length, which can be attenuated by BMP signaling.

2.4 Discussion

In this study, we investigated a role for the kinesin-2 motor KIF17 in HH-dependent cerebellar development. Our work revealed that *Kif17* is expressed in both SHH-producing Purkinje cells and SHH-responsive CGNPs. Purkinje cell-specific *Kif17* deletion phenocopies germline *Kif17* deletion, resulting in reduced EGL thickness due to reduced HH target gene expression and decreased CGNP proliferation. Conversely, CGNP-specific *Kif17* deletion increased EGL thickness due to increased HH target gene expression and increased CGNP proliferation (Figure 2.17). This work identifies dual and opposing roles for KIF17 in HH-dependent cerebellar development– first, as a positive regulator of HH signaling through regulation of SHH protein levels within Purkinje cells, and second, as a negative regulator of HH signaling through regulation of GLI transcription factors in CGNPs.

2.4.1 KIF17 function in SHH-producing Purkinje cells

Here we demonstrated that KIF17 is required in Purkinje cells to mediate proper HH-dependent cerebellar development and that KIF17 regulates SHH protein levels within Purkinje cells. Specifically, we visualized intracellular SHH utilizing a C-terminal antibody, which revealed reduced SHH protein in *Kif17* mutant cerebella, both within the presumed endoplasmic reticulum/Golgi apparatus and more broadly within Purkinje cell bodies. Notably, SHH is translated as a 45 kDa precursor protein, which undergoes auto-catalytic cleavage into a 19 kDa N-terminal fragment and 25 kDa C-terminal fragment (Bumcrot et al., 1995; Lee *et al.*, 1994; Porter *et al.*, 1995). The N-terminal fragment is dually-lipidated with cholesterol at the C-terminus and palmitate at the N-terminus to produce active ligand (reviewed in (Petrov et al., 2017)). While the 25 kDa C-terminal SHH fragment does not transduce HH signaling, the C-terminal HH

fragment does target N-HH to axons and growth cones in the developing retina of *Drosophila melanogaster* (Chu *et al.*, 2006). One model for KIF17 action in Purkinje cells is the transport of SHH-containing vesicles along microtubules to distinct locations within these cells. This model has precedence with a previously described role for KIF17 in the vesicular trafficking of NR2B in the hippocampus (Yin *et al.*, 2012; Yin *et al.*, 2011). Further, this is consistent with the reduced levels of SHH protein in *Kif17* mutants, as NR2B levels are also reduced when its vesicular trafficking is disrupted in *Kif17* mutants. This model is also consistent with the results from KIF17 gain-of-function experiments demonstrating increased intracellular SHH protein accumulation (this study). Altogether, the data in this paper propose KIF17 may be responsible for cytoplasmic trafficking of SHH within cerebellar Purkinje cells. However, we cannot rule out similar trafficking-related effects of KIF17 on other HH pathway components, such as SCUBE2 and DISP, both of which regulate SHH protein release from cell surfaces. We also cannot distinguish between KIF17-mediated effects on SHH trafficking versus potential impacts on SHH protein stability. Distinguishing between these possibilities would require robust methods to culture Purkinje cells *ex vivo*, which are currently lacking. Further, while we did not observe any gross morphological changes or the density of Purkinje cells, we cannot distinguish whether the loss of KIF17 impacts overall Purkinje cell function or the secretion of other Purkinje cell-derived ligands, such as IGF-1.

2.4.2 KIF17 regulation of GLIs in CGNPs

In addition to a non-cell autonomous role for KIF17 in Purkinje cells, we also established a cell autonomous role for KIF17 in CGNPs, where *Kif17* deletion results in a HH gain-of-function phenotype – increased CGNP proliferation and upregulation of several HH target genes. CGNP-

specific *Kif17* deletion results in reduced protein levels of all three HH transcriptional effectors, GLI1, GLI2, and GLI3. Previous work established GLI1 and GLI2 as transcriptional activators in the developing cerebellum where *Gli2* deletion results in a HH loss-of-function phenotype (Corrales *et al.*, 2006; Corrales *et al.*, 2004). Given these roles for GLI1 and GLI2, we were surprised to find that CGNP-specific *Kif17* deletion results in a HH gain-of-function phenotype. However, the concomitant loss of GLI3 repressor in *Kif17* mutant CGNPs suggests that GLI repressor function is a significant mediator of CGNP proliferation. Notably, reduction of GLI activator and repressor protein is consistent with previous work where cerebellar-specific Suppressor of fused (*Sufu*) deletion also results in increased CGNP proliferation (Jiwani *et al.*, 2020). GLI3 also acts during early embryonic cerebellar development in mesencephalon and rhombomere 1 patterning through the regulation of *Fgf8* expression (Blaess *et al.*, 2008). Here we also show that loss of one *Gli3* allele is sufficient to drive cerebellar hyperplasia, likely due to increased HH signaling. Together, these data suggest that KIF17 in CGNPs promotes GLI3 repressor formation to restrict proliferation in the postnatal cerebellum, consistent with previous work demonstrating central roles for other kinesin-2 motors in GLI processing (Endoh-Yamagami et al., 2009; Huangfu and Anderson, 2005; Huangfu *et al.*, 2003).

GLIs require primary cilia for proper processing and transcriptional activity (reviewed in (Bangs and Anderson, 2017)). Further, studies have established ciliary tip localization of KIF17 (Dishinger *et al.*, 2010), similar to GLI transcription factor localization during HH activation (Santos and Reiter, 2014; Wen *et al.*, 2010). One model for KIF17 regulation of GLI protein levels in CGNPs is through ciliary trafficking or localization. Notably, this is consistent with recent work demonstrating that GLI interactions with KIF7 promote ciliary localization (Haque et al., 2022). Unfortunately, the lack of suitable KIF17 antibodies precludes rigorous testing of this hypothesis.

Other possible roles for KIF17 in CGNPs include the regulation of GLI trafficking and stability as well as interactions with other ciliary proteins that regulate GLI processing, such as SUFU, KIF7, or PKA (Ding et al., 1999; He et al., 2014; Tuson *et al.*, 2011). We observe that SUFU does localize to the tips of cilia with the loss of KIF17, although at a reduced proportion. This may be due to KIF17 interacting with SUFU or due to the reduced abundance of GLI transcription factors. Previous literature demonstrates that the loss of GLI2 or GLI3 results in a loss of ciliary SUFU (Tukachinsky *et al.*, 2010).

It is important to note the contradictory results of CGNP proliferation *in vitro* with germline and CGNP-specific *Kif17* deletion. While the CGNP-specific *Kif17* deletion increased CGNP proliferation *in vivo*, germline *Kif17* mutants display reduced CGNP proliferation *in vivo*. One hypothesis to explain this contradiction is KIF17's function in Purkinje cells in regulating SHH ligand is upstream to GLI processing, therefore the cell autonomous defect cannot be observed until the CGNPs are isolated and grown in culture. While we do note reduced GLI3 repressor in the germline mutants, it will be essential to determine the levels of GLI activator (GLI1 and GLI2) in germline *Kif17* deletion CGNPs is similarly reduced or below the levels seen in conditional deletion CGNPs. Furthermore, we observed increased proliferation in the absence of HH stimulation in germline and CGNP-specific *Kif17* deletion CGNPs *in vitro*. This result could be due to reduced levels of BMP signaling. In support of that hypothesis, *Bmp10* expression was reduced in germline *Kif17* deletion CGNPs. Further, the addition of recombinant BMP ligands, BMP2 and BMP10, reduced the levels of CGNP proliferation *in vitro* in *Kif17* conditional deletion CGNPs, lowering proliferation levels to match $Kif17^{fl/fl}$ controls.

2.4.3 Kinesin motors and HH signaling

While previous studies have explored the requirement for kinesin and dynein motors in HH-responding cells (reviewed in (Bangs and Anderson, 2017)), the current study highlights a novel role for kinesin motors in HH-producing cells, complementing new work examining KIF3B and SHH in the developing limb bud (Wang *et al.*, 2022). It is important to note that the single loss of KIF17 in the developing cerebellum results in a HH loss-of-function phenotype, demonstrating other kinesin-2 motors cannot rescue or compensate the loss of KIF17. An outstanding question is whether KIF17 functions in HH-producing cells in other tissues. Notably, the subgranular zone of the hippocampus and subventricular zone rely on proper HH signaling for neurogenesis (Ahn and Joyner, 2005; Breunig et al., 2008; Han et al., 2008; Machold et al., 2003). While KIF17 has a well-defined role in NR2B trafficking in the hippocampus (Yin *et al.*, 2012; Yin *et al.*, 2011), the potential contribution of KIF17 to HH signaling in the hippocampus has not yet been examined.

In addition to its neural-specific contributions, KIF17 has several described functions in the testes, although loss-of-function studies have yet to be performed (Chennathukuzhi *et al.*, 2003; Kimmins et al., 2004; Kotaja *et al.*, 2006; Macho *et al.*, 2002; Saade *et al.*, 2007). Desert Hedgehog (DHH) is expressed in Sertoli cells, and *Dhh* deletion results in a loss of HH-responsive Leydig cells (Clark *et al.*, 2000). While we did not observe infertility in *Kif17* mutant mice, it will be of interest to investigate the consequences of *Kif17* deletion on HH-dependent spermatogenesis. Future studies investigating the contribution of other kinesin-2 motors, particularly KIF3A/KIF3B, in HH-producing cells (e.g., in the notochord or zone of polarizing activity) will be of high interest. Finally, this work raises the question of potential contributions from KIF3C, another accessory kinesin-2 motor, to HH signal transduction.

2.5 Materials and Methods

Reagents

Antibodies utilized (Table 2.1); primers used for RT-qPCR (Table 2.2);

Animal models

Kif17^{lacZ} germline mutant mice have been previously described (Lewis *et al.*, 2017). These mice were maintained on two different congenic C57BL/6J and 129S4/SvJaeJ backgrounds after backcrossing for at least 10 generations. *Kif17*^{fl} animals carrying *Kif17* conditional alleles were generated from the initial knock-in allele from EUCOMM through crossing *Kif17*^{tm1A} animals to ubiquitous Flippase mice obtained from The Jackson Laboratory [strain 011065, (Wu et al., 2009)] to generate *Kif17*^{tm1C}*/Kif17*^{flox} mice. These mice were maintained on a congenic C57BL/6J background. *Atoh1Cre* animals were obtained from The Jackson Laboratory [strain 011104, (Matei *et al.*, 2005)] and maintained on a C57BL/6J background. Mice carrying the *Shh*^{Cre} allele [strain 005622] were provided by Dr. Deb Gumucio and previously described (Harfe *et al.*, 2004). These mice were backcrossed for at least 10 generations to C57BL/6J animals to create a congenic line. All animal procedures were reviews and approved by the Institutional Animal Care and Use Committee (IACUC) at the University of Michigan, USA. Experiments performed in this paper were completed with littermate controls.

Wholemount X-gal staining

Postnatal cerebella were dissected in 1X PBS (pH 7.4) and cut in half with a razor before fixation (1% formaldehyde, 0.2% glutaraldehyde, 2 mM $MgCl_2$, 5 mM EGTA, 0.02% NP-40) on ice for 20 min. After fixation, the cerebella were washed 3 x 5 min with 1X PBS (pH 7.4) on a

rocking platform. Beta-Galactosidase activity was detected with X-gal staining solution [5 mM $K_3Fe(CN)_6$, 5 mM $K_4Fe(CN)_6$, 2 mM $MgCl_2$, 0.01% Na deoxycholate, 0.02% NP-40, 1 mg/ml X-gal]. The signal was developed for 24 h at 37°C, changing the staining solution after 12 h. After staining, cerebella were washed 3 x 5 min with 1X PBS (pH 7.4) and post-fixed in 4% paraformaldehyde for 30 min at room temperature on a rocking platform, followed by 3 x 5 min washes in 1X PBS (pH 7.4). Cerebella were photographed using a Nikon SMZ1500 microscope and stored in 1X PBS (pH 7.4).

Section Immunofluorescence

Section immunofluorescence was performed as described in (Allen *et al.*, 2011). Briefly, cerebella were dissected in 1X PBS (pH 7.4) and cut in half using a razor. For all experiments except for beta-galactosidase and SHH visualization, cerebella were fixed with 4% paraformaldehyde (Electron Microscopy Sciences) for 1 h on ice. For beta-galactosidase immunofluorescence, cerebella were fixed (1% formaldehyde, 0.2% glutaraldehyde, 2 mM $MgCl_2$, 5 mM EGTA, 0.02% NP-40) on ice for 20 min. For SHH visualization, cerebella were fixed in Sainte Marie's solution (95% ethanol, 1% acetic acid) at 4°C on a rocking platform for 24 h. Following fixation, cerebella were washed 3 x 5 min with 1X PBS (pH 7.4) on a rocking platform and cryoprotected overnight in 1X PBS + 30% sucrose on a rocking platform. Then, cerebella were washed 3 x 1 h in 50% OCT (Fisher Scientific, 23-730-571) before embedding in 100% OCT. Sections were collected on a Leica CM1950 cryostat at 12 μm thickness for all experiments, except for SHH visualization, which were sectioned at 9 μm thickness. Slides were then washed 3 x 5 min with 1X PBS (pH 7.4). For mouse primary antibodies, citric acid antigen retrieval (10 mM citric acid + 0.5% Tween-20, pH 6.0) at 92°C for 10 min was performed prior to primary antibody

incubation. Primary antibodies were diluted in blocking buffer (3% bovine serum albumin, 1% heat-inactivated sheep serum, 0.1% Triton X-100) and incubated overnight at 4°C in a humidified chamber. After primary antibody incubation, slides were washed 3 x 10 min with 1X PBST^{X} (1X PBS + 0.1% Triton X-100, pH 7.4). Secondary antibodies were diluted in blocking buffer and incubated for 1 h at room temperature, followed by 3 x 5 min 1X PBST^{X} washes. Nuclei were labeled using DAPI (0.5 μg/mL in blocking buffer) for 10 min and washed twice with 1X PBS. Coverslips were mounted using Immu-mount aqueous mounting medium (Thermo Fisher Scientific, 9990412). Images were taken on a Leica SP5X upright confocal (2 photon). A list of all the primary and secondary antibodies and their working concentrations is provided in Table S1.

Fluorescent in situ hybridization

Cerebella were dissected in 1X PBS (pH 7.4) and cut in half using a razor. Cerebella were fixed with 10% neutral buffered formalin (Fisher, 245-685) on a rocking platform at room temperature for 24 h. Following fixation, cerebella were washed 3 x 5 min with 1X PBST^{X} on a rocking platform and cryoprotected overnight in 1X PBS + 30% sucrose on a rocking platform. Cerebella were then washed 3 x 1 h with 50% OCT compound before embedding in 100% OCT. Sections were collected on a Leica CM1950 cryostat at 12 μm thickness. Slides were processed using RNAscope Multiplex Fluorescent Detection kit (ACD, 323110) using a protocol adapted from (Holloway, 2021). Prior to probe hybridization, samples underwent antigen retrieval for 15 minutes and treated with Protease Plus (ACD, 322381) for 5 minutes. Probes used in this paper were *Mm-Gli1* (ACD, 311001) and *E.coli-lacZ* (ACD, 313451). After probe detection, slides were subsequently stained using the above-described section immunofluorescence protocol.

RT-qPCR

Cerebella were dissected in 1X PBS, and RNA was isolated using a PureLink RNA Mini Kit (ThermoFisher Scientific, 12183025). Following isolation, 2 μg of RNA were used to generate cDNA libraries using a High-Capacity cDNA reverse transcription kit (Applied Biosystems, 4368814). RT-qPCR was performed using PowerUP SYBR Green Master Mix (Applied Biosystems, A25742) in a QuantStudio 3 Real-Time PCR System (Applied Biosystems). Primers used in this paper can be found in Table S2. Gene expression was normalized to *Gapdh*, except for Figure 3B, where expression was normalized to *Calb1*, and relative expression analyses were performed using the $2(^{-ddCT})$ method. For RT-qPCR analysis, biological replicates were analyzed in triplicate.

Weight analyses

For weight measurements, the date litters were born were noted as postnatal day 0 and were dissected on postnatal day 10. Pups were first weighed and then placed on ice briefly before decapitation. The cortices and cerebella were dissected in 1X PBS (pH 7.4). To weigh cortices and cerebella, a specimen jar was first filled with PBS on an analytical scale. The tissue was transferred with forceps to the specimen jar, and its weight was recorded. Genotyping samples were taken after dissection, allowing the weights to be recorded without prior knowledge of the genotype.

Hematoxylin and Eosin Staining and Cerebellar Area Quantification

Tissue sections were washed 1 x 5 minutes in water, stained with hematoxylin for 5 minutes, then rinsed in water and 1X PBS (pH 7.4) for 10 seconds. Slides were counterstained with eosin solution, rinsed in water and dehydrated in an ethanol and xylene series (1 x 1 minutes

in 95% ethanol, 2 x 2 minutes in 100% ethanol, 2 x 2 minutes in 100% xylene). Slides were mounted using Cytoseal 60 mounting media and imaged on a Nikon SMZ1500 stereomicroscope. For cerebellar area quantitation, we analyzed 2-5 sections per animal and a minimum of 2 animals per genotype. Cerebellar area measurements were collected using the area measure function on ImageJ.

EGL and PC Dendrite quantitation

To measure the thickness of the external granule layer (EGL) and PC dendrites, ImageJ software was utilized. Images were first blinded before measuring. For EGL thickness, the area was divided by the length of the EGL. For PC dendrite length, measurements were taken just below the bottommost nuclei in the EGL to the center of Purkinje cell nuclei within the molecular layer. For each animal, at least three images were acquired in the posterior lobes and an additional three images in the anterior lobes.

EdU incorporation assay (in vivo)

On postnatal day 9, pups were intraperitoneally injected with 100mg/kg of EdU (Invitrogen, A10044), dissolved in 1X PBS (pH 7.4). 24 h later, cerebella were dissected and processed for section immunofluorescence as described above. Prior to primary antibody incubation, EdU incorporation was visualized with an azide staining solution [100 mM Tris HCl (pH 8.3), 0.5 mM $CuSO_4$, 50 mM ascorbic acid, 50 μM Alexa Fluor 555 Azide, Triethylammonium Salt (Thermo Fisher Scientific, A20012)] for 30 min at room temperature. Sections were then washed 3 x 10 min in $PBST^X$ (1x PBS + 0.1% Triton X-100, pH 7.4), followed by immunofluorescence staining as described above.

Section digoxigenin in situ hybridization

Section digoxigenin *in situ* hybridization was performed as previously described (Allen at al., 2011; Wilkinson, 1992). First, cerebella were dissected in 1X PBS (pH 7.4) and fixed for 24 h with 4% paraformaldehyde at 4°C on rocking platform. After fixation, cerebella were washed 3 x 5 min with 1X PBST^{W} (1X PBS + 0.1% Tween-20, pH 7.4) and cryoprotected with 1X PBS + 30% sucrose overnight on a rocking platform. The next day, cerebella were subjected to 3 x 1 h washes with 50% OCT before embedding in 100% OCT. Cerebella were sectioned on Leica CM1950 cryostat at 20 μm thick sections. Probe hybridization was performed with the indicated digoxigenin probes at a concentration of 1 ng/μl overnight at 70°C. The sections were incubated in AP-conjugated anti-DIG antibody (Table S1). AP-anti-DIG was visualized with BM Purple (Roche, 11442074001), and signal was developed for 4 h at 37°C. After the signal was developed, development was stopped with 3 x 5 min washes with 1X PBS (pH 4.5). Sections were post-fixed in 4% PFA + 0.2% glutaraldehyde for 30 min, then washed 3 x 5 min in 1X PBS (pH 7.4). Sections were dried with 70% ethanol wash before drying at 60°C for 10 min. Coverslips were mounted using Glycergel (DAKO, C056330-2) preheated to 60°C. Images were taken on a Nikon SMZ1500 microscope.

Western blot analysis

For cerebellar lysates – Cerebella were dissected in 1X PBS (pH 7.4) and lysed in radioimmunoprecipitation assay buffer [50 mM Tris-HCl (pH 7.2), 150 mM NaCl, 0.1% Triton X-100, 1% sodium deoxycholate, 5 mM EDTA] containing protease inhibitor (Roche, 11836153001) and 1 mM phenylmethylsulfonyl fluoride (PMSF; Sigma, 10837091001). Extracts

were cleared by centrifugation at 21130 rcf for 10 min at 4°C. Total protein concentration was determined with the Pierce BCA protein assay kit (Thermo Fisher Scientific), utilizing 50 μg of cerebellar lysate for each sample. Lysates were mixed with 6X Laemmli buffer and denatured at 95°C for 10 min. Protein was separated by SDS-PAGE (5% separating gel for GLI1 and GLI2, 6.25% for GLI3 and 12% for SHH) and transferred onto Immuno-Blot PVDF membranes (Bio-Rad) at 100 v for 100 min on ice. For most blots, primary antibodies were diluted in blocking buffer [30 g/L bovine serum albumin with 0.2% NaN_3 in 1X TBST (Tris-buffered saline, 0.5% Tween-20, pH 7.4)]. Blots were incubated with primary antibodies overnight at 4°C on a rocking platform. For detecting SHH, the primary antibody was diluted in 1X TBST and blots were incubated with primary antibody for 1 h at room temperature on a rocking platform. All primary antibodies and concentrations used can be found in Table S1. After incubation with primary antibody, blots were washed 3 x 10 min in 1X TBST. Peroxidase-conjugated secondary antibodies (Table S1) were diluted in blocking buffer, and blots were incubated with secondary antibodies for 1 h at room temperature on a rocking platform. After secondary incubation, blots were washed 4 x 10 min in 1X TBST, following incubation with Amersham ECL Prime Western Blotting Detecting Reagent (GE Healthcare, RPN2232) for 2 min and then exposed to HyBlot CL autoradiography film (Fisher Scientific, NC9556985) and developed using a Konica Minolta SRX-101A medical film processor. Relative levels were obtained by taking the integrated density value of each band, subtracting the background of the lane, and normalizing to the integrated density of housekeeping protein (CALB-1, VINCULIN, β-TUB) minus the background of the lane.

For Cos7 overexpression lysates – COS-7 cells were transiently transfected with the relevant DNA constructs using Lipofectamine 2000 (Invitrogen, catalog number 11668). The media was collected, and cells were lysed 48 h after transfection in HEPES lysis buffer (25 mM

HEPES pH 7.4, 115 mM KOAc, 5 mM NaOAc, 5 mM MgCl2, 0.5 mM EGTA and 1% Triton X-100) containing protease inhibitor (Roche, catalog number 11836153001) and 1 mM PMSF (Sigma, 10837091001). Culture media and extracts were cleared by centrifugation at 15,000 rpm for 10 min at 4°C. Total protein concentration was determined for cell lysates with the Pierce BCA protein assay kit (Thermo Fisher Scientific), utilizing 50 μg of cell lysate for each sample. Collected culture media was diluted 1:5 in HEPES lysis buffer before mixing with 6X Laemmli buffer and denatured at 95°C for 10 min. Protein was separated by SDS-PAGE using 12% gels and transferred onto Immuno-Blot PVDF membranes (Bio-Rad). Membranes with cell lysates were treated identical to cerebellar lysates, as described above.

Tamoxifen induction

To conditionally delete *Shh* in $Shh^{CreER/lacZ}$ mice, neonatal pups were injected intraperitoneally with 50 mg/kg of tamoxifen (Sigma, T5648-1G) dissolved in corn oil once daily on postnatal days 7, 8 and 9. On postnatal day 10, cerebella were collected and processed for section immunofluorescence described above.

Cerebellar granule neuronal progenitor cultures

The protocol was adapted from (Lee *et al.*, 2009). Postnatal day 8 animals were anesthetized on ice briefly before decapitation. Cerebella were dissected in 1X PBS (pH 7.4) and placed in Hibernate-A media (BrainBits, HA). Tissue was then washed once with 1X PBS (pH 7.4). Cerebella were incubated in digestion media [0.25% Trypsin-EDTA (Gibco, ILT25200056) + 1 mg/mL DNAse I (Roche, 10104159001)] for 5 min at 37°C followed by trituration with a P1000 pipette, and subsequent incubation for 15 min at 37°C, shaking the dish every 5 minutes.

After digestion, the pieces of tissue were further broken up with a P1000 pipette and transferred to a conical containing isolation media [DMEM (Gibco, 11965-092) + 10% calf bovine serum (ATCC 50-189-025NP) + 1x Penicillin-Streptomycin-Glutamine (Gibco, 10378016)]. The digested tissue was spun down 800 rcf for 8 min to pellet the cells. Digestion media was removed, and the pellet was washed with twice more isolation media. The pellet was fully resuspended in isolation media and passed through a 70 μm cell strainer. Single cell suspensions were spun down and resuspended in 1 mL of isolation media, which was then added to the top of a 30%/60% Percoll gradient (Sigma/Cytiva, P1644) before spinning at 800 rcf for 20 min. Initially, 100% Percoll was diluted with 10X PBS to make 90% Percoll. For 60% Percoll, 90% Percoll was diluted in L15 complete media [Leibovitz's L-15 Medium without phenol red (Gibco, 21083027) + 10% calf bovine serum (ATCC 50-189-025NP) + 1x Penicillin-Streptomycin-Glutamine (Gibco, 10378016)]. For 30% Percoll, 90% Percoll was diluted in isolation media. CGNPs were isolated from the 30%/60% Percoll interphase and washed with isolation media. Finally, CGNPs were resuspended in neuronal media [Neurobasal media (Gibco, 21103049) + 1% calf bovine serum (ATCC 50-189-025NP) + 1x Penicillin-Streptomycin-Glutamine (Gibco, 10378016) + 1x B27 supplement (Gibco, 17504044)] and counted using a hemocytometer and plated at appropriate densities onto chambers or wells that were incubated with laminin (Sigma, L2020). CGNPs were cultured at 37°C, 5% CO2, 95% humidity in neuronal media. For activation of Hedgehog signaling, either SHH C.M. collected from COS-7 cells was added to the media (1:10) or 500 nM of SAG (Enzo Life Sciences, ALX-270-426-M001) dissolved in DMSO was added to the media. To antagonize HH signaling, BMP2 (Peprotech, 120-02) was used at 100 ng/mL, and BMP10 (Peprotech, 120-40) was used at 10 ng/mL. Half media changes were done every 24 hours for the

duration of the cultures. 24 h before fixation, 10 μM EdU (Invitrogen, A10044), dissolved in DMSO, was administered to the culture.

Genotyping with beta-galactosidase fluorescence

For co-culturing *Kif17*$^{+/-}$ and *Kif17*$^{-/-}$ CGNPs, we utilized BetaFluor β-gal assay kit (Promega 70979-3) to distinguish between *Kif17*$^{+/-}$ and *Kif17*$^{-/-}$ littermates at postnatal day 8. Briefly, while dissected cerebella were on ice in Hibernate-A media, half of the cortex placed in TrypLE express (Invitrogen, ILT12604013) for 15 minutes at 37°C before lysing with reporter lysis buffer (Promega, E397A). Samples were spun at 15,000 rpm for 10 min at 4°C, and supernatant removed to a fresh tube. Lysates were then plated in triplicate in clear bottom 96-well plate and incubated with assay mixture for 30 min at 37°C before reading fluorescence. Genotyping samples taken at dissection later confirmed beta-galactosidase assay results.

Cerebellar granule neuronal progenitor culture immunofluorescence

Culture media was removed gently before coverslips were fixed in 4% paraformaldehyde for 30 min at room temperature. Coverslips were washed 3 x 5 min with 1X PBST^{X}, then were stained with EdU staining solution [100 mM Tris HCl (pH 8.3), 0.5 mM $CuSO_4$, 50 mM ascorbic acid, 50 μM Alexa Fluor 555 Azide, Triethylammonium Salt (Thermo Fisher Scientific, A20012)] for 30 min at room temperature. Coverslips were washed 3 x 5 min with 1X PBST^{X} and then blocked with blocking buffer (3% bovine serum albumin, 1% heat-inactivated sheep serum, 0.1% Triton X-100) for either 1 h at room temperature or 4°C overnight. Primary antibodies were diluted in blocking buffer. Coverslips were removed from the plate and were placed onto the diluted primary antibodies on top of parafilm for 1 h at room temperature. Coverslips were placed back in

the well and were washed 3 x 5 min with 1X PBST^{X}. Secondary antibodies were diluted in blocking buffer and were added to a fresh piece of parafilm. Coverslips were placed onto the parafilm and incubated with the secondaries for 1 h at room temperature. After secondary incubation, nuclei were labeled using DAPI (0.5 ng/mL in block buffer) for 10 minutes. Coverslips were then washed 3 x 5 min with PBST^{X}. Before mounting onto a slide with Immu-mount aqueous mounting medium (Thermo Fisher Scientific, 9990412), coverslips were briefly dipped in water. Images were taken on a Leica SP5X upright confocal (2 photon).

CGNP microplate assays

To quantify EdU incorporation *in vitro*, a Click-iT EdU proliferation assay (Thermo Fisher Scientific, C10499) was used in CGNPs *in vitro*. 24 h after plating, EdU was added to the culture (10μM, dissolved in DMSO). 48 h after plating, the assay was completed according to the manufacturer's protocol. To measure BrdU incorporation, a colorimetric BrdU Cell Proliferation ELISA Kit (Abcam, ab126556) was utilized. 48 h after plating (2 d *in vitro*), BrdU was administered to the culture. 48 h after BrdU addition (4 d *in vitro*), the assay was completed according to the manufacturer's protocol. To quantify the number of viable CGNPs *in vitro*, a CellTiter-Glo® Luminescent Cell Viability Assay (Promega, G7570) was used on cultures grown for 4 d *in vitro*. The assay was performed according to the manufacturer's protocol.

Immunoprecipitation of tagged proteins

COS-7 cells were transiently transfected with the relevant DNA constructs using Lipofectamine 2000 (Invitrogen, 11668). Cell lysates (1 mg) were pre-cleared with Protein-G–agarose beads (Roche, catalog number 11719416001) for 1 h at 4°C. MYC- or HA-tagged proteins

were immunoprecipitated from pre-cleared lysates using either anti-MYC or anti-HA antibodies for 2 hours at 4°C. Following immunoprecipitation, the lysates were incubated with Protein-G–agarose beads for 1 h at 4°C. The Protein-G–agarose beads were subjected to 5 x 8 min washes in HEPES lysis buffer and resuspended in 30 µl of 1X PBS and 6X Laemmli buffer. The samples were boiled for 10 min and proteins were separated using SDS-PAGE and analyzed by western blotting. Visualization and quantitation were identical to the above-described western blot analysis.

Image quantitation

To quantify intensity of SHH immunofluorescent signal, ImageJ software was used to measure the fluorescence integrated density of individual Purkinje cell bodies, subtracting the background measured from the internal granule layer. Per mouse, at least 5 images from the posterior lobes were measured, and an additional 5 images of the anterior lobes. To quantify fluorescent *Gli1* fluorescence, ImageJ software was used to measure the integrated density fluorescent signal contained to either the external granule layer (EGL, CGNPs) or lower molecular layer to inner granule layer (IGL, Bergmann glia and CGNs). At least six images were analyzed per mouse; three images for each posterior and anterior lobes. For all image analyses, images were blinded.

Quantitation and statistical analysis

All the data are mean ± s.d. All statistical analyses were performed using GraphPad Prism (www.graphpad.com). Statistical significance was determined by using a two-tailed Student's t-test for comparison of two groups or one way ANOVA analysis for more than two groups.. For all

the experimental analyses, a minimum of three mice of each genotype were analyzed, each *n* represents a mouse. For *in vitro* experiments, a minimum of three biological replicates were analyzed, each *n* represents a biological replicate. All the statistical details (statistical test used, adjusted *P*-value, statistical significance and exact value of each *n*) for each experiment are specified in the figure legends.

2.6 Acknowledgements.

We thank past and present Allen lab members for their valuable feedback and suggestions. We also thank Joe Besharse (Medical College of Wisconsin) for providing the *Kif17* mutant mice. We thank Adrian Salic (Harvard) for sharing the SUFU antibody. We thank Suzie Scales (Genentech) and Martin Engelke (Illinois State University) for their insightful comments. We thank Ryan Passino (University of Michigan) for technical assistance with the CGNP assays. We thank members of the Department of Cell and Developmental Biology who provided access to equipment, including the O'Shea, Engel, and Spence labs. PAX6 and LIM1/2 antibodies were obtained from the Developmental Studies Hybridoma Bank, created by the Eunice Kennedy Shriver National Institute of Child Health and Human Development of the National Institutes of Health and maintained at The University of Iowa, Department of Biology, Iowa City, IA 52242, USA. Finally, we acknowledge the Biomedical Research Core Facilities Microscopy Core, which is supported by the Rogel Cancer Center, for providing access to confocal microscopy equipment.

2.7 Author Contributions

Conceptualization: B.W., B.L.A. Data Curation: B.W., B.S.C., N.E.F. Formal Analysis: B.W., N.E.F. Funding Acquisition: B.W., B.L.A. Investigation: B.W., B.S.C., B.L.A. Methodology: B.W. Project Administration: B.L.A. Resources: K.J.V. Supervision: B.L.A. Validation: B.W. Visualization: O.Q.M. Writing/editing: B.W., B.L.A.

2.8 Tables

Table 2.1 Table of Antibodies

Antibody	Source	Catalogue Number	Application	Concentration used
Mouse IgG1 anti PAX6	DSHB	PAX6	IF	1:20 on tissue sections, 1:40 on coverslips
Rabbit anti Calbindin (CALB-1)	SWANT	CB38	IF/WB	1:10,000 (IF), 1:2000 (WB)
Chicken anti Beta-galactocidase	ICL	CGAL-45A-Z	IF	1:2000
Mouse IgG1 anti LIM1+2	DSHB	4F2	IF	1:20
Rabbit anti Ki67	Abcam	ab15580	IF	1:1000 on tissue sections, 1:2000 on coverslips
Rabbit anti SOX2	Seven Hills Bioreagent	WRAB-1236	IF	1:2000
Goat anti SHH (N-terminus)	R&D systems	AF464	WB	0.5 μg/mL

Rabbit anti HA	Bethyl Labs	A190-108A	WB	1:10,000
Mouse IgG1 anti Beta-tubulin (B-Tub)	DSHB	E7	WB	1:2000
Goat anti SHH (C-terminus)	R&D systems	AF445	IF	10 μg/mL
Goat anti BOC	R&D systems	AF2385	WB	1:4000
Rabbit anti Giantin	Biolegend (Covance)	924302	IF	1:1000
Goat anti GLI3	R&D systems	AF3690	WB	1:1000
Rabbit anti GLI1	Cell Signaling Technology	2534	WB	1:1000
Goat anti GLI2	R&D systems	AF3635	WB	1:1000
Rabbit anti VINCULIN	Cell Signaling Technology	13901	WB	1:1000
Mouse IgG1 anti MYC	Santa Cruz	sc-40	IP/WB	1:150 (IP), 1:1000 (WB)
Mouse IgG1 anti HA	Covance	MMS-101	IP/WB	1:300 (IP), 1:1000 (WB)
Mouse IgG2a anti ARL13B	NeuroMAB	73-287	IF	1:100 on tissue sections, 1:200 on coverslips
Rabbit anti Gamma-Tubulin	Sigma	T3559	IF	1:4000 on tissue sections, 1:8000 on coverslips
Goat anti SUFU	Adrian Salic Lab	N/A	IF	1:750
Alexa Fluor 488 goat anti-mouse IgG1	Invitrogen	A21121	IF	1:500

Alexa Fluor 647 goat anti-mouse IgG1	Invitrogen	A21240	IF	1:500
Alexa Fluor 647 donkey anti-rabbit IgG	Invitrogen	A31573	IF	1:500
Cy3 AffiniPure Donkey anti-Chicken IgY	Jackson Immunoresearch	703-165-155	IF	1:500
AP-conjugated anti-DIG antibody	Roche (Millipore Sigma)	11093274910	SISH	1:4000
Polyclonal Donkey anti Goat HRP	R&D systems	HAF109	WB	1:1000-5000
Peroxidase AffiniPure Donkey Anti-Rabbit IgG	Jackson Immunoresearch	711-035-152	WB	1:5000
Peroxidase AffiniPure Donkey Anti-Mouse IgG	Jackson Immunoresearch	715-035-150	WB	1:5000
Alexa Fluor 488 donkey anti-goat IgG	Invitrogen	A11055	IF	1:500
AffiniPure goat anti-mouse-light-chain secondary antibody	Jackson Immunoresearch	115-035-174	WB	1:50,000
Alexa Fluor 488 goat anti-mouse IgG2a	Invitrogen	A21131	IF	1:500

Table 2.2 Table of RT-qPCR primers

Gene	forward primer (5-3)	reverse primer (5-3)	Reference
Gapdh	GTGGTGAAGCAGGCATCTGA	GCCATGTAGGCCATGAGGTC	[Han et al., 2017 (PLoS Biology)]

Kif17	CATGCACACGGTACACAAC	GAACGGGAGGAGTCCTTATTC	designed by BW
Atoh1	AGTCAATGAAGTTGTTTCCC	ACAGATACTCTTATCTGCCC	[Hor et al., 2021 (Journal of Neuroscience)]
Gli1	GTGCACGTTTGAAGGCTGTC	GAGTGGGTCCGATTCTGGTG	[Han et al., 2017 (PLoS Biology)]
Ptch1	GAAGCCACAGAAAACCCTGTC	GCCGCAAGCCTTCTCTAGG	[Han et al., 2017 (PLoS Biology)]
Ptch2	CCCGTGGTAATCCTCGTGGCCTCTAT	TCCATCAGTCACAGGGGCAAAGGTC	[Shimokawa et al., 2008 (JBC)]
Ccnd1	AGACCTGTGCGCCCTCCGTA	CAGCTGCAGGCGGCTCTTCT	[Han et al., 2017 (PLoS Biology)]
Shh	GCTGTGGAAGCAGGTTTCG	GGAAGGTGAGGAAGTCGCTC	[Madison et al., 2005 (Development)]
Scube2	TGACTACCTGGTGATGCGGAAAAC	CAGTGGCGTGTGGGAAGAGTCA	[Lin et al., 2015 (J Bone Miner Res.)]
Boc	TTCATCCCCTTCTGCCTATG	ACCATTGTGTACTGGCACGA	[Mille et al., 2014 (Dev Cell)]
Ki67	CATTGACCGCTCCTTTAGGTATGAAG	TTGGTATCTTGACCTTCCCCATCAG	[Mille et al., 2014 (Dev Cell)]
Gli2	CCTTCACCCACCTTCTTGG	CTTGTTCTGGTTGGCATCATTT	[Scales et al., 2022 (PLoS Genetics)]

Gli3	CACATGCATCAACAG ATCCTAAGC	AGGGATAGGTCTCT GTGTTGGAAAT	[Scales et al., 2022 (PLoS Genetics)]
Bmp10	ATGGGGTCTCTGGTT CTGC	CAATACCATCTTGC TCCGTGAA	[Liu et al., 2017 (J Biol Chem.)]

2.9 Figures

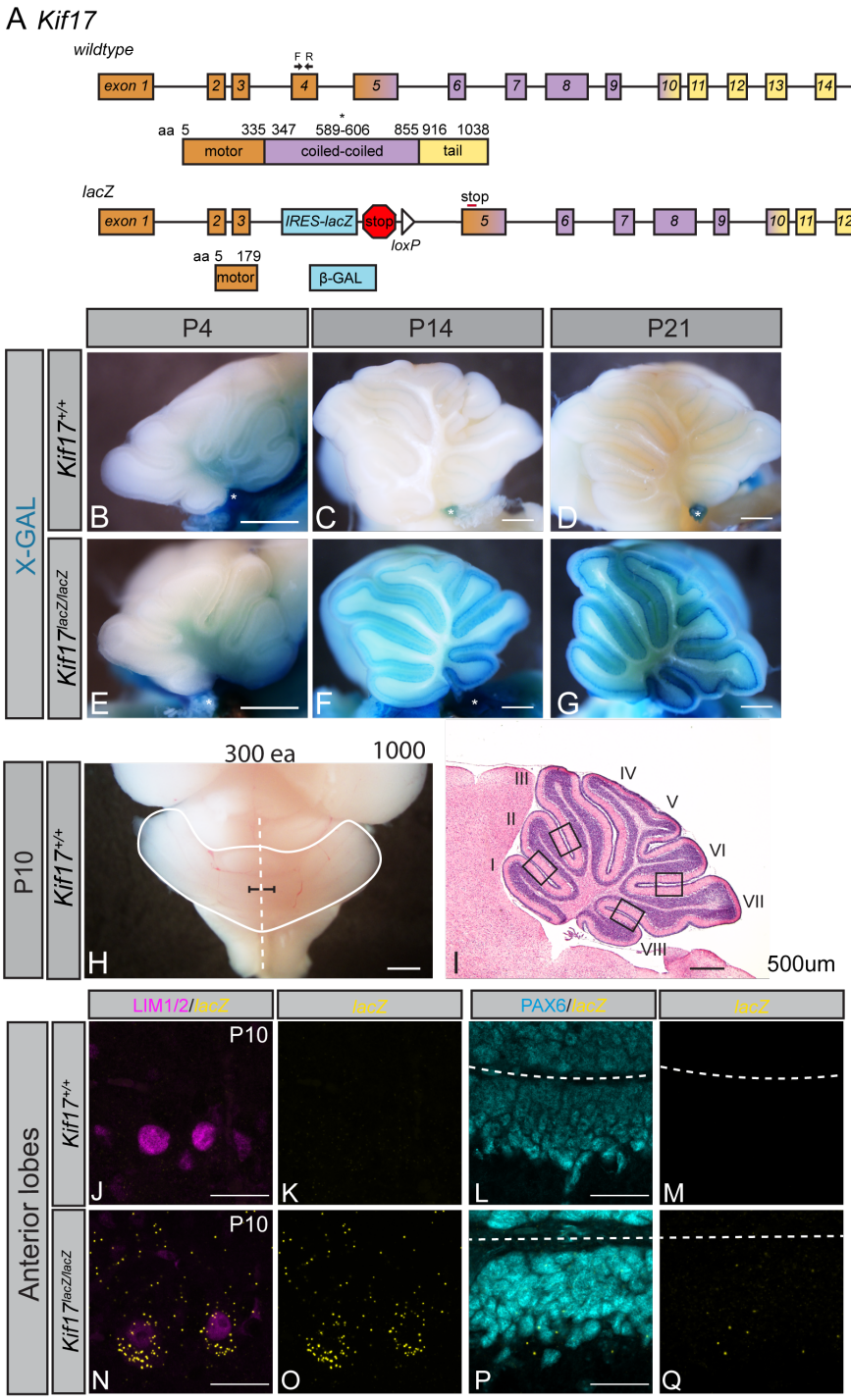

Figure 2.1 Schematic of *Kif17*^{lacZ} allele, orientation of sectioning analysis, timeline of *Kif17* expression during postnatal cerebellar development.

Schematic of *Kif17 wildtype* and *lacZ* alleles (A) and the polypeptides they encode. The *wildtype* allele encodes for three domains (motor domain, orange; coiled-coiled, purple; tail, yellow), while *lacZ* allele contains exon 4 deletion and *IRES-lacZ* insertion. The *lacZ* insertion contains a stop codon at the end of the cassette, and deletion of exon 4 results in a frameshift and premature stop codon within exon 5 (red line). Asterisk in wildtype polypeptide denotes the binding site of the commercial antibody in the paper initially describing this allele. Whole-mount X-gal stain of *Kif17*$^{+/+}$ (B-D) and *Kif17*$^{lacZ/lacZ}$ (E-G) cerebella from postnatal day 4 (P4) to postnatal day 21 (P21). Asterisks denote endogenous Beta Galactosidase in the choroid plexus (Trifonov et al., 2016). Scale bar (A-F), 500 μm. Whole-mount image of P10 *Kif17*$^{+/+}$ cerebella (H), indicating where mid-sagittal sections were taken for this paper (black brackets) for a depth of 300 μm into the tissue. Hematoxylin and eosin-stained section of P10 Kif17$^{+/+}$ cerebella (I), indicating numbering of the lobes. For this paper, lobes I-III are considered anterior, while VI-VIII are considered posterior. Boxes indicate where images were obtained. Fluorescent *in situ* hybridization detection of *lacZ* (yellow, J-Q) in anterior cerebellar lobes of P10 *Kif17*$^{+/+}$ (J-M) and *Kif17*$^{-/-}$ (N-Q) mice. Immunofluorescent detection of LIM1/2 (magenta; J, N) and PAX6 (cyan; L, P) were used to visualize Purkinje cells and CGNPs, respectively. Scale bar (J, L, N, P), 25 μm.